

Second Messenger-mediated flagellum assembly
during
the *Caulobacter Crescentus* cell cycle

Inauguraldissertation

zur
Erlangung der Würde eines Doktors der Philosophie
vorgelegt der
Philosophisch-Naturwissenschaftlichen Fakultät der Universität Basel

Von

Yaniv Cohen
aus Warth-Weinigen (TG) und Israel

Basel 2014

Genehmigt von der Philosophisch-Naturwissenschaftlichen Fakultät

auf Antrag von

Prof. Dr. U. Jenal und Prof. Dr. C. Dehio

Basel, den 11.12.2012

Prof. Dr. Jörg Schibler

Table of Contents

1	Introduction	5
1.1	The second messenger c-di-GMP	5
1.1.1	The making and breaking of c-di-GMP	6
1.1.2	Regulation of c-di-GMP cellular levels.....	8
1.1.3	c-di-GMP effectors.....	11
1.2	<i>Caulobacter crescentus</i> cell cycle and development.....	15
1.3	The <i>C. crescentus</i> cell cycle regulation	17
1.3.1	<i>ctrA</i> transcription	18
1.3.2	CtrA phosphorylation	19
1.4	c-di-GMP and <i>C. crescentus</i> development.....	21
1.5	The flagellum.....	23
1.5.1	The <i>C. crescentus</i> flagellar architecture.....	23
1.5.2	The regulation of flagellar biogenesis in <i>C. crescentus</i>	25
1.5.3	The flagellum and c-di-GMP signalling.....	26
2	Aim of this work.....	29
3	Results.....	30
3.1	Re-setting a flagellar polarization pathway during a bacterial cell cycle with a second messenger	30
3.2	Additional results TipF	90
3.2.1	TipF is cell cycle regulated but its degradation does not depend on known adaptor proteins of the ClpXP degradation pathway.....	91
3.2.2	c-di-GMP independent TipF mutants are stable in a strain lacking c-di-GMP and restore flagellum assembly.....	94
3.2.3	A CtrA mutant is able to partially suppress a deletion of TipF.....	98

3.2.4	The chemotaxis arrays in the <i>tipF</i> deletion mutant.....	102
3.2.5	Yeast two-hybrid screen for proteins interacting with TipF.....	103
3.2.6	Material and methods.....	108
3.3	The flagellin modification protein FlmA interacts with cyclic diguanosine monophosphate in an unspecific manner	111
3.3.1	Introduction.....	112
3.3.2	Results and Discussion.....	113
4	Bibliography	122
5	Appendices	136
5.1	De- and repolarization mechanism of flagellar morphogenesis during a bacterial cell cycle	137
5.2	Acknowledgements.....	152
5.3	Curriculum Vitae	153

1 Introduction

1.1 The second messenger c-di-GMP

Nucleotide-based second messengers can serve as message carriers inducing a variety of cellular cascades by binding specifically to their targets, thus transducing signals originating from changes in the surroundings or in intracellular conditions into cellular responses. The bacterial second messenger cyclic-di-guanosine monophosphate (c-di-GMP) was first identified as an allosteric activator of cellulose synthesis in *Gluconacetobacter xylinus*^{1,2} and was later shown to modulate several of the main activities of the bacterial cell such as transcription³⁻⁵, translation^{6,7}, enzymatic activities^{1,8}, and specific proteolysis^{9,10}. This influences multiple cellular processes such as motility, virulence, biofilm formation, cell cycle progression and cell differentiation^{11,12}. In summary, c-di-GMP is regarded as a bacterial life style modulator¹³ inducing the transit from a motile, single state to adhesive multicellular state. Low cellular levels of c-di-GMP are generally correlated with a motile and solitary lifestyle and with acute stages of infection of a range of bacterial pathogens, whereas high c-di-GMP concentrations promote a sessile, biofilm associated lifestyle and a chronic state of infection (Fig. 1).

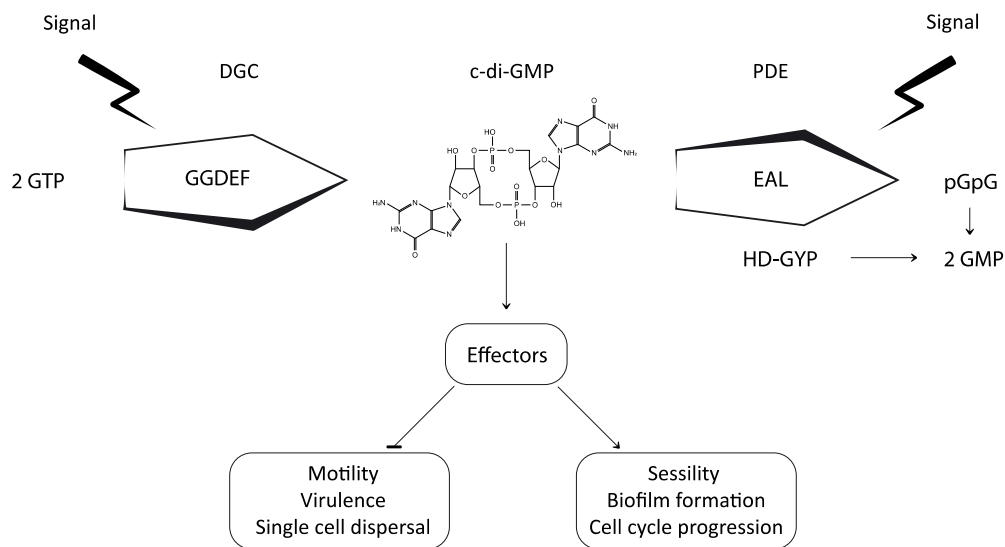


Figure 1: Overview of c-di-GMP signalling. DGC proteins harbouring the catalytic domain GGDEF and PDE proteins carrying the catalytic domain EAL regulate c-di-GMP cellular levels in response to environmental or intracellular signals. c-di-GMP binding proteins, so called effectors proteins translate c-di-GMP cellular levels into a cellular response and modulate the activity of target systems. Low levels of c-di-GMP promote motility and virulence, whereas high c-di-GMP cellular levels induce sessility and biofilm formation. Adapted from ¹⁴.

1.1.1 The making and breaking of c-di-GMP

C-di-GMP is the result of the condensation reaction of two GTP molecules. This process is catalysed by the activity of the widely distributed diguanylate cyclase enzymes (DGC)^{15–18}. GTP binds to catalytic active GGDEF domains, which form a homodimer thereby allowing the anti parallel alignment of the GTP molecules and the formation of two intermolecular phosphodiester bonds¹⁴. C-di-GMP degradation is promoted by the activity of the specific phosphodiesterases (PDE) that harbor the active domain EAL or HD-GYP.

Active EAL domains¹⁹ bind a single c-di-GMP molecule within their TIM-barrel-like fold^{20,21} and catalyse the asymmetrical hydrolysis of an ester bond. This reaction utilizes a conserved glutamate as a general base that together with two Mg^{2+} cation(s)²² coordinates and activates a water molecule for the nucleophilic attack. The attack of the hydroxide ion on the electrophilic phosphorus center leads to the breakage of the sugar phosphate bond producing the linear product dinucleotide 5'-

phosphoguananylyl-(3'-5')-guanosine (pGpG), which is then hydrolyzed to GMP by other unknown phosphoesterases²³. Sequence alignment of EAL domains revealed the presence of 10 conserved charged or polar residues²⁴ that were identical in all active proteins. Four conserved residues residues Glu⁵²³, Asn⁵⁸⁴, Glu⁶¹⁶, Asp⁶⁴⁶, (TBD1265) including the Glu residue of the EAL signature sequence bind the metal ion, whereas the conserved Glu⁷⁰³ (TBD1265) functions as a general base, coordinating the catalytic water molecule (Fig. 2). The role of Asp⁶⁴⁶ (TBD1265) is a matter of debate, nevertheless mutation of this residue caused significant changes in the catalytic parameters^{21,22,24}. The functional role of conserved residues Arg⁵²⁷, Glu⁵⁴⁶, Lys⁶⁶⁷, and Gln⁷²³ (TBD1265) is presently unknown²⁴.

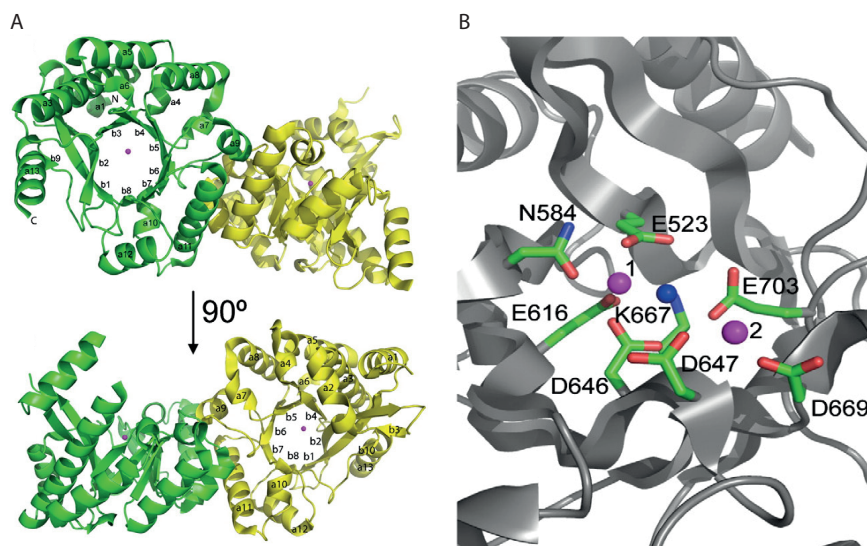


Figure 2 : Crystal structure of the TBD1265 EAL domain (PDB code 2r6o). Overall structure of the apoprotein dimer (A). Close-up view of the active site with bound Mg²⁺ (denoted by magenta spheres). The potential catalytic water molecule is shown as a blue sphere, whereas the amino acid residues in contact with the metal ions and water are shown as sticks along a TBD1265 ribbon (B). Adopted from²⁴.

In addition to the catalytic center itself, a conserved motif known as loop 6^{22,25} was shown to play an important role in the EAL domain activity²². It is presumed that this loop motif modulates the quaternary structure of the protein forming a dimer interface in the active conformation. Alteration of single amino acids in loop 6 or in Glu²⁶⁸ (EAL_{RocR}), which interacts with the loop and stabilized its position changes the catalytic parameters of the protein dramatically²² (Fig 3). This is an indication that

the loop 6 motif might be involved in signal transduction and activity regulation. The metal-dependent phosphohydrolase HD-GYP domain is less common and able to degrade *c*-di-GMP directly into GMP²⁶. The structure of HD-GYP domains reveal differences in the overall fold and an active site with a binuclear metal center²⁷.

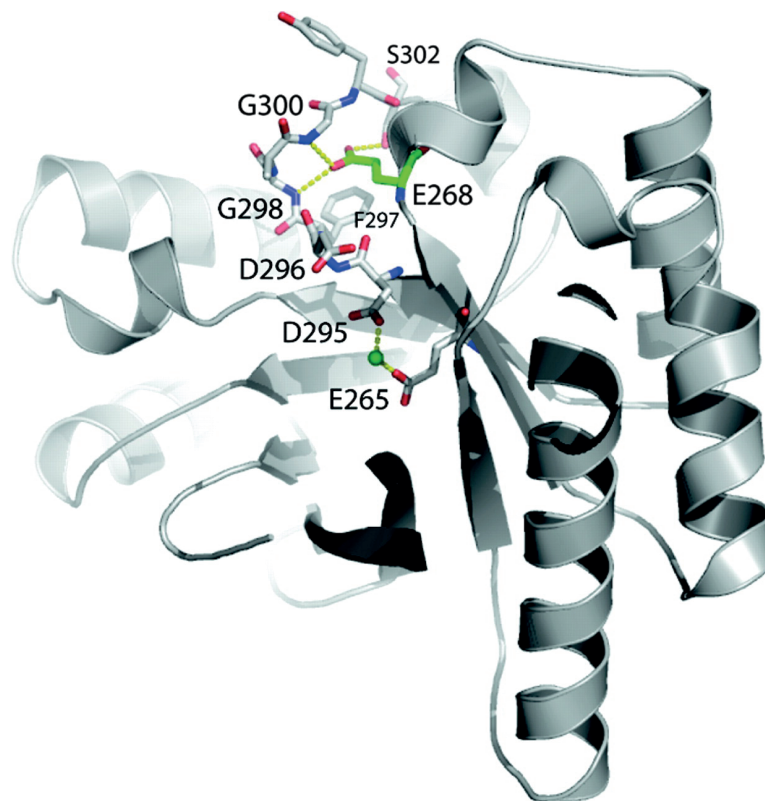


Figure 3: Structural model of EAL_{RocR}. The residues of loop 6 and Glu²⁶⁸ are highlighted. The hydrogen bonds formed between Glu²⁶⁸ and the loop residues Gly³⁰⁰ and Ser³⁰² are represented by the broken lines. The Mg²⁺ ion is shown as the ball. Adopted from^{21,22}.

1.1.2 Regulation of *c*-di-GMP cellular levels

The cellular levels of *c*-di-GMP are tightly regulated with the enzymatic activities of DGCs and PDEs being subject to multiple regulation cascades. DGCs and PDEs are generally composed of the catalytic active domain fused to diverse sensory and regulatory domains such as PAS, HAMP, GAF and REC^{28–30}, which govern the activity of the GGDEF and EAL domains. This enables the integration of diverse signals into the *c*-di-GMP signaling system and modulates the cellular levels of *c*-di-GMP.

Moreover, proteins involved in the *c*-di-GMP turnover are subject to temporal and spatial regulation. In *Escherichia coli* for example, several GGDEF and EAL encoding

genes are under the control of the σ^5 (RpoS)^{31,32}, a general stress response master regulator, which activates these genes only upon entry into stationary phase. In *C. crescentus*, spatial regulation and localization of c-di-GMP signaling elements in addition to specific proteolysis represent a further layer of regulation controlling c-di-GMP cellular levels. E.g. PdeA is a *C. crescentus* PDE³³ that co-localizes with its antagonist the DGC DgcB to the flagellated pole of the swarmer cell. During G1 to S phase transition, PdeA is recruited to the polar protease ClpXP where it is degraded setting DgcB activity free and leading to a c-di-GMP accumulation¹⁰.

DGCs are subject feedback regulation by their own product. This regulatory mechanism is well-documented for PleD, a *C. crescentus* response regulator with two receiver domains arranged in tandem (REC1-REC2) and a GGDEF catalytic domain^{8,34}. PleD is activated by phosphorylation of its first REC domain (REC1), which induces conformational changes of the REC1-REC2 stem that promote the formation of PleD homodimers. The resulting homodimer organization allows free rotation of the GGDEF domains that are connected to the REC1-REC2 stem over a flexible linker peptide. Once bound to GTP molecules, the GGDEF domains are reorganizing in a form that enables substrate proximity. The available crystal structures of PleD provided insight into the mechanism of non-competitive product inhibition by domain immobilization^{17,34} (Fig. 4). Dimeric c-di-GMP is able to crosslink GGDEF domains in a nonproductive conformation either to a neighboring REC or GGDEF domain. C-di-GMP interacts with the GGDEF domain over the primary inhibitory site (I_p) characterized by an RxxD motif⁸ and with a secondary inhibitory site (I_s) located on the surface of a neighboring GGDEF or REC domain. In both of the resulting domain organizations, the GGDEF active sites are immobilized resulting in PleD inactivation once the product levels reach the inhibition constant ($1\mu\text{M}$)^{14,17}.

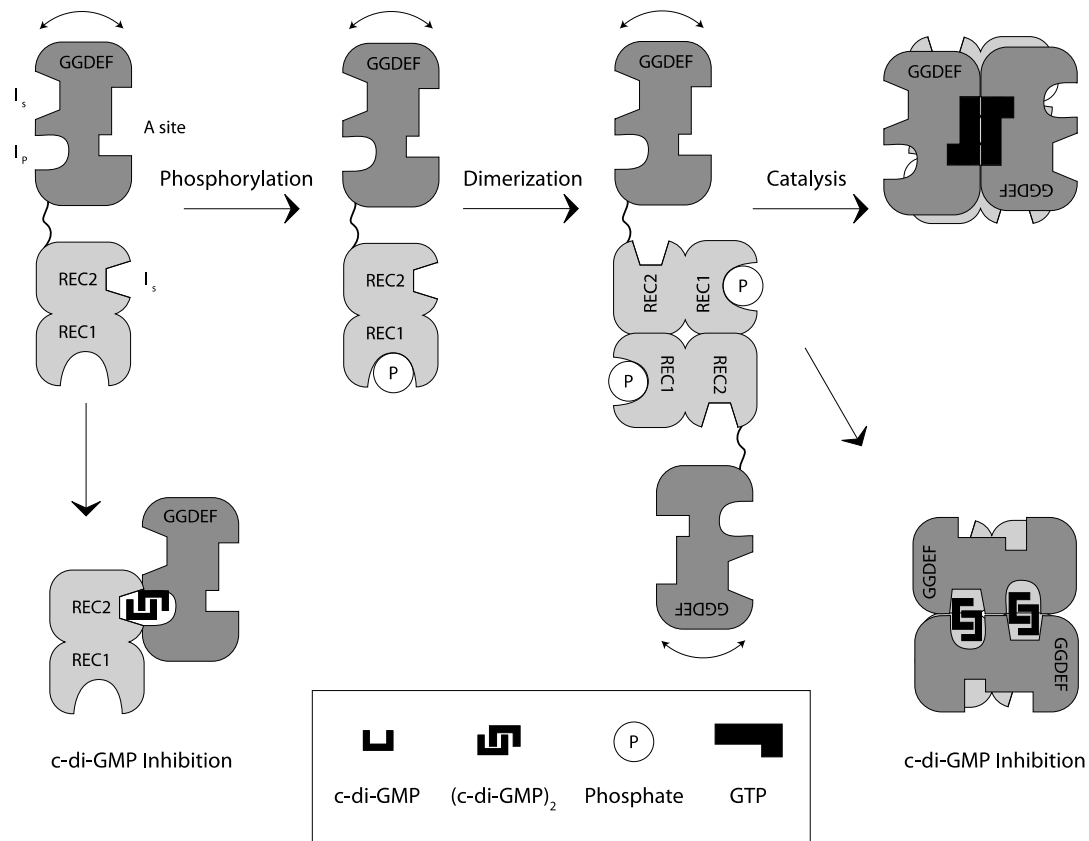


Figure 4: Model of PleD regulation. The catalytic GGDEF domain is connected to the receiver domains REC1-REC2 over a flexible linker peptide. Phosphorylation of the receiver domain REC1 results in dimerization and enzymatic activity. The two forms of domain organization resulting in allosteric product inhibition by domain immobilization are shown (lower panel). Inhibition occurs by binding of $(\text{c-di-GMP})_2$ to the I_s at the REC2 and to the I_p at the GGDEF domain or by crosslinking two GGDEF domains over I_s and I_p . Adapted from³⁵.

GGDEF and EAL containing proteins display an additional composition as about one third of GGDEF containing protein and two thirds of the EAL containing proteins contain both domains (composite proteins)²⁹ It was shown for several composite proteins that one of these domains lost its catalytic activity and is involved in signal transduction mechanism^{19,26,31,36} (see c-di-GMP effectors). This is for instance the case in *C. crescentus* PdeA, whose phosphodiesterase activity is strongly stimulated by GTP binding to the degenerate and catalytically inactive GGDEF domain³³. However, several composite proteins retain both catalytic activities³⁷. There is precedence for bifunctional enzymes involved in signal transduction, include protein

His-kinases/phosphatases of the two-component regulatory systems or the SpoT proteins catalyzing both synthesis and degradation of the bacterial nucleotide second messenger, (p)ppGpp³⁸. This arrangement of two catalytic domains with opposite activities within one polypeptide might serve as an additional regulatory mechanism controlling the cellular levels of c-di-GMP.

1.1.3 c-di-GMP effectors

The paradigm of second messenger signal transduction requires an additional component. An adaptor molecule (effector) that is able to translate the cellular levels of c-di-GMP into a specific cellular response. So far, several c-di-GMP effectors were reported interfering with numerous cellular activities on several levels, including transcription, translation, allosteric regulation, and protein stability³⁹. During the evolutionary process, c-di-GMP effectors evolved from different initial molecules generating a high degree of variability of c-di-GMP signal integration (Table 1).

Degenerated GGDEF and EAL domains These proteins apparently have evolved from c-di-GMP enzymes that retained their ability to bind c-di-GMP in the allosteric (DGC) or substrate-binding site (PDE) though lost their enzymatic capacity. The *Pseudomonas aeruginosa* protein FimX⁴⁰⁻⁴² harbouring degenerate GGDEF and EAL domains is one example for this effectors class. Upon binding to c-di-GMP FimX localizes to one cell pole where it mediates type IV pili assembly⁴². Binding of c-di-GMP to the C-terminal EAL domain triggers a long-range (~ca. 70 Å) conformational change in the N-terminal REC domain and the adjacent linker promoting FimX localization^{41,42}. Another example is PelD⁴³. The Pel exopolysaccharide is involved in *P. aeruginosa* biofilm formation. Pel biogenesis is stimulated by c-di-GMP both on the transcriptional^{3,44} and post-translational level^{43,45}. Activation of the Pel biosynthesis machinery by c-di-GMP involves the c-di-GMP receptor protein PelD. Despite of limited primary sequence homology, secondary structure analysis of PelD revealed a near identical fold to the catalytic domain of the PleD diguanylate cyclase⁴⁵. PelD binds c-di-GMP at a conserved RXXD motif that normally serves as

allosteric inhibition site for active diguanylate cyclases like PleD. Mutations in the RxxD motif of PelD abolished c-di-GMP binding and Pel stimulation⁴³.

AAA σ 54 Regulatory Domain In *P. aeruginosa*, c-di-GMP modulates the activity of the transcriptional regulator FleQ³, which antagonistically controls the expression of flagellar and PEL exopolysaccharide genes. FleQ is an enhancer binding protein belonging to the NtrC family of sigma54-specific transcription activators. It harbors an N-terminal input domain, an AAA⁺/ATPase sigma54-interaction domain and a DNA binding domain. It is suggested that FleQ controls gene expression by a mechanism that involves binding to two sites in the promoter of the operon it controls. FleN and FleQ forming a protein complex, that in the absence of c-di-GMP induces a distortion of pel DNA and represses the *pelA* promoter activity. Once bound with c-di-GMP, FleQ undergoes a conformational change that induces a cascade of conformational changes in the FleQ/FleN/DNA complex and enables *pelA* promoter activity⁴⁴.

REC Domain The *Vibrio cholerae* transcription regulator VpsT⁵ consists of an N-terminal receiver (REC) domain and a C-terminal helix-turn-helix (HTH) domain, with the latter mediating DNA binding. Unlike other REC domains, the VpsT REC domain is extended by an additional helix at its C terminus enabling c-di-GMP binding. This inversely controls extracellular matrix production and motility⁵. Upon c-di-GMP binding VpsT forms oligomers on DNA binding sites thus regulating promoters activity⁴⁶.

cNMP binding domain in *Xanthomonas campestris* the global regulator Clp^{47,48} a member of the large CRP/FNR transcription family, induces a number of virulence genes (among others the cellulase gene *engXCA*, the protease gene *ptr1*, and the flagellin gene *fliC*⁴⁹) upon a drop in the cellular level of c-di-GMP. Clp shows high sequence similarity to the *E. coli* catabolite activation protein CAP a cAMP receptor protein and contains a conserved cyclic nucleotide monophosphate (cNMP) binding

domain that binds c-di-GMP. The binding of c-di-GMP induces a conformational rearrangement affecting the affinity of Clp to its target promoters, thus repressing virulence genes transcription.

PilZ Domain The PilZ domain was identified in a bioinformatics analysis as c-di-GMP effector⁵⁰. Additionally this domain is found at the C-terminus of cellulose synthetase BcsA of the *Gluconacetobacter xylinus*, the first enzyme shown to be regulated by c-di-GMP². PilZ domains have been found to bind to c-di-GMP with variable affinities, ranging from sub- μM to μM ^{33,51-53} and to induce a variety of cellular cascades, including virulence, motility and exopolysaccharides synthesis. The PilZ domain has a β -barrel topology with a conserved short unstructured loop at the N-terminus, the so-called c-di-GMP switch. Conserved RxxxR and D/NxSxxG sequence motifs were demonstrated to mediate c-di-GMP binding⁵². The interaction of c-di-GMP to arginine residues in the switch portion induces a conformational change in the overall fold of the protein that facilitates the signal transduction as shown for YcgR. YcgR, an *E.coli* PilZ domain containing protein was demonstrated to bind to the stator complex of the flagellar motor and to regulate flagellar rotation^{54,55} in response to c-di-GMP. Although it seems that protein-protein interaction is the preferred mode of action of the reported PilZ receptors, additional mechanisms are reported. In *Klebsiella pneumoniae*, the PilZ domain protein MrkH binds DNA in a cyclic di-GMP-dependent manner to activate transcription of the type III fimbriae⁴. Due to the vast domain architectures of PilZ-containing proteins^{50,52} additional signal transduction mechanisms seem to be plausible.

Riboswitch c-di-GMP-controlled riboswitches regulate splicing⁵⁶ or translational initiation of mRNA. Two classes of riboswitches were identified: the first class is GEMM⁵⁷, an RNA domain localized in the 5' untranslated region of target mRNA that specifically binds c-di-GMP with high affinity and, in response, controls translation of downstream genes. Both ON- and OFF-switches of GEMM have been reported. The second class consists of a RNA c-di-GMP binding structure that upon binding induces

folding changes at atypical splice site junctions to modulate alternative RNA processing⁵⁸.

PNPase The polynucleotide phosphorylase (PNPase) is part of the RNA degradosome complex⁵⁹, a multiprotein complex involved in mRNA degradation. C-di-GMP was shown to directly interact with *E. coli* PNPase and, in response, increase its 3' oligonucleotide polymerase activity⁶⁰. Moreover, a set of dedicated c-di-GMP catalytic enzymes, DosC (DGC) and DosP (EAL), seem to adjust c-di-GMP levels available to the PNPase within the degradosome complex in response to oxygen availability⁶⁰.

Protein	Organism	Domain	Biological output	Reference
GGDEF and/or EAL domain-containing proteins				
FimX	<i>P. aeruginosa</i>	REC/PAS/GGDEF/EAL	Twitching motility	[^{40,41}]
PelD	<i>P. aeruginosa</i>	TM/TM/TM/TM/GAF /GGDEF	Exopolysaccharide (EPS) production	[^{43,45}]
LapD	<i>P. aeruginosa</i>	HAMP/GGDEF/EAL	Biofilm escape	[⁶¹]
PopA	<i>C. crescentus</i>	REC/REC/GGDEF	Cell cycle progression	[⁹]
Transcription factors				
FleQ	<i>P. aeruginosa</i>	FLEQ/AAA/HTH	Motility, EPS	[³]
Bcam1349	<i>B. cenocepacia</i>	cNMP/HTH	Biofilm formation and virulence	[⁶²]
VpsT	<i>V. cholerae</i>	LuxR-HTH	EPS production	[⁶³]
Clp	<i>X. campestris</i>	cNMP/HTH	Virulence	[^{47,48,64}]
PilZ domain-containing proteins				
YcgR	<i>E. Coli</i>	YcgR-N/PilZ	Motility	[^{54,55,65}]

Alg44 (PA4608)	<i>P. aeruginosa</i>	PilZ	Alginate production	[⁶⁶]
XC1028	<i>X. campestris</i>	PilZ	Motility, virulence and biofilm formation	[⁶⁷]
PilZ (XCC6012)	<i>X. campestris</i>	PilZ	Virulence	[⁶⁸]
PP4397	<i>P. putida</i>	YcgR-N/PilZ	N/A	[⁶⁹]
PlzD (VCA0042)	<i>V. cholerae</i>	YcgR-N/PilZ	Virulence	[⁵²]
PilZ (XAC1133)	<i>X. axonopodis</i>	YcgR-N/PilZ	Virulence	[⁷⁰]
MrkH	<i>K. pneumoniae</i>	PilZ	Virulence and biofilm formation	[⁴]
Riboswitches				
Class I	<i>V. cholerae</i>	NA	Gene expression	[⁵⁷]
Class II	<i>C. difficile</i>	NA	Translational control	[⁵⁸]
Other RNA regulating proteins				
PNPase	<i>E. coli</i>	NA	RNA degradation	[⁶⁰]

Table 1: Specific c-di-GMP effector molecules. adapted from⁷¹.

1.2 *Caulobacter crescentus* cell cycle and development

The aquatic α -proteobacterium *Caulobacter crescentus* undergoes a complex cell cycle, which is characterized by an asymmetric cell division. Each division gives rise to genetically identical but morphologically distinct cells (Fig. 5). The motile daughter cell (swarmer cell) is equipped with polar adhesive pili and a rotary flagellum and needs to first differentiate into a non-motile stalked cell in order to initiate chromosome replication and cell division. This differentiation process is irreversible and involves multiple morphological changes; flagellum and pili are shed, and replaced by a long cellular extension, the stalk, that carries an exopolysaccharide adhesion, the holdfast, at its tip⁷². During the obligate swarmer-to-stalked cell

differentiation the chromosome replication block is suspended with cells transiting from G1-phase (gap) to S-phase (DNA synthesis). As cells progress through division a new flagellum and adhesive pili are synthesized at the pole opposite the stalk. In contrast to the newborn swarmer cell, the stalked cell progeny initiates chromosome replication and cell division immediately⁷³ thereby continuously producing new swarmer progeny⁷⁴. Chromosome replication initiates only once per cell cycle⁷⁵ and is intimately linked to the cell developmental stage. Precise timing of assembly and loss of polar organelles is regulated by cell cycle and relay on signal transduction via the second messenger molecule c-di-GMP^{10,76,77}. This provides an excellent platform to explore the c-di-GMP signal transduction in relation to polar organelles development.

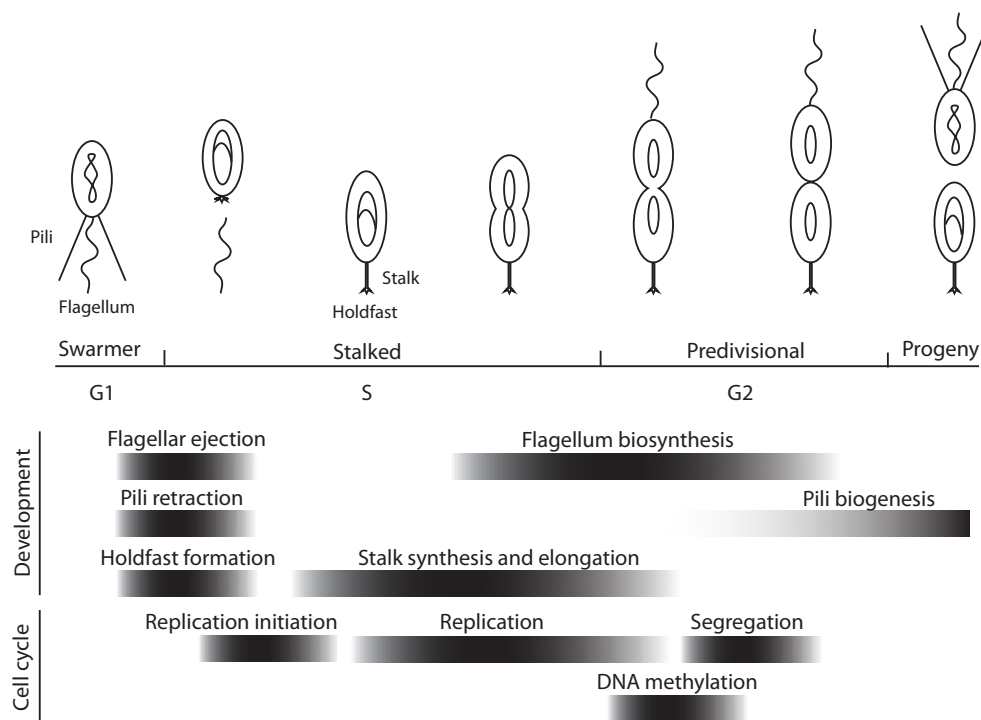


Figure 5: *C. crescentus* cell cycle and development. A schematic of the developmental stages of *C. crescentus* cell division and differentiation from the flagellated, piliated swarmer cell into a sessile surface attached stalked cell. Coincident with pole differentiation, the incipient stalked cell initiates chromosome replication. The grey bars represent morphogenetic and cell cycle events, bar position and length represent time windows. Adapted from⁷⁸.

1.3 The *C. crescentus* cell cycle regulation

The coordination of multiple processes that cooperatively assemble the *C. crescentus* cell cycle process requires numerous regulatory layers that orchestrate the single events spatially and temporally into one linear event. This is achieved by the oscillation of regulatory factors that create a signalling network. The main output of this regulatory network is the oscillation of CtrA, a response regulator that is composed of a receiver domain with a conserved histidine phosphorylation pocket and a C-terminal DNA binding domain^{79,80}. CtrA recognizes a specific DNA motif⁸¹, the CtrA box, that is located in the promoter region of its target genes. Once bound, CtrA can act as repressor or activator. At least 95 genes are directly regulated by CtrA⁸², among these are genes involved in chromosome replication, cell division and developmental processes⁸², such as *fla*⁷⁹, *che*⁸³, *divK*⁸⁴ and *ftsZ*⁸⁵. CtrA is regulated on multiple levels including phosphorylation, transcription, localization and proteolysis^{84,86,87} that dictate CtrA levels and activity. In the swarmer cell, high levels of active CtrA-P result in the inhibition of chromosome replication⁸⁸ as CtrA binds to sites within the origin of replication (Cori). This neutralizes the activity of DnaA, a key bacterial replication initiation factor that also binds to the Cori^{89,90}. During the swarmer-to-stalked cell differentiation CtrA is recruited to the incipient stalked pole where it is degraded by the polar ClpXP protease⁹¹. The removal of CtrA relieves the replication block and allows cells to enter S-phase. Removal of CtrA also leads to the transcription of *gcrA*⁹², which encodes an additional cell cycle regulator required for chromosome replication, cell elongation and polar development⁹³ (Fig. 6). The accumulation of GcrA during S-phase then leads to restart of *ctrA* transcription⁹⁴. Buildup of CtrA levels in the predivisional cell subsequently inactivate the *gcrA* promoter and direct the degradation of DnaA by the ClpP protease⁹⁰. In the late predivisional cell CtrA activity is sequestered asymmetrically by phosphorylation at the new swarmer pole and dephosphorylation and degradation at the stalked pole⁸⁰. This asymmetric distribution differentially sequesters CtrA into the progeny cells during division, thereby contributing to the different cell cycle and cell differentiation fates of the two daughter cells.

1.3.1 *ctrA* transcription

The transcription of *ctrA* is regulated during the cell cycle via a hierarchical transcription cascade, in which every element controls the regulation of the next, creating a closed regulatory circuit composed of DnaA, GcrA, CtrA, and CcrM^{82,94,95}. The transcription of *ctrA* is initiated from two promoters, P1 and P2⁹⁶. While the weaker P1 promoter is negatively autoregulated, the stronger P2 promoter is part of a positive feedback loop. P1 is first activated in S-phase through the action of the other global transcription regulator, GcrA⁹⁴. GcrA activation requires that the replication fork has moved through this region, leaving the P1 promoter in a hemimethylated state^{75,97}. As CtrA levels build up, the P2 promoter is activated and at the same time CtrA stimulates the transcription of *ccrM*, encoding a DNA methyltransferase with high specificity for GANTC sites. CcrM methylation of GANTC sites represses the activity of the P1 promoter and activates transcription of *dnaA*⁹⁶, a key factor for replication initiation in the next round of cell division. The activity of P2 promoter leads to further accumulation of CtrA in the predivisive cell, which is then phosphorylated and increases its affinity to the target genes promoters⁹⁸. Recently SciP^{99,100}, a small regulatory protein whose promoter is CtrA regulated, was shown to bind next to the CtrA binding box and to modulate the activity of CtrA controlled genes. Elevated cellular levels of SciP in the swarmer cell lead to reduction of CtrA levels since SciP inactivates the *ctrA* P2 promoter. Thus SciP serves as the negative feedback loop^{99,100}.

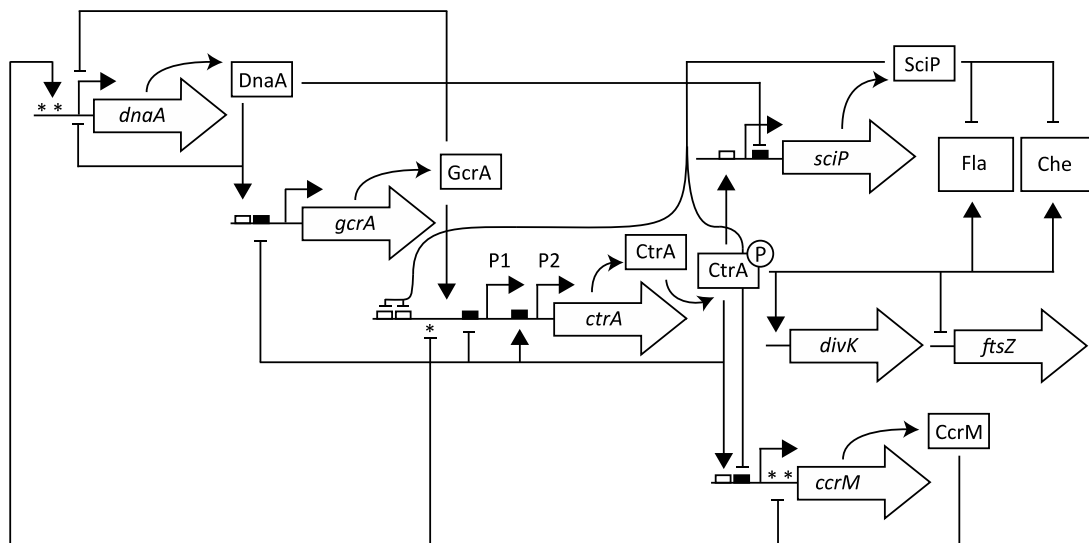


Figure 6: Topology of *ctrA* transcription and regulation. The regulatory circuit composed of *dnaA*, *gcrA*, *ccrM*, *sciP*, and *ctrA* is shown. Each regulator activates the next in the cascade and the inhibitory loop regulating the temporal activity of the promoters creating a closed cycle that regulates the oscillation of the cell cycle regulators. The main outputs of CtrA regulation and SciP inhibition are indicated. Adapted from^{84,100}.

1.3.2 CtrA phosphorylation

The oscillation of CtrA between a phosphorylated and dephosphorylated state and the asymmetric distribution of the different states in the predivisive cell is the result of an elaborate spatial distribution of the responsible phosphorelay system. The phosphorylation state of CtrA is determined by the bifunctional hybrid histidine kinase CckA^{96,101} and the histidine phosphotransfer (HPT) protein ChpT¹⁰². Proteins regulating the CckA-ChpT phosphorelay are positioned asymmetrically at the poles of the predivisive cell, thereby creating a gradient of activated CtrA and eventually, after cytokinesis has taken place, establishing two different cell fates^{103,104}. The histidine kinase DivJ¹⁰⁵ is localized to the stalked pole where it acts as a kinase for the single-domain response regulator DivK¹⁰⁶. The flagellated pole in contrast, accommodates a second histidine kinase, PleC^{103,104}, that acts as DivK phosphatase. DivK shuttles between the poles with changing phosphorylation states, until cytokinesis is completed and the cell is compartmentalized and each cell type inherits different levels of DivK-P, which dictates a different cell programme^{84,102}. In

the stalked cell, DivK-P binds to DivL¹⁰⁷, an unorthodox tyrosine kinase and prevents its interaction with CckA. In this situation CckA acts as phosphatase leading to the dephosphorylation of CtrA. In contrast, DivK-P levels are low at the flagellated pole allowing the interaction of DivL with CckA^{108,109} and the stimulation of CckA autophosphorylation leading to CtrA phosphorylation (Fig. 7).

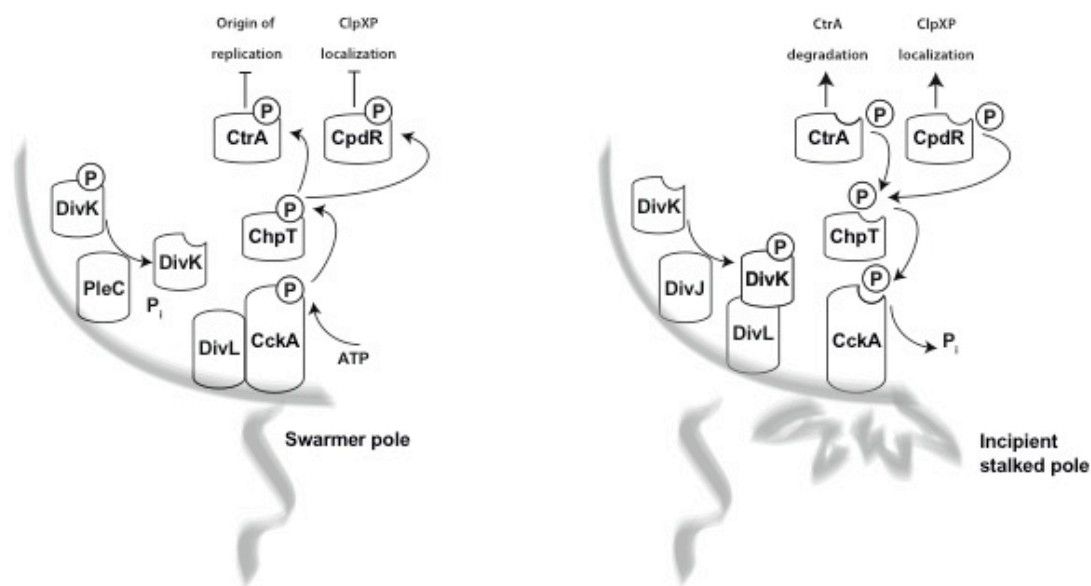


Figure 7: Model of the phosphorelay regulating spatially CtrA phosphorylation. The DivK phosphorylation state is determined by the phosphatase and kinase activity of PleC and DivJ. DivK~P interacts with DivL and inhibits DivL CckA interaction resulting in phosphatase activity of CckA and dephosphorylation of CtrA and CpdR. In contrast, dephosphorylation of DivK by PleC promotes DivL CckA interaction reversing CckA activity ultimately driving CtrA and CpdR phosphorylation. Adapted from¹⁰⁸.

Upon entry into S-phase, CtrA is specifically removed through proteolysis by ClpXP, an essential AAA⁺ protease whose transcription is CtrA regulated^{82,110,111}. The ClpX ATPase energizes the substrate unfolding and the translocation into the degradation cavity composed of tetradecamer complex of ClpP peptidase^{112,113}. A degradation tag, a short N-or C-terminal amino acid sequence that is located directly on the substrate or on the adapter molecule, mediates substrate recognition¹¹⁴. During swarmer to stalked cell transition, ClpXP is localized to the incipient stalked cell pole¹¹⁵. This process coincides with CtrA localization to the same pole where the

degradation of CtrA takes place¹¹⁰. The proteolysis of CtrA is the integration point of two control mechanisms. The first originates from the PleC-DivJ-DivK phosphorylation switch that, through the modulation of CckA activity (see above), activates CpdR, a single-domain response regulator that is required for the localization of the ClpXP protease to the cell pole¹¹⁶. Phosphorylation of CpdR is controlled by the CckA-ChpT phosphorelay that also mediates CtrA phosphorylation and activity¹¹⁷. Thus, through the coincident modulation of CtrA and CpdR phosphorylation states, CckA coordinates cell type specific activity and stability of CtrA¹¹⁷. The second signal required for CtrA degradation is c-di-GMP. Elevated levels of c-di-GMP activate the effector protein PopA. PopA is an unorthodox response regulator harboring two receiver domains fused to a degenerated GGDEF domain that retained its ability to bind c-di-GMP via a conserved I-site (see above). Once bound, PopA recruits CtrA to the degradation machinery via its direct interaction with the RcdA helper protein⁹¹ (Fig. 8).

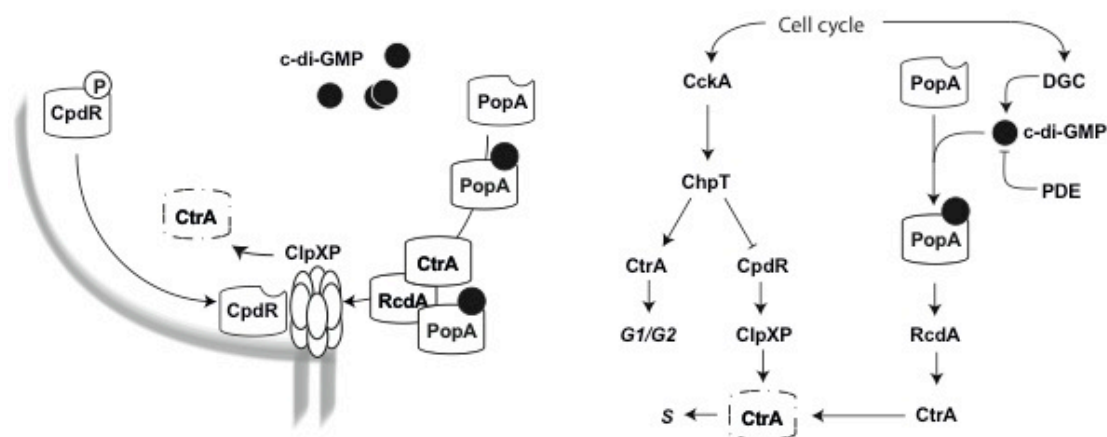


Figure 8: Model for CtrA degradation. The CckA-ChpT phosphorelay inversely regulates CtrA and CpdR activity through phosphorylation signal. Dephosphorylated CpdR recruits the ClpXP protease to the pole, whereas additional c-di-GMP mediate signaling activate the recruitment of CtrA over PopA to the same pole where ClpXP degrades CtrA. Adapted from⁹.

1.4 c-di-GMP and *C. crescentus* development

The fluctuation of CtrA activity during the cell cycle is accompanied by fluctuations of c-di-GMP levels that control many aspects of polar organelle development such as flagella, holdfast, and stalk biogenesis^{10,16,76,77}. While c-di-GMP levels are low in

swarmer cells, the concentration quickly increases during the transition to stalked cells. Likewise, in dividing cells a characteristic spatial gradient is observed with low c-di-GMP levels in the swarmer and high levels in the stalked compartment¹¹⁸. This characteristic distribution is governed through strict temporal and spatial control of several enzymes involved in c-di-GMP turnover. The swarmer cell maintains low c-di-GMP levels through the activity of the PDE PdeA¹⁰. At the same time the DGC PleD is kept in its inactive state in swarmer cells by the PleC phosphatase. The PleD response regulator harbors a catalytic GGDEF domain and is directly controlled by the PleC-DivJ-DivK phosphorylation switch^{16,102}. While PleC keeps PleD in its inactive state in the swarmer cell, PleD is activated by DivJ mediated phosphorylation during the stalked cell transition⁷⁶. At the same time, PdeA is degraded by the ClpXP protease, freeing the activity of its antagonist DGC, DgcB¹⁰. Together this leads to an accumulation of c-di-GMP in sessile stalked and predivisional cells. Asymmetric distribution of PleD and PdeA in the predivisional cell sets up a spatial gradient of c-di-GMP with low cellular levels in the swarmer compartment and high cellular levels in the stalked compartment¹¹⁸. Mutants that lack PleD and DgcB show characteristic pole differentiation defects¹¹⁹. This includes the failure to eject the flagellum and to assemble a polar stalk and adhesive holdfast^{76,120} (Fig. 9). These observations strongly indicate a prominent role for c-di-GMP in *C. crescentus* cell fate determination^{10,34,76,91}.

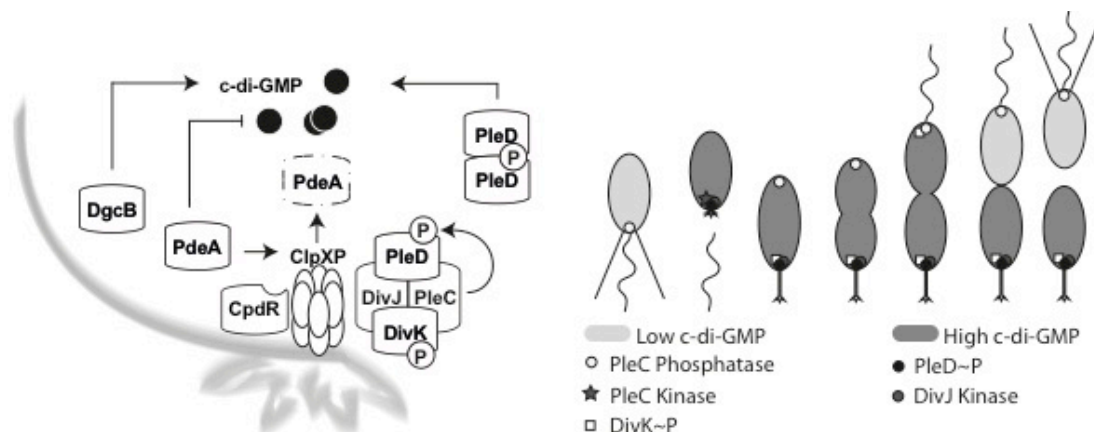


Figure 9: Model for c-di-GMP accumulation and distribution in the cell. During the swarmer to stalked pole transition, ClpXP mediates degradation of PdeA unleashing DgcB activity and PleD is activated by DivJ-DivK-PleC leading to PleD localization and rapid c-di-GMP accumulation. The distributions of c-di-GMP, PleD, PleC, DivK and DivJ during the cell cycle are indicated (left panel). Adapted from^{10,16,118}.

1.5 The flagellum

Locomotion is an advantage for the bacterial cell as the ability to move into favorable surroundings is a crucial for growth and survival in nutrient poor environments. One means of locomotion is the flagellum, an elaborate nanomachine, which enables the cell to harness the proton or sodium ion motive force to generate a mechanical force by the rotation of a long filament. The rotation of the flagellum is controlled by an array of chemoreceptors that can sense a wide range of environmental signals (chemotaxis). Changes in the surroundings induce a rotational response, clockwise or contra clockwise that facilitates the forward locomotion allowing bacteria to reach a beneficial environment.

1.5.1 The *C. crescentus* flagellar architecture

The flagellar motor consists of a rotor and a stator part. The stator is assembled in the inner membrane of bacterial cells from two integral membrane proteins, MotA and MotB, that form a complex of four MotA and two MotB protomers¹²¹. It has been estimated that at least 11 copies of the MotA-MotB complex, anchored to the peptidoglycan over MotB¹²², assemble around the rotary part of the motor. The rotor is composed of several proteins that assemble into ring structures in and around the inner membrane where they form the MS ring switch complex. The MS ring is made of 26 copies of FliF subunits^{123,124} that serve as assembly platform for the switch complex composed of FliG, FliM, and FliN. The interaction between FliG and MotA is responsible for the torque generation¹²⁵, whereas FliM and FliN modulate the direction of motor rotation in response to signals from the chemoreceptor array¹²⁶. The C ring accommodates the type three secretion system (T3SS)¹²⁷ that facilitates the secretion of the flagellar distal elements, the rod, the

hook and the filament. The rod is composed of three proteins FlgB, FlgC and FlgF forming a cylindrical channel that spans the periplasmic space and is embedded in the peptidoglycan layer and the outer membrane via the P-ring (FlgI) and the L-ring (FlgH) structures. These are the only flagellar elements that are secreted via the Sec pathway^{128,129} and not via the T3SS. The rod structure has a double function as a structural element that connects the motor to the hook protein (FlgE) and as a part of the T3SS as the proteins that assemble the hook and filament travel over the periplasmic space within the rod. Once the hook proteins are secreted, they are self assembled into a short tubular structure, which is thought to function as a universal joint to smoothly transmit the torque produced by the motor¹³⁰ to the filament and enables the secretion of the filament subunits. The filament itself, is composed of FljJ, FljK, FljL, FljM, FljN, and FljO¹³¹ subunits, grows to a tremendous length up to 15 μM ¹³² and serves as a screw propeller to convert rotary motion of the motor into a mechanical drive (Fig. 10).

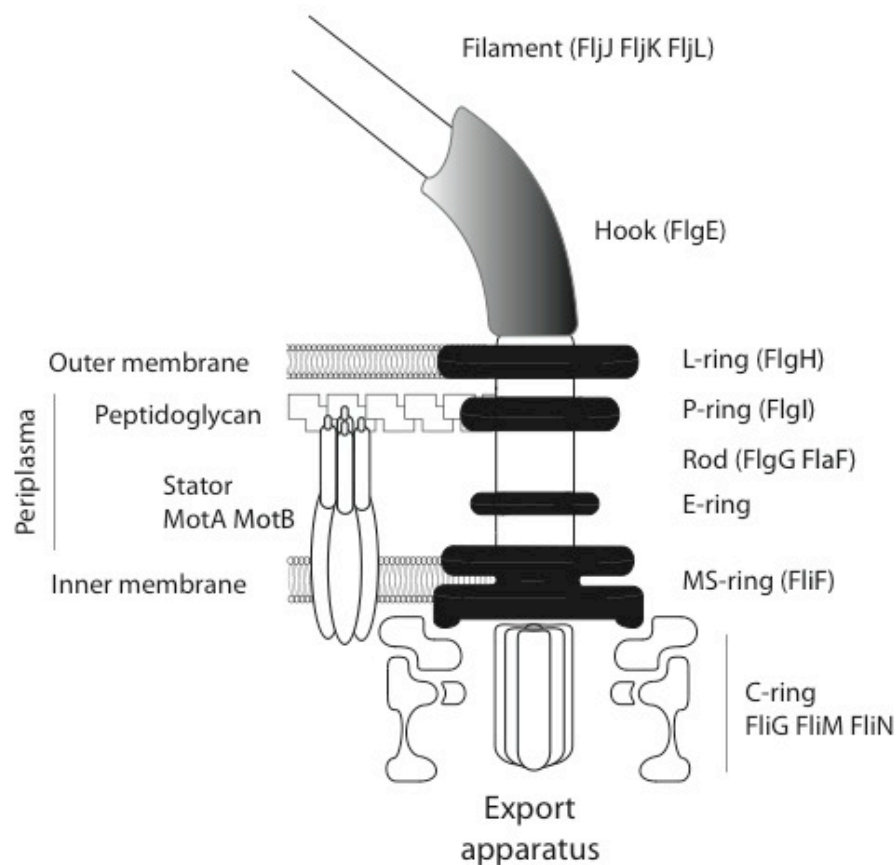


Figure 10: Schematic representation of the *C. crescentus* flagellum. The main structures are indicated as well as the proteins composing the structure. In addition, the position of the flagellum relative to the cell membrane is shown. The *C. crescentus* flagellum is presumed to have an additional ring structure (E-ring) which is unique and is missing in *E. coli* and *S. typhimurium*. Adapted from^{133,134}.

1.5.2 The regulation of flagellar biogenesis in *C. crescentus*

The *C. crescentus* flagellum biogenesis regulation is unique as flagellar gene expression is not only coordinated with the ongoing construction of the rotary device but is also tied to the cell cycle. The flagellum is assembled in the late predivisive cells and is active only for a short time during the cell cycle during which chromosome replication is inhibited (G1 phase). Upon swarmer cell differentiation into a stalked cell the flagellum is ejected. The flagellar genes cluster into operons that are regulated in a hierarchical manner forming transcriptional classes. These correspond to the flagellar structural checkpoints that are built sequentially and activate the next wave of gene expression. The activation of each class is dependent on the successful assembly of the previous class of proteins. Class I is reserved for the response regulator CtrA that acts as general activator of class II genes⁷⁹, the products of which assemble into the MS ring, the switch complex and the T3SS (basal body). In addition to the structural elements, class II includes regulatory elements that couple the transcription initiation of class III and class IV to the assembly of the flagellar basal body. FliD is an NtrC-like transcriptional regulator that is required for the transcription initiation of sigma 54-dependent class III and IV genes^{135,136}. The activity of FliD is dependent on an additional factor, FliX¹³⁷. FliX is a 15 kD membrane associated protein required for class III and IV expression. It has been postulated that FliX, by some unknown mechanism, senses the assembly state of the class II encoded part of the basal body and in response regulates FliD activity through a direct interaction¹³⁸. Furthermore, it was shown that the stability of the two proteins is co-dependent and stabilized FliX deregulates FliD activity and leads to the expression of class III protein in a class II mutant background. Once activated, the class III gene products are secreted via the T3SS and assembled into rod and hook structure. The class IV mRNA translation is inhibited, as long as the hook

structure is not assembled, by the activity of the class III gene product FlbT¹³⁹ that binds the flagellin mRNA 5' untranslated region¹⁴⁰. The mechanism by which hook assembly is sensed and transmitted to FlbT is unknown (Fig 11).

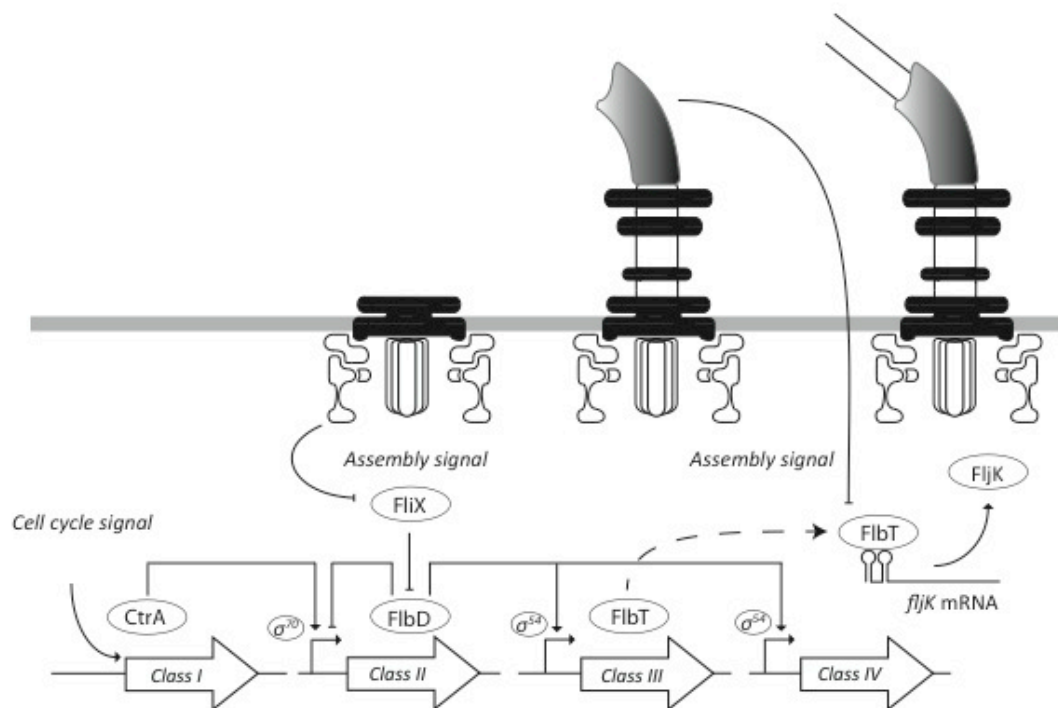


Figure 11: Regulation of flagellar gene expression and assembly during *C. crescentus* flagellar biogenesis: The regulatory cascade is indicated in the lower panel, the corresponding progression of flagellar assembly is indicated in the upper panel. Class II transcription is activated by CtrA. The class II gene product FliX inhibits FliD by direct interaction, as long as the MS switch complex is not assembled. The nature of signal inactivating FliX is unknown. Class III and IV flagellar genes are activated by FliD, whereas the class III gene product FlbT binds the flagellin 5' UTR mRNA (class IV) until the basal body hook, is fully assembled. Adapted from^{134,138}.

1.5.3 The flagellum and c-di-GMP signalling

C-di-GMP induces the switch between a motile and a sessile life style of bacterial cells. In recent years several c-di-GMP mediated mechanisms affecting flagellar function were described. One example is the *E. coli* PliZ domain effector protein YcgR, which upon binding to c-di-GMP modulates flagellar rotation through a direct

interaction with the motor protein MotA. This interaction presumably results in strengthened electrostatic interactions between MotA and the rotor component FlgG generating a force that opposes motor rotation. A stepwise decrease of torque production and thus increased motor curbing was observed with increasing numbers of stator subunits interacting with YcgR⁵⁵. Alternative models propose that activated YcgR binds to the switch complex and biases flagellum rotation towards a counter-clockwise orientation and thus smooth swimming⁶⁵.

In *C. crescentus*, the cellular levels of c-di-GMP are affecting the flagellum in several ways. A mutant lacking the DGC PleD fails to eject the flagellum during the swarmer to stalked cell transition, resulting in hypermotile cells and the stabilization of the FlhF MS ring protein^{76,110,120,141}. In contrast, a strain expressing a constitutive active allele of *pleD* (*pleD**) produces high cellular levels of c-di-GMP and, as a consequence, assembles an intact but paralyzed flagellum. The paralysis of the flagella at high c-di-GMP levels was associated with the activity of the c-di-GMP effector proteins DgrA and DgrB³³. It was shown that *dgrA* and *dgrB* deletion mutants are able to retain motility even under high cellular levels of c-di-GMP. All of the above shows that the flagellar rotation and ejection in *C. crescentus* is c-di-GMP regulated.

In addition, c-di-GMP regulates flagellar assembly in *C. crescentus*. TipF¹⁴² and TipN^{142,143} were identified in a screen for mutants with reduced motility. Deletion mutants of *tipN* show delocalized flagella^{142,143}, whereas *tipF* mutants fail to assemble any external flagellar structures¹⁴². TipN was demonstrated to localize to the bacterial septum and to mark the position of the new pole. The observation that ectopic expression of *tipN* resulted in ectopic stalks argued that TipN is sufficient for the initiation of pole development. In addition, TipN is essential for normal pole development as *tipN* deletions misorient axis polarity, fail to localize the PleC phosphatase and polar organelles¹⁴³. TipF localizes to the new pole in a TipN dependent manner, although no direct interaction was found. While *tipF* mutants are unable to assemble the flagellum, flagellar genes of class II, III, and IV are transcribed in this mutant background¹⁴⁴ and the respective proteins are present in the cell but are not secreted. This indicates that an early checkpoint of flagellar

assembly is defect in the absence of TipF. This is supported by the observation that FliG failed to localize to the pole opposite the stalk in the absence of TipF¹⁴². The *tipF* gene encodes an EAL domain protein and putative PDE. Primary structure analysis of TipF EAL domain indicates that all of the catalytic residues are conserved (Table 2) with the exception of Lys³³² (Gln⁶⁴⁷ TBD1265). In addition, TipF variants with a deletion in the EAL domain show the same phenotypes as *tipF* deletion mutants¹⁴². This creates a direct link between c-di-GMP signalling and flagellar assembly and/or positioning. However, the exact mechanism of this process is yet to be determined.

Proteins ^A	Conserved residues										Activity ^B
	1	2	3	4	5	6	7	8	9	10	
1. CB15 TipF	E211	R215	E233	N269	E311	D331	K332	K352	E396	Q415	?
2. TBD1265	E523	R527	E546	N584	E616	D646	D647	K667	E703	Q723	Yes
3. TDB1269	E	R	E	N	E	D	D	K	E	Q	Yes
4. TDB1660	E	R	E	N	E	D	D	K	E	Q	Yes
5. TDB1456	E	R	E	N	E	D	D	K	E	Q	Yes
6. EC YahA	E	R	E	N	E	D	D	K	E	Q	Yes
7. SFV 3559	E	R	E	N	E	D	D	K	E	Q	Yes
8. CV0542	E	R	E	N	E	D	D	K	E	Q	Yes
9. CV2505	E	R	E	N	E	D	D	K	E	Q	Yes
10. SO2039	E	R	E	N	E	D	D	K	E	Q	Yes
11. NE0566	E	R	E	N	E	D	D	K	E	Q	Yes
12. EC YdiV	E	H	E	Q	L	G	N	M	G	Q	No
13. STM1344	E	T	V	A	A	A	N	M	A	Q	No
14. BS Ykul	E	R	I	D	E	D	N	K	E	Q	No
Residue role (interaction)	Me1	P2	G1	Me1, P1	Me1	Me1, Me2	Me2	Water-1, E616	Me2	E523, K667	

Table 2: Primary structure analysis of TipF EAL domain revealing a subset of conserved residues.

Sequence alignment of the following proteins was used to identify conserved residues: *T. denitrificans* TBD1265 (Q3SJE6; aa 487–758), TBD1269 (Q3SJE2; aa 442–705), TBD1660 (Q3SIB5; aa 443–698), TBD1456 (Q3SIW6; aa 955–1212); *E. coli* YahA (P21514; aa 73–362); *Shi. flexneri* SFV_3559 (Yhjk; Q83J53; aa 395–649); *C. violaceum* CV0542 (Q7P0M4; aa 362–612), CV2505 (Q7NV41; aa 146–401); *She. Oneidensis* SO2039 (Q8EFE2; aa 1–233); *N. europaea* NE0566 (Q82WU5; aa 1–415); *E. coli* YdiV (P76204; aa 1–237); *S. typhimurium* STM1344 (CdGR; Q8ZPS6; aa 1–237); *B. subtilis* Ykul (BSU14090; O35014; aa 1–407) (A). Hydrolysis of c-di-GMP (B). Adapted from²⁴

2 Aim of this work

The second messenger cyclic-di-guanosine monophosphate (c-di-GMP) is known to control multiple aspects of bacterial growth and development. In *C. crescentus*, polar developmental such as the synthesis of polar organelles is c-di-GMP dependent. However, the adaptor molecules that sense c-di-GMP and mediate the signal to the appropriate targets are not identified yet.

The main goal of this work was to investigate whether and how putative downstream elements are involved in c-di-GMP signalling and to understand the respective signal transduction mechanisms. Previous results had linked the EAL domain containing protein TipF to flagellar assembly. The focus of this work was to investigate the c-di-GMP signal transduction mechanism involved in TipF activation and the identification of the processes of c-di-GMP mediated flagellar assembly. In an additional project, we identified the flagellar glycosylation protein FlmA as a putative c-di-GMP binding protein. Follow up studies should investigate c-di-GMP binding specificity of FlmA.

3 Results

3.1 Re-setting a flagellar polarization pathway during a bacterial cell cycle with a second messenger

Nicole Davis*, Yaniv Cohen*, Stefano Sanselicio, Coralie Fumeaux, Ricardo Guerrero-Ferreira, Elizabeth Wright, Urs Jenal, Patrick Viollier

Statement of my work

I contributed to this work by performing the experiments presented in Figures 2, 3C-D, 4A, 7A-E, S1, and S2A-B

ABSTRACT

Morphogenesis relies on the implementation and subsequent amplification of polarity cues, often imparted by nucleotide signals, at key times during the eukaryotic cell cycle. Analogous mechanisms are not known for the bacterial cell cycle. We uncovered a polarization mechanism in the bacterium *Caulobacter crescentus* that is triggered and amplified by cyclic-di-GMP signaling upon the G1→S transition to seed flagellum morphogenesis at the new pole via the TipF receptor protein. We show that c-di-GMP-binding induces the polarization of TipF and the recruitment of downstream effectors, including flagellar switch proteins and the PflI positioning factor, into a complex with the TipN landmark protein that preselects the polar site. Importantly, c-di-GMP not only induces TipF polarization and activation, but also its stability, thereby enforcing the removal of this factor from the maturing old pole during the G1→S transition. This novel c-di-GMP-governed reinforcement mechanism ensures a robust amplification and swift removal of TipF-dependent polarization during each cell cycle.

INTRODUCTION

Cell polarity is fundamental to intracellular organization and morphogenesis in all forms of life, yet little is known on how polarity-dependent cues are implemented, reinforced and removed during the bacterial cell cycle. The cell cycle regulator Cdc42, a member of the Rho-family of GTPases, is critical for polarization in baker's yeast *Saccharomyces cerevisiae* and many other eukaryotes. In response to cell cycle signals, Cdc42 polarizes and promotes the nucleation of actin cables that, in turn, enhance the polarization of Cdc42 in its active GTP-bound form (Cdc42•GTP). Polarized Cdc42•GTP recruits polarity effectors to the bud site and ultimately drives bud emergence. Underlying this polarization are “landmark” proteins that are positioned in the mother and inherited by newborn cells to dictate the future bud site (Slaughter, Smith, & Li, 2009).

Here we describe a conceptually analogous polarized nucleotide-signaling pathway that triggers and reinforces morphogenesis during a bacterial cell cycle. We show that polar flagellation in the Gram-negative α -proteobacterium *Caulobacter crescentus* (henceforth *Caulobacter*) is cued by the activation, polarization and stabilization of a bis-(3'-5')-cyclic dimeric guanosine monophosphate (c-di-GMP) receptor protein (TipF) upon the G1→S transition to seed flagellar assembly at the pre-determined polar site. We show that TipF recruits the Pfl placement factor into a flagellar positioning complex containing the TipN landmark protein while also binding and recruiting the switch component of flagellar base to the newborn pole. Importantly, the c-di-GMP-induced stabilization and localization amplifies the

polarization while synchronizing this specific morphogenetic process with other c-di-GMP induced developmental events that are triggered during the G1→S transition.

A myriad of polarized macromolecular assemblages were recently uncovered in bacteria and time-lapse imaging indicates that mechanisms must exist that coordinate protein polarization with cell cycle progression to ensure their appropriate inheritance in the progeny. The bacterial flagellum is such a polar assemblage, and while, polar flagellation is not uncommon, the mechanisms of polarization during the cell cycle are largely mysterious. Arguably the preeminent model system for bacterial cell cycle studies, *Caulobacter* has long been known to assemble polar flagellum in a cell cycle-controlled fashion. At the predivisional cell stage *Caulobacter* is overtly polarized, bearing a cylindrical extension of the cell envelope (the stalk) at the old pole and a newly assembled flagellum whose rotation is activated at cytokinesis at the opposite pole. Cytokinesis yields a motile swarmer cell that resides in a G1-like, non-replicative state and a dividing stalked cell that in S-phase. Two master transcriptional regulators of the cell cycle, CtrA and GcrA, reinforce the transcriptional program at sequential stages of the cell cycle. CtrA is present in G1-phase, proteolytically removed during the G1→S transition and reappears later in S-phase. GcrA accumulates during the G1→S transition, inducing the synthesis of CtrA along with polarity and cell cycle proteins.

The synthesis of early flagellar structural constituents, including the FliF MS-ring protein and two components of the switch complex (FliG and FliM), is induced by CtrA late in S-phase. The newly synthesized flagellar

parts are assembled from the inside of the cell outward, first with an organizational platform in the inner membrane (the MS-ring) from to which the switch complex on the cytoplasmic side of the membrane is tethered. The assembly of subsequent structures follows suit, ultimately ending with the elaboration of the external parts such as the hook and the flagellar filament (see. Fig. 3F).

Superimposed on these temporal patterns, are spatial cues that guide flagellar proteins to the appropriate site of assembly at the new cell pole opposite the stalk. The new cell pole is marked by TipN a polytopic coiled coil protein that is pre-positioned at this site when the new poles emerge from cytokinesis (Fig. 1)(Huitema, Pritchard, Matteson, Radhakrishnan, & Viollier, 2006; Lam, Schofield, & Jacobs-Wagner, 2006). At cytokinesis, TipN is recruited to the division plane from the poles, a redistribution that ensures that cell polarity cues are available for the flagellar polarization in the next cell cycle. Indeed, flagella are mispositioned in the absence of *tipN* mutants, indicating that TipN is required for the proper placement, but not the assembly, of the flagellum(Huitema et al., 2006; Lam et al., 2006). A flagellar misplacement defect has also been observed in mutants lacking the PflI positioning factor, a bitopic membrane proteins with a proline-rich domain at the C-terminus facing the cytoplasm that is localized to the future flagellated pole before the synthesis of early flagellar components. While the spatial relationship between TipN and PflI remains unexplored, TipN recruits TipF, a polytopic membrane protein that positively, regulates for flagellum biogenesis (Huitema et al., 2006). In the absence of TipN, TipF localizes to sites of misplaced flagella raising the possibility that mislocalized TipF is responsible

for the flagellar misplacement phenotype of a *tipN* mutant. This is supported by the observation that *tipF* deletion mutants lack external flagellar structures such as the hook and filament (Huitema et al., 2006).

TipF features C-terminal EAL domain facing the cytoplasm which in other related proteins confers c-di-GMP specific phosphodiesterase activity (Christen, Christen, Folcher, Schauerte, & Jenal, 2005). C-di-GMP is a ubiquitous bacterial second messenger that promotes an adhesive, surface-grown multi-cellular state called biofilm, while its absence favors the motile adventurous single cell state. C-di-GMP levels are regulated by the antagonistic enzymatic activities of diguanylate cyclases (DGC) and phosphodiesterases (PDE). DGCs harbor a catalytically active GGDEF domain that promotes the condensation of two GTP molecules into c-di-GMP. In contrast, EAL or HD-GYP domain catalyze the asymmetric hydrolysis of c-di-GMP into linear pGpG (Christen et al., 2005; Schirmer & Jenal, 2009). In *C. crescentus* multiple DGCs and PDEs modulates c-di-GMP levels during the cell cycle to promote development and cell cycle progression (Abel et al., 2011; R. Paul et al., 2008; R. Paul, Weiser, Amiot, & Chan, 2004). Whereas G1 swarmer cells contain low levels of c-di-GMP, levels quickly increase during G1→S transition (R. Paul et al., 2008). Then, at cell division c-di-GMP levels diminish in the flagellated G1 (swarmer) chamber, while being maintained in the stalked compartment (Christen et al., 2010).

The observation that TipF localizes to the site of flagellar assembly at the new cell pole together with the finding that a *tipF* mutant fails to assemble a complete flagellar structure, argued that TipF may act as a phosphodiesterase locally at the newborn pole to promote flagellar

assembly(Huitema et al., 2006). A role for TipF as PDE at the site of flagellum assembly would be in line with the general consensus that high levels of c-di-GMP inhibit flagellar-based motility through different possible mechanisms(Boehm et al., 2010; Wolfe & Visick, 2008). Here we explore the spatiotemporal relationship of c-di-GMP and TipF in polar flagellum biogenesis during the *Caulobacter* cell cycle.

RESULTS

c-di-GMP binds to and activates TipF at the newborn pole

To dissect the mechanism and function of TipF at the newborn pole, we first considered the several unusual sequence features in TipF compared to c-di-GMP -specific phosphodiesterase (PDE) belonging to the same family. For example, TipF features a Lys at position 332 instead of an Asp in related proteins (Fig. 1D). Moreover, a Glu-Ser-Phe (ESF, residues 211-213) triplet replaces the defining Glu-Ala-Leu (EAL) motif normally found in related PDEs. To explore whether the sequence conservation reflects a functional requirement for the residues at these positions, we engineered alanine mutations at several conserved positions implicated in coordinating the cofactor (Mg^{2+} or Mn^{2+}), the substrate or the nucleophile (E211A, D331A and K352A, filled triangles in Fig. 1D). Neither of these mutant proteins could support TipF function (motility on 0.3% soft agar plates) when expressed in a $\Delta tipF$ background from P_{xyI} on a low copy plasmid, indicating that all of these residues play a key role in TipF function (Fig. 1E).

To test if TipF is an active PDE, we purified soluble, hexa-histidine tagged forms of TipF wild type and TipF(E211A) mutant. Both proteins were truncated variants lacking the first 110 amino acids, which include the two predicted trans-membrane domains. Circular dichroism (CD) spectra suggested that the secondary structures of purified TipF wild type and E211A mutant were unchanged (Fig. S1A). We next assayed PDE activity of both proteins by HPLC analysis using c-di-GMP as substrate (Fig. 2A). No cleavage of c-di-GMP to the linear pGpG was observed with either TipF wild type or the E211A mutant (Fig. 2A, right panel), even after extended incubation times of up to 24 h (Fig. S1B, 1C). By contrast, control PDE YahA from *E. coli* converted all of the c-di-GMP to pGpG in less than 5 min (Fig. 2A left panel).

In the absence of detectable PDE activity, we asked if TipF wild type or the E211A mutant can bind c-di-GMP using an iso-thermal calorimetry (ITC)-based binding assay (Fig. 2B). Successive injections of 10 μ L of a 118 μ M solution of c-di-GMP into the ITC reaction chamber containing 32.5 μ M of WT TipF was accompanied with the characteristic heat release indicating specific and high affinity binding of c-di-GMP (Fig. 2B, left panel). The resulting integrated titration peaks were fitted to a sigmoidal enthalpy curve and a dissociation constant (K_D) of 0.4 (+/- 0.2 μ M) between WT TipF and c-di-GMP was derived. By contrast, only background (non-specific) heat release was observed when an equimolar amount of TipF(E211A) was in the chamber (Fig. 2B, middle panel, note the different scales in the panels). Together, these results demonstrate that TipF is not a PDE and that while TipF wild type binds c-di-GMP with high affinity, the E211A mutant is unable to bind the

ligand. On the basis of these results we hypothesize that c-di-GMP binding is necessary for TipF to signal motility and that TipF(E211A) is non-functional because it fails to bind c-di-GMP and, in response, is not activated. In support of this view, we show below that depleting *Caulobacter* cells of c-di-GMP by overexpression of PA5295, a potent heterologous PDE from *Pseudomonas aeruginosa*, phenocopies the localization and flagellar assembly defect caused by the absence of TipF or the “c-di-GMP-blind” E211A mutant (see Fig. 5E, 5F).

If TipF is activated without hydrolysing c-di-GMP, then analogous mutations that are known to specifically cripple catalytic activity of PDEs (without interfering with c-di-GMP binding) should still retain function. To test this prediction, we engineered mutants Q197A, R215L and E396A (Fig. 1D, open triangles) and found the mutant proteins R215L and E396A to confer motility in $\Delta tipF$ cells indistinguishable from that of WT TipF, while Q197A could also support motility albeit with reduced efficiency (data not shown).

On the basis of these genetic and biochemical experiments, we conclude that TipF is a c-di-GMP binding protein and signals motility function(s) upon binding of the second messenger.

TipF cues the polar assembly of the flagellar base.

How TipF cues motility is not well understood. Transmission electron micrographs previously suggested that TipF signals the construction of the polar flagellum, or at least the external structures, since the flagellar hook and the filament (Fig. 3F) are absent from $\Delta tipF$ cells (Huitema et al., 2006). Moreover, live-cell fluorescence imaging in wild type (WT) and $\Delta tipF$ mutant

cells expressing a derivative of the FliG switch (C-ring) protein (Fig. 3F) harboring a carboxy (C-) terminal fusion to GFP (FliG-GFP) in addition to the endogenous FliG, showed that localization of FliG-GFP to the new pole depends on TipF (Fig. 3C, S2A). To demonstrate that TipF promotes the formation of the switch structure at the cell pole, we conducted live cell imaging of the FliM switch protein (Fig. 3A, 3F) harboring a C-terminal moiety to GFP (FliM-GFP) that was expressed from P_{van} on a plasmid. By analogy to other flagellar systems, FliG is predicted to interact with FliM and to tether the switch to the MS-ring base plate in the inner membrane. Our finding that FliM-GFP is diffuse in the cytoplasm of $\Delta fliG$ cells, but sequestered to the flagellated pole in WT cells, is consistent with this notion (Fig. 3A). Next, we imaged FliM-GFP in $tipF^+$ and $\Delta tipF$ cells that carry the $fliM::Tn5$ mutation (to avoid interference from untagged, endogenous FliM) and observed diffuse fluorescence in $\Delta tipF$ cells, akin to that of $\Delta fliG$ cells. By contrast, in $tipF^+$ cells FliM-GFP was properly localized at the newborn pole opposite the stalk. Thus, consistent with the dependence of polar localization of FliM on FliG, when FliG localization is compromised in $\Delta tipF$ cells, FliM is also unable to localize in the absence of TipF.

Since two switch proteins (FliG and FliM) are no longer polarized in the absence of TipF, we investigated if this is also the case for the MS-ring protein FliF. The MS-ring is the earliest known flagellar structure to assemble and tethers the switch complex to the cytoplasmic membrane. Similar to the situation for FliG-GFP, only few polar foci were seen when FliF-GFP was expressed in $\Delta tipF$ cells, arguing that neither the MS-ring, nor the switch complex assemble in $\Delta tipF$ cells (Fig. 3C, 3D, S2A and S2B). By contrast,

FliF-GFP and FliG-GFP show normal polar localization when expressed in $\Delta fliF$ and $\Delta fliG$ cells, respectively (Fig. S2A and S2B). Together this argued that TipF promoted polar clustering of FliG independent of FliF. To bolster this finding using an independent imaging approach, we conducted high-resolution analysis of WT and $\Delta tipF$ poles by electron cryo-tomography (ECT) (Fig. 3E, S2C and S2D) in which intracellular structures that are preserved in their native (cryogenically vitrified) state are visualized *in situ* by virtue of their natural contrast (electron density). Whole-cell imaging of WT and $\Delta tipF$ cells followed by structural refinement using segmentation algorithms of 2D projections from 3D tomograms revealed densities of the MS-ring and switch at the cytoplasmic membrane of WT poles, but no such structures at $\Delta tipF$ poles. As expected, flagellar (sub)structures traversing the OM and S-layer reflecting regions of the rod, P- and L-rings and the hook emanated from the poles of WT cells. These structures were also absent from $\Delta tipF$ cells. However, chemoreceptor arrays that normally assemble at the same pole and at the same time as the flagellum, but via a flagellum-independent pathway, were seen in the $\Delta tipF$ mutant pole thus confirming that the site was imaged where a flagellum should have been (Fig. 3E, right panel).

The important role of TipF in the formation of the MS-ring and switch was further corroborated using strains in which FliG is tethered to FliF by way of FliF-FliG translational fusion (i.e. within single polypeptide) encoded within the endogenous *fliF* locus. This fully functional FliG-FliF fusion protein (Jenal & Shapiro, 1996) could not direct FliM-GFP into polar clusters in the absence of TipF, indicating that TipF function is beyond merely facilitating the recruitment of FliG to the membrane via FliF and that TipF stimulates polar clustering of

FliG (data not shown). In support of this conclusion, polar clusters of FliG, although dependent on TipF, still formed in $\Delta fliF$ cells (Fig. S2A). Moreover, below we show that TipF interacts directly with FliG in a yeast-two-hybrid assay.

Taken together, these experiments support the conclusion that the formation of the polar MS- and C-rings is cued by TipF and that TipF possibly acts at the earliest known (nucleation) step in flagellum biogenesis, switch and MS-ring formation, respectively.

The PflI flagellar positioning factor is recruited into a polar complex by TipF

In addition to the structural components of the flagellum, a polarly localized ancillary protein, PflI, was recently identified that is required for proper positioning of the flagellum. PflI, a bitopic membrane protein with a proline-rich C-terminal domain facing the cytoplasm, is expressed and recruited to the future flagellum assembly site before most flagellar proteins (Obuchowski, 2008). How PflI is localized to the newborn pole is unclear, but it does not require the MS-ring protein FliF. We uncovered three lines of evidence that prompted us to explore whether PflI localization was dependent on TipF. First, we observed that TipF synthesis precedes that of FliF and other flagellar proteins whose expression is activated by the CtrA master transcriptional regulator (see Fig. 7F). Second, we noted that, similar to PflI, FliF is also dispensable for the polar sequestration of TipF (data not shown). Finally, we found that mCherry tagged TipF (TipF-mCherry) expressed from the endogenous *tipF* locus in lieu of untagged TipF co-

localizes with PflI-GFP expressed from P_{van} on a plasmid (Fig. 1C). Moreover, since $\Delta tipF$ cells (unlike $\Delta pflI$ cells) are aflagellate, we wondered if TipF recruits PflI to the pole. To test this possibility, we expressed PflI variants harboring a C-terminal fusion to YFP or GFP either from its own promoter at the native chromosomal locus or from a plasmid in $\Delta pflI$ cells and imaged in the wild type or $\Delta tipF$ context. While the expected polar foci of PflI-YFP (and PflI-GFP) were readily seen in $tipF^+$ cells, only dispersed fluorescence from PflI-YFP or PflI-GFP was seen in the envelope of $\Delta tipF$ cells (Fig. 3B and S3A). Conversely, PflI does not noticeably affect TipF localization, as indicated by the apparent normal localization of TipF-GFP (expressed in lieu of endogenous TipF from the $tipF$ locus) in $\Delta pflI$ compared to WT cells (Fig. S3B).

To identify which region of PflI is required for TipF-dependent localization, we imaged mutant PflI-GFP derivatives lacking either the trans-membrane domain [PflI($\Delta 4-28$)], the coiled-coil region [PflI($\Delta 28-92$)] or one of two adjacent stretches in the proline-rich region [PflI($\Delta 93-142$) or PflI($\Delta 142-194$)] expressed from P_{van} on a plasmid in $\Delta pflI$ cells (Fig. S3C). While the deletion of the coiled-coil domain had no dramatic effect of PflI localization, deletion of the trans-membrane domain or the proline-rich region strongly interfered with polar sequestration. PflI lacking the proline-rich region is distributed in the membrane, as is the case for full-length PflI-GFP expressed in the absence of TipF, suggesting that TipF recruits PflI to the newborn pole, directly or indirectly, via the proline-rich domain.

Since TipF is recruited to this site by the TipN landmark protein (Fig. S3B), we predicted that PflI localization should also be dependent on TipN.

Indeed, PflI-YFP or PflI-GFP foci are mispositioned near or within the stalk in $\Delta tipN$ cells, a pattern resembling the misplacement of TipF-GFP in the absence of TipN (Fig. 3B and S3A). The formation of these (mislocalized) PflI foci in $\Delta tipN$ cells is still TipF-dependent as indicated by the fact that upon introducing a $\Delta tipF$ mutation into $\Delta tipN$ cells, PflI-GFP adopts a disperse disposition in the envelope (Fig. S3A). Conversely the $\Delta pflI$ mutation does not seem to change the mislocalization of TipF-GFP in $\Delta tipN$ cells (Fig. S3B). Thus, flagellar assembly and recruitment events at the newborn pole proceed in the order: TipN > TipF > [(PflI)(FliF/G/M)].

To test if this localization dependency is reflected in physical interactions among the proteins, we conducted pull-down experiments from extracts derived of cells harboring an empty vector control or a plasmid expressing either a TipF or PflI derivative with a C-terminal TAP (Tandem Affinity Purification) tag from the P_{van} promoter. Owing to the instability of TipF (described below), we conducted the pull-down experiments in mutant backgrounds ($\Delta tipN$ and $fliB::Tn5$, when appropriate) in which TipF abundance is increased (Fig. 4A). This likely results from a post-transcriptional mechanism as $tipF$ transcription is unchanged in a $tipN$ and $fliB$ mutant (Fig. S4A). Immunoblotting of TipF-TAP and PflI-TAP pull-down samples with antibodies to PflI (Fig. 4B) or TipF (Fig. 4C) provided evidence that TipF and PflI interact (directly or indirectly), albeit the interaction seems relatively weak. By contrast, co-immunoprecipitation of PflI with TipF-GFP using monoclonal antibodies to GFP was more efficient (Fig. S4B). We conclude that PflI resides in a complex with TipF. To investigate if TipF and PflI also associate with TipN, we probed blots containing the TipF-TAP (Fig.

4D) and PflI-TAP (Fig. 4E) pull-down samples with polyclonal antibodies to TipN and detected TipN in these samples as well, but not in the control samples. Thus, TipF and PflI also interact with TipN.

Lastly, in an attempt to identify TipF client proteins in an unbiased fashion, we conducted a yeast-two-hybrid screen with soluble TipF (lacking trans-membrane segments, residues 1-90 aa) as bait to probe a genomic prey library of *C. crescentus*. The screen was conducted in a yeast strain that ectopically expressed the diguanylate cyclase YdeH from *E. coli*, thereby mimicking a c-di-GMP containing environment. When selecting for interaction of bait and prey by scoring for growth in the absence of adenine, we identified two positive clones encoding Gal4-AD fusions to two C-terminal fragments of FliG (FliG_C), residues 192-340 and residues 236-340 (Fig. 4F).

In sum, we conclude that TipF interacts directly with FliG_C and recruits PflI into a flagellar positioning complex with TipN at the newborn pole.

c-di-GMP signals TipF localization and activation

Having established that polar localization of PflI and flagellar assembly are regulated by the c-di-GMP-receptor TipF, we investigated if c-di-GMP is required for TipF function. To this end, we first asked if TipF(E211A) that is unable to bind c-di-GMP and cannot support motility, can promote the polar localization of PflI. As shown in Fig. 6A, neither the E211A derivative, nor the D331A or K352A mutants were able to tag PflI to the cell pole. Furthermore, the E211A mutation phenocopied flagellar assembly defect of the $\Delta tipF$ deletion as reflected in a failure to express the FlgE hook protein (Fig. 3F, 5F).

If TipF signaling is triggered by binding of c-di-GMP, then cells depleted for c-di-GMP should also be unable to localize PflI and to express the FigE hook protein similar to $\Delta tipF$ or $tipF(E211A)$ mutant cells. To test this prediction, we heterologously expressed the potent *P. aeruginosa* PDE PA5295 (Duerig, Nicollier, Schwede, & Amiot, 2009) in strains carrying the *pflI-yfp* reporter and imaged the resulting cells. PA5295, but not the catalytically inactive mutant PA5295-AAL [carrying an analogous mutation to TipF(E211A) at position E328], was previously shown to reduce c-di-GMP levels beyond detection (Duerig et al., 2009). We found that induction of PA5295 caused the dispersion of PflI-YFP from the pole into the envelope and prevented FigE expression, akin to $\Delta tipF$ or $tipF(E211A)$ mutant cells (Fig. 5A). Interestingly, however, c-di-GMP depletion has a much stronger effect on transcription of the *flgE* gene than the $\Delta tipF$ or $tipF(E211A)$ mutation, indicating that c-di-GMP modulates another step of flagellum biogenesis independently of TipF (see below).

Next, we explored if c-di-GMP depletion also affects TipF-GFP or TipN-GFP localization. As shown in Fig. 5B, 5C TipF was completely delocalized from the poles upon c-di-GMP-depletion, while TipN localization was only weakly affected. Thus, c-di-GMP promotes TipF localization and activity. If so, then a mutation in TipF that prevents c-di-GMP binding and activity, such as TipF(E211A), should be unable to localize when c-di-GMP is present. Live-cell fluorescence imaging confirmed that TipF(E211A)-GFP is delocalized when expressed from P_{xyI} promoter on a plasmid in $\Delta tipF$ cells (Fig. 6B). Next, we also determined the subcellular localization of the other TipF mutants and found TipF(D331A)-GFP to be dispersed and TipF(K352A)-GFP to cluster at

the stalked pole but not at the newborn pole (Fig. 6B). Thus, these mutations interfere with c-di-GMP binding or structural changes that are induced by c-di-GMP to prevent TipF and PflI from localizing to the newborn pole and inducing flagellar assembly at this site.

Bypassing the requirement of c-di-GMP for TipF signaling

To illuminate how c-di-GMP activates TipF and induces its polar localization, we isolated intragenic suppressor mutations that restore motility to *tipF(E211A)* or *tipF(D331A)* cells. These suppressor mutations are either missense mutations in two proximal residues (F280S or F284L) within the c-di-GMP-binding (EAL) domain or a duplications of a triplet amino acid (either ADA or DTV, residues 121-124 or 128-130, respectively) within the coiled-coil motif in front of the EAL-domain (Fig. 1B, 1E). Importantly, the two missense mutations were isolated irrespective of the genetic background, i.e. *tipF(E211A)* or *tipF(D331A)*. Since F280S and F284L are not allele-specific suppressors, we suspected that they would both also be able to overcome the localization defect of D331A and E211A by driving the proteins from dispersion into an active and polarized state. C-terminal fusions of GFP to the four TipF double mutants (E211A/F280S, E211A/F284L, D331A/F280S and D331A/F284L) revealed that these proteins indeed regained the capacity to cluster at the pole and to recruit PflI-YFP to polar sites (Fig. 6C, D).

Next, we tested if these TipF double mutants were able to resist delocalization induced by depletion of c-di-GMP. In the presence of c-di-GMP, WT TipF-YFP and the two E211A double mutant derivatives (E211A/F280S and E211A/F284L) were all polar (Fig. S5A). By contrast, depletion of c-di-

GMP delocalizes WT TipF-YFP, while polar foci of the E211A/F280S and E211A/F284L derivatives persisted (Fig. 5D). In support of the conclusion that the E211A/F280S and E211A/F284L mutants are active and localized in the absence of the signal induced by c-di-GMP, we found that the E211A/F284L mutant protein, like the E211A single mutant, is unable to bind or hydrolyze c-di-GMP *in vitro* (Fig. 2A, B), although its secondary structure is conserved (Fig. S1).

To test if these c-di-GMP-bypass mutants confer motility in the absence of c-di-GMP, we determined the FlgE steady-state levels (cell-associated and the shed hook accumulating in the supernatant) in WT and *tipF* single and double mutant cells by immunoblotting (Fig. 5F). These experiments showed that FlgE levels are reduced in c-di-GMP-depleted cells, even in the presence of the E211A/F280S and E211A/F284L TipF versions. This effect seems to be mediated by a second, c-di-GMP-dependent event that acts on *flgE* transcription, as indicated by the reduction of β -galactosidase activity from the P_{flgE} -*lacZ* transcriptional reporter to $30\pm 1\%$ (E211A/F280S) and $30\pm 1\%$ (E211A/F284L) compared to WT, much below that observed in the $\Delta tipF$ single mutant ($57\pm 1\%$) (Fig. 5E). Consistent with the conclusion that at least one additional c-di-GMP-dependent event exists that controls the assembly and possibly the placement of the flagellum, expression of the hook gene as monitored using P_{flgE} -*lacZ* activity is further reduced to 21% when c-di-GMP is depleted in $\Delta tipF$ cells. A similar c-di-GMP-dependent effect was seen on transcription of the *fliL* flagellin gene, using the P_{fliL} -*lacZ* transcriptional reporter (Fig. S5B). In this case, however, c-di-GMP-depletion reduced *fliL*

transcription in $\Delta tipF$ cells from near full WT levels (*fliL* transcription is not affected by $\Delta tipF$ mutation) to $32\pm 2\%$.

We conclude that TipF localization is at least partially uncoupled from c-di-GMP in two suppressor mutants and that c-di-GMP controls, in addition to the TipF branch, at least one more pathway in flagellum assembly.

TipF cell cycle abundance is tightly regulated and dependent on c-di-GMP

Immunoblotting experiments using polyclonal antibodies to TipF raised the possibility that the TipF protein is stabilized upon binding to c-di-GMP. The abundance of wild type TipF expressed from P_{xyI} (i.e. using the transcriptional and translational regulatory signals of the *xyIX* gene) in $\Delta tipF$ cells is significantly higher than those of the TipF(E211A) mutant variant under the same conditions (Fig. 5F), suggesting that TipF is regulated at the level of stability by c-di-GMP. Indeed stability measurements of wild type TipF and TipF(E211A) under normal (Fig. 7B, D) or c-di-GMP depleted (Fig. 7A, C) conditions (using PA5295 as described above) approximated the half-life of WT TipF at a level of more than 2 hours in the presence of c-di-GMP and below 20 min in its absence. By contrast, for TipF(E211A) we determined half-life values of about 10-20 min irrespective of the presence or absence of c-di-GMP, demonstrating that TipF(E211A) is not significantly destabilized upon c-di-GMP depletion (Fig. 7A, C). Remarkably, the half-life of E211A/F284L (~40 min) was higher than that of TipF(E211A) but lower than that of WT TipF. Again, the stability of this mutant was largely insensitive to the presence or absence of c-di-GMP, consistent with the robust polarization of

TipF(E211A/F284L) even in the absence of c-di-GMP (see above). Thus, in the absence c-di-GMP TipF is unable to bind c-di-GMP and adopt an active conformation, it is delocalized from the cell pole and, at the same time is destabilized. These events can be uncoupled from c-di-GMP with a mutation of F284L, which not only activates the TipF(E211A) mutant form constitutively, but at the same time protects it from proteolysis *in vivo*.

In search for a candidate protease that destabilizes TipF *in vivo*, we found that ClpX, the ATP-dependent chaperone component of the ClpXP protease, controls the cell cycle-dependent accumulation of endogenous (untagged) TipF expressed from its native chromosomal location. Poisoning ClpXP activity by expression of a dominant negative (catalytically inactive) ClpX variant (ClpX*)(Osterås, Stotz, Schmid Nuoffer, & Jenal, 1999) from P_{xyI}, results in TipF accumulation. Immunoblotting revealed TipF to be absent from G1-phase (swarmer) cells, induced during the G1-S transition (40 min) and again destabilized at the time of division (Fig. 7F). Blocking ClpX function using the *clpX** allele, resulted in TipF accumulation in G1 cells, presumably owing to a failure to degrade TipF in the swarmer progeny (Fig. 7E). Together with the observation that TipF stability critically depends on the presence of c-di-GMP, this strongly argued that TipF is rapidly degraded in the swarmer progeny as a result of a drop in c-di-GMP levels in this cell type(Christen et al., 2010).

As a result of the ClpXP-mediated elimination of TipF in G1 swarmer cells, TipF accumulation is dictated primarily by the time of its synthesis. Since the cell cycle pattern of TipF resembles that of GcrA, a master transcriptional regulator that activates transcription of a myriad of cell cycle-

regulated genes at the G1-S transition and is itself induced at this time, we hypothesized that GcrA induces the expression of TipF at the G1-S transition. In support of this idea, previous mRNA profiling experiments using DNA microarrays showed that *tipF* mRNA levels diminish when GcrA is depleted (Holtzendorff et al., 2004). Probing a P_{tipF} -*lacZ* transcriptional reporter in a GcrA-depletion strain (Fig. 7G), we found that *tipF* promoter activity depends on GcrA. Moreover, quantitative chromatin-immunoprecipitation (qChIP) analysis using polyclonal antibodies to GcrA showed that GcrA binds to the *tipF* promoter (Fig. 7H). The induction of TipF expression at the transcriptional level by GcrA and the concordant surge in c-di-GMP levels at the G1-S transition ensure that TipF is active and ready to prime flagellum biosynthesis at the newborn pole, while a drop in c-di-GMP in the incipient G1 daughter cells results in the removal of TipF, thus resetting flagellar polarity cascade.

DISCUSSION

With the coordinated induction of TipF and c-di-GMP at the G1→S transition, a robust polarized pathway for flagellum biogenesis is launched and simultaneously tuned to other c-di-GMP dependent differentiation events, including stalk biogenesis and the removal of the replication inhibitor/transcriptional activator CtrA. The implementation, the robust propagation and then the sudden re-setting of polarity during the cell cycle is a hallmark of bacterial, fungal and metazoan model systems, but the

underlying signals and mechanisms are not well understood, let alone in bacterial systems.

The c-di-GMP mechanisms unearthed here illustrate how during a primitive bacterial cell cycle, flagellar polarity is first signaled and implemented, and then ultimately re-set. At least three sequential mechanisms are involved and mediated by distinct effectors: TipN, c-di-GMP and ClpXP. The first mechanism, active during the late stages of constriction at the end of the preceding cell cycle, involves the deposition of the TipN landmark signal at the newborn pole to allow the correct interpretation of the polarity axis in the progeny. This ensures that the subsequent events, triggered by c-di-GMP at the G1→S, are executed at the correct (newborn) pole (Fig. 1A).

The second mechanism involves a double selection by two parallel “AND” gates (the “GcrA-gate” and “c-di-GMP-gate”) that must be met for TipF-dependent implementation of flagellar polarity to proceed. The GcrA-gate (Fig. 1A) licenses TipF expression with the induction of the transcriptional regulator GcrA that activates transcription of genes encoding polarity (PodJ, controls pilus assembly), development (PleC, regulates CtrA), division (MipZ, inhibits the FtsZ tubulin) and cell cycle (HU, nucleoid organizing protein) determinants, along with *tipF*. While the accumulation of GcrA seems to be coupled to the initiation of chromosome replication via the DnaA replication initiator protein (Collier, McAdams, & Shapiro, 2007) and is thus under a cell cycle cue, other unknown mechanism may help enforce this gate to promote the fluctuation of GcrA. With the synthesis of TipF, the surge of c-di-GMP at the G1→S (Christen et al., 2010; R. Paul et al., 2008) directly induces the

activation and subsequent recruitment of TipF and its client proteins to the newborn (TipN-marked) pole to promote flagellum assembly (the “c-di-GMP-gate”).

The third mechanism is discernable and involves the onset of a diminution in TipF levels during cytokinesis, when flagellar biogenesis is completed and the flagellum is energized. While it is unclear if the ClpXP protease regulates TipF stability as function of the cell cycle as for many of its substrates, ClpX activity is required to prevent the ectopic accumulation of TipF in the G1 progeny cell. Under conditions that preclude binding of c-di-GMP by TipF, either by mutation of the c-di-GMP binding site in TipF or by depletion of c-di-GMP from cells, polar localization is prevented and TipF is quickly turned over. The levels of c-di-GMP are rapidly depleted during compartmentalization in the G1 (swarmer) progeny, while they are maintained in the S (stalked) progeny. Therefore, a critical role can be attributed to this c-di-GMP reduction in the ClpX-dependent removal of TipF in the G1 progeny and, thus, in re-setting flagellar polarity for the G1 cell.

The diminution of c-di-GMP in compartmentalized G1 cells is governed by the PleC histidine kinase/phosphatase that is sequestered to the flagellar pole and partitions exclusively with the G1 progeny to de-activate the PleD response regulator with its c-di-GMP-synthase (GGDEF) output domain by de-phosphorylation (R. Paul et al., 2008). The resulting trough in c-di-GMP should disperse TipF from the pole and induce proteolytic removal, thereby terminating flagellar assembly. This event is coordinated with the onset of flagellar rotation regulated by the DgrA/B PilZ-domain proteins, paralogous c-di-GMP receptor proteins that prevent precocious activation of flagellar

rotation in the presence of bound c-di-GMP (Christen et al., 2007). The PleC-dependent reduction in c-di-GMP levels in the motile G1 progeny, is thought to release the inhibition of flagellar rotation by DgrA/B. PleC not only de-phosphorylates the PleD c-di-GMP synthase/response regulator, but also the DivK single domain response regulator, a cell fate determinant that promotes the transcriptional activation of G1-phase genes by CtrA (perhaps reinforced by other factors) (Biondi et al., 2006) and the accumulation of the swarmer cell specific c-di-GMP phosphodiesterase PdeA (Abel et al., 2011). Thus, the removal of TipF that clears the flagellar polarization pathway coincides with the implementation of the G1 transcriptional landscape by CtrA and with a reduction of c-di-GMP levels that directly promotes motor function in this cell type. By contrast, the transcriptional re-programming by GcrA and the resulting induction of TipF at the onset of S-phase thus reinstates the c-di-GMP-dependent flagellar polarity with the coincident activation of the PleD-kinase DivJ.

An imbalance in c-di-GMP abundance in the two progeny cells also occurs in the compartmentalized *Pseudomonas aeruginosa* pre-divisional cell. Interestingly, the FimX EAL-GGDEF hybrid protein of *P. aeruginosa* that promotes the assembly of retracting Type IV (polar) pili (Tfp) for twitching motility shares biochemical and cytological properties with TipF. FimX is a polarized EAL domain protein that can influence the positioning of Tfp (Kazmierczak, Lebron, & Murray, 2006; Navarro, De, Bae, Wang, & Sondermann, 2009). It also binds c-di-GMP and this causes a (long-range) conformational change in the adjacent domain (Qi et al., 2011). How FimX scouts the pole, how it signals Tfp assembly and how its localization is

coordinated with cell cycle progression is unknown. Our *tipF* suppressor genetics points to a functional relationship between triplet duplications in the coiled-coil motif and missense mutations in the EAL domain. Helical wheel analysis predicts the alpha-helicity to be maintained by the insertion, while causing a shift of the hydrophobic region that could cause structural reorganization presumed to underlying the functional modifications of TipF and interactions with its flagellar and polarity targets.

Within the flagellar polarization cascades TipF bears perhaps the most functional resemblance to the FlhF GTPase studied in *vibrios*, *pseudomonads* and *Campylobacter jejuni*. FlhF is itself polarized and recruits the MS-ring protein FliF to the polar site of flagellation in *V. cholera* (Correa et al., 2005; Kusumoto et al., 2006; Pandza et al., 2000). However, despite the pervasive polar flagellation found across most bacterial lineages, the principal target of FlhF in polar flagellation and the underlying temporal relationships are unknown. By contrast, TipF associates with PflI, TipN and the flagellar switch protein FliG. The soluble portion of TipF (encompassing the predicted coiled-coil and EAL domains) interacts directly with the C-terminal portion of FliG. FliG is emerging as an important regulatory hub for diverse modes of motility control. EpsE of *Bacillus subtilis* and YcgR of *E. coli/Salmonella enterica* are thought to arrest flagellar rotation by disengaging or curbing the flagellar motor (Blair, Turner, Winkelman, Berg, & Kearns, 2008; Boehm et al., 2010; K. Paul, Nieto, Carlquist, Blair, & Harshey, 2010). Moreover, the nucleoid binding protein H-NS and the enzyme fumarate reductase (FRD) bind to FliG, perhaps to regulate motility in response to metabolic fluctuations or to maintain the homeostasis of motility with chromosome organization or

environmental conditions that H-NS responds to (K. Paul, Brunstetter, Titen, & Blair, 2011). With the important role of FliG switch protein in regulating the direction of rotation of the flagellum it is perhaps not surprising that the aforementioned FliG-binding proteins regulate rotation. However, because of its central role early in flagellar erection, assembly regulators that act on FliG might also be expected. TipF is the first representative of this class with a function(s) that may go beyond regulating FliG. In fact, polar sequestration of FliG and FliF is independent of each other but strongly affected by TipF. Our evidence that another, TipF-independent, but c-di-GMP dependent flagellar assembly step exists (Fig. 5E-F) provides another example of the unexpected regulatory complexity in flagellar assembly. As established from seminal work in other systems, flagellation is fine-tuned through external signals. As shown here, this pathway also ingrates information from pre-existing spatial landmarks for polar c-di-GMP-mediated signals that are periodically removed and re-established, thus reinforcing small nucleotide polarization pulses that drive morphogenesis at key times in the bacterial cell cycle.

Material and Methods

Strains, plasmids, and media

The bacterial strains and plasmid used in this study are listed in Table S1. *Caulobacter crescentus* strains were grown in peptone yeast extract (PYE, Ely, 1991) or in minimal media supplemented with 0.2% glucose or 0.3% D-xylose (M2G or M2X, Ely, 1991) at 30°C with constant shaking (150 rpm). When selection was required antibiotics in the following concentrations were added: (solid/liquid media in µg/ml): gentamycin (5/0.5), kanamycin (20/5), nalidixic acid (20/not used) and oxytetracycline (5/2.5). For inducible gene expression the medium was supplemented with 1 mM vanillate, 0.3% xylose or 1 mM IPTG. For synchronization experiments newborn swarmer cells were isolated by Ludox gradient centrifugation (Jenal, 1996) and released into fresh minimal medium. For synchronization with inducible constructs, 1 mM vanillate was added to the growth medium 2 h prior synchrony.

E. coli strains were grown in Luria Broth (LB) at 37 °C. When necessary for selection the following antibiotic concentrations were used: (solid/liquid media in µg/ml) ampicillin (100/50), gentamycin (20/15), kanamycin (50/30) and oxytetracycline (12.5/12.5).

Microscopy

DIC and fluorescence microscopy were performed on a DeltaVision Core (Applied Precision, USA)/Olympus IX71 microscope equipped with an UPlanSApo 100x/1.40 Oil objective (Olympus, Japan) and a coolSNAP HQ-2 (Photometrics, USA) CCD camera. Cells were placed on a patch consisting of 1% agarose in water (Sigma, USA). Images were processed using ImageJ software (NIH, USA) or Photoshop CS3 (Adobe, USA) software. Bacteria cell and protein localization signals were analyzed with MicrobeTracker (V0.931) and MATLAB software. Cryo-electron Tomography

was performed as described in (Kudryashev, Cyrklaff, Wallich, Baumeister, & Frischknecht, 2010).

Protein purification

Rosetta BL21pLysS *E.coli* strain was transformed with respective plasmids and used for protein overexpression. Cultures with an optical density at 600nm of 0.4 were induced with 1mM isopropyl-b-D-thiogalactopyranoside (IPTG) and incubated for 4h at RT with constant shaking, cells were collected by centrifugation. The cell pellets were resuspended in buffer consisting of 20mM Tris-HCl pH7, 250mM NaCl, 5mM imidazole, 10mM MgCl₂, 1% glycerol and Complete mini cocktail of protease inhibitors, EDTA free at the concentrations specified by the manufacturer (Roche). The cells were lysed using French press, and the crude extracts were centrifuged at 15,000g for 40 min at 4⁰C. The cleared lysates were incubated with preequillibrated Profinity IMAC Ni-resin (Bio-Rad) for 1h at 4⁰C and washed subsequently with lysis buffer and washing buffer containing 20 mM imidazole. The proteins were eluted using 350mM imidazole.

Phosphodiesterase Assay

TipF_{WT}, TipF_{E211A} and TipF_{E211A/F284L}, were tested for c-di-GMP phosphodiesterase activity. As a control YahA, a class A phosphodiesterase from *E. coli* was used. 10mM final concentration of each protein was incubated with 100mM c-di-GMP in 50mM Tris-HCl pH8, 50mM NaCl, 5mM MgCl₂, 1mM DTT at RT. Samples were taken at time points 0, 1h, 2h and overnight. The reactions were stopped by heating at 99⁰C for 5 min, diluted with 5mM NH₄HCO₃ pH8 buffer, filtered (0.22mm), and analyzed on a Resource Q ion-exchange chromatography column (GE Healthcare).

Circular Dichroism Spectroscopy.

Circular dichroism (CD) measurements were performed with an AVIV 26A DS spectropolarimeter. Spectra were recorded at room temperature from 250 to 190 nm, with a resolution of 1.0 nm, response time of 3 s, bandwidth of 1 nm and 3 accumulations. CD samples were prepared by adjusting the protein concentration to 30 μ M in 50 mM Tris buffer at pH 8. A control spectrum of pure buffer solution was subtracted from all samples.

Isothermal titration calorimetry

The interaction of TipF with cyclic-di-GMP was measured with a VP-ITC isothermal titration calorimeter from MicroCal (Northampton, MA). Four different experiments were performed with three different protein batches measured under the same conditions (50 mM Tris/HCl, 50 mM NaCl, pH 8.0 at 25°C). All integrated titration peaks produced sigmoidal enthalpy curves for the interaction between TipF and cyclic di-GMP. The average dissociation constant, K_D , was 0.4 (+/- 0.2 mM), the stoichiometry of binding, n , was 0.35 (+/- 0.1) and the enthalpy of reaction was -2.1 (+/- 0.3 kcal/mol). Two additional experiment were performed at 35°C, the average dissociation constant, K_D , was 0.3 (+/- 0.1 mM), the stoichiometry of binding, n , was 0.3 (+/- 0.02) and the enthalpy of binding, ΔH^0 , was -4.75 (+/- 0.25) kcal/mol. All solutions were degassed and equilibrated at desired temperature before using. The delay between the injections was set to 5 min to ensure re-equilibration between injections. Data were evaluated using Origin software (OriginLab) provided by Microcal (Northampton, MA). TipF_{E211A} and TipF_{E211A/F284L} binding experiments were contacted under the above-specified conditions.

Motility Assays

The spontaneous, non-allele specific *tipF* suppressor mutants were obtained by plating 2.5µl of an overnight culture of PV1928 (P_{xyI} -*tipF*(E211A)); PV2152 (P_{xyI} -*tipF*(D331A)); and PV2151 (P_{xyI} -*tipF*(K352A)) to 0.3% PYE swarm agar supplemented with Tetracycline (1µg/ml). The plates were incubated for seven days after which spontaneous motile colonies developed. The plasmids were isolated, sequenced, and shown to contain the initial primary mutation (E211A, D331A, or K352A) and an additional second-site mutation within the *tipF* coiled-coil or EAL domains.

Yeast two-hybrid analysis

Yeast two hybrid screen was performed using the system described in. The EAL domain of TipF fused to the Gal4-DBD (DNA binding domain) was expressed in *Saccharomyces cerevisiae* PJ69-4A from plasmid pGBD Kan^R. YdeH, an active DGC that produces c-di-GMP, was expressed in the same strain from plasmid p426-cm-YdeH or the empty plasmid p426. For screening, a *C. crescentus* library was transformed into the strain containing the before mentioned plasmids. The library contains *C. crescentus* genomic DNA fragments between 500 to 3000 bp, obtained after partial digest of genomic DNA using the enzymes HinPIL, MspI and Taq1, fused to the *gal4-AD* (activator domain) in three reading frames (J. Luciano). Transformants were screened on SD medium lacking leucine, tryptophan, uracil and either adenine or histidine. Prey-plasmids of positive clones were isolated and retransformed in PJ69-4A containing the Gal4-DBD-TipF-EAL or the Gal4-DBD. Interaction strength and self-activity were tested with these strains on

selective medium to check for the activation of reporter genes. Inserts of confirmed interactors were sequenced to ensure in-frame coding sequence with the Gal4-AD.

References

- Abel, S., Chien, P., Wassmann, P., Schirmer, T., Kaefer, V., Laub, M. T., Baker, T. A., et al. (2011). Regulatory Cohesion of Cell Cycle and Cell Differentiation through Interlinked Phosphorylation and Second Messenger Networks. *Molecular Cell*, *43*(4), 550–560. doi:10.1016/j.molcel.2011.07.018
- Biondi, E. G., Reisinger, S. J., Skerker, J. M., Arif, M., Perchuk, B. S., Ryan, K. R., & Laub, M. T. (2006). Regulation of the bacterial cell cycle by an integrated genetic circuit. *Nature*, *444*(7121), 899–904. doi:10.1038/nature05321
- Blair, K. M., Turner, L., Winkelman, J. T., Berg, H. C., & Kearns, D. B. (2008). A molecular clutch disables flagella in the *Bacillus subtilis* biofilm. *Science*, *320*(5883), 1636–8. doi:10.1126/science.1157877
- Boehm, A., Kaiser, M., Li, H., Spangler, C., Kasper, C. A., Ackermann, M., Kaefer, V., et al. (2010). Second messenger-mediated adjustment of bacterial swimming velocity. *Cell*, *141*(1), 107–16. doi:10.1016/j.cell.2010.01.018
- Christen, M., Christen, B., Allan, M. G., Folcher, M., Jenö, P., Grzesiek, S., & Jenal, U. (2007). DgrA is a member of a new family of cyclic diguanosine monophosphate receptors and controls flagellar motor function in *Caulobacter crescentus*. *Proceedings of the National Academy of Sciences of the United States of America*, *104*(10), 4112–7. doi:10.1073/pnas.0607738104
- Christen, M., Christen, B., Folcher, M., Schauerte, A., & Jenal, U. (2005). Identification and characterization of a cyclic di-GMP-specific phosphodiesterase and its allosteric control by GTP. *The Journal of biological chemistry*, *280*(35), 30829–37. doi:10.1074/jbc.M504429200
- Christen, M., Kulasekara, H. D., Christen, B., Kulasekara, B. R., Hoffman, L. R., & Miller, S. I. (2010). Asymmetrical distribution of the second messenger c-di-GMP upon bacterial cell division. *Science (New York, N.Y.)*, *328*(5983), 1295–7. doi:10.1126/science.1188658
- Collier, J., McAdams, H. H., & Shapiro, L. (2007). A DNA methylation ratchet governs progression through a bacterial cell cycle. *Proceedings of the National Academy of Sciences of the United States of America*, *104*(43), 17111–6. doi:10.1073/pnas.0708112104
- Correa, N. E., Peng, F., Klose, K. E., Correa, N. E., Peng, F., & Klose, K. E. (2005). Roles of the Regulatory Proteins FlhF and FlhG in the *Vibrio cholerae* Flagellar Transcription Hierarchy Roles of the Regulatory Proteins FlhF and FlhG in the *Vibrio cholerae* Flagellar Transcription Hierarchy, *187*(18). doi:10.1128/JB.187.18.6324
- Duerig, A., Nicollier, M., Schwede, T., & Amiot, N. (2009). Second messenger-mediated spatiotemporal control of protein degradation regulates bacterial cell cycle progression. *Genes & Development*, *23*(1), 93. doi:10.1101/gad.502409.tion

- Holtzendorff, J., Hung, D., Brende, P., Reisenauer, A., Viollier, P. H., McAdams, H. H., & Shapiro, L. (2004). Oscillating global regulators control the genetic circuit driving a bacterial cell cycle. *Science (New York, N. Y.)*, *304*(5673), 983–7. doi:10.1126/science.1095191
- Huitema, E., Pritchard, S., Matteson, D., Radhakrishnan, S. K., & Viollier, P. H. (2006). Bacterial birth scar proteins mark future flagellum assembly site. *Cell*, *124*(5), 1025–37. doi:10.1016/j.cell.2006.01.019
- Jenal, U., & Shapiro, L. (1996). Cell cycle-controlled proteolysis of a flagellar motor protein that is asymmetrically distributed in the *Caulobacter* predivisional cell. *The EMBO journal*, *15*(10), 2393–406.
- Kazmierczak, B. I., Lebron, M. B., & Murray, T. S. (2006). Analysis of FimX, a phosphodiesterase that governs twitching motility in *Pseudomonas aeruginosa*. *Molecular microbiology*, *60*(4), 1026–43. doi:10.1111/j.1365-2958.2006.05156.x
- Kudryashev, M., Cyrklaff, M., Wallich, R., Baumeister, W., & Frischknecht, F. (2010). Distinct in situ structures of the *Borrelia* flagellar motor. *Journal of Structural Biology*, *169*(1), 54–61. doi:10.1016/j.jsb.2009.08.008
- Kusumoto, A., Kamisaka, K., Yakushi, T., Terashima, H., Shinohara, A., & Homma, M. (2006). Regulation of polar flagellar number by the *flhF* and *flhG* genes in *Vibrio alginolyticus*. *Journal of biochemistry*, *139*(1), 113–21. doi:10.1093/jb/mvj010
- Lam, H., Schofield, W. B., & Jacobs-Wagner, C. (2006). A landmark protein essential for establishing and perpetuating the polarity of a bacterial cell. *Cell*, *124*(5), 1011–23. doi:10.1016/j.cell.2005.12.040
- Navarro, M. V. A. S., De, N., Bae, N., Wang, Q., & Sondermann, H. (2009). Structural analysis of the GGDEF-EAL domain-containing c-di-GMP receptor FimX. *Structure (London, England : 1993)*, *17*(8), 1104–16. doi:10.1016/j.str.2009.06.010
- Obuchowski, P. (2008). PflI, a protein involved in flagellar positioning in *Caulobacter crescentus*. *Journal of bacteriology*, *190*(5), 1718–29. doi:10.1128/JB.01706-07
- Osterås, M., Stotz, a, Schmid Nuoffer, S., & Jenal, U. (1999). Identification and transcriptional control of the genes encoding the *Caulobacter crescentus* ClpXP protease. *Journal of bacteriology*, *181*(10), 3039–50.
- Pandza, S., Baetens, M., Park, C. H., Au, T., Keyhan, M., & Matin, a. (2000). The G-protein FlhF has a role in polar flagellar placement and general stress response induction in *Pseudomonas putida*. *Molecular microbiology*, *36*(2), 414–23.
- Paul, K., Brunstetter, D., Titen, S., & Blair, D. F. (2011). A molecular mechanism of direction switching in the flagellar motor of *Escherichia coli*. *Proceedings of the National Academy of Sciences of the United States of America*, *108*(41), 17171–6. doi:10.1073/pnas.1110111108
- Paul, K., Nieto, V., Carlquist, W. C., Blair, D. F., & Harshey, R. M. (2010). The c-di-GMP binding protein YcgR controls flagellar motor direction and speed to affect chemotaxis by a “backstop brake” mechanism. *Molecular cell*, *38*(1), 128–39. doi:10.1016/j.molcel.2010.03.001
- Paul, R., Jaeger, T., Abel, S., Wiederkehr, I., Folcher, M., Biondi, E. G., Laub, M. T., et al. (2008). Allosteric regulation of histidine kinases by their cognate response regulator determines cell fate. *Cell*, *133*(3), 452–61. doi:10.1016/j.cell.2008.02.045

- Paul, R., Weiser, S., Amiot, N., & Chan, C. (2004). Cell cycle-dependent dynamic localization of a bacterial response regulator with a novel diguanylate cyclase output domain. *Genes & Dev*, 18(6), 715–727. doi:10.1101/gad.289504.
- Qi, Y., Chuah, M. L. C., Dong, X., Xie, K., Luo, Z., Tang, K., & Liang, Z.-X. (2011). Binding of cyclic diguanylate in the non-catalytic EAL domain of FimX induces a long-range conformational change. *The Journal of biological chemistry*, 286(4), 2910–7. doi:10.1074/jbc.M110.196220
- Schirmer, T., & Jenal, U. (2009). Structural and mechanistic determinants of c-di-GMP signalling. *Nature reviews. Microbiology*, 7(10), 724–35. doi:10.1038/nrmicro2203
- Slaughter, B. D., Smith, S. E., & Li, R. (2009). Symmetry breaking in the life cycle of the budding yeast. *Cold Spring Harbor perspectives in biology*, 1(3), a003384. doi:10.1101/cshperspect.a003384
- Wolfe, A. J., & Visick, K. L. (2008). Get the message out: cyclic-Di-GMP regulates multiple levels of flagellum-based motility. *Journal of bacteriology*, 190(2), 463–75. doi:10.1128/JB.01418-07

Table S1 Strains and Plasmids

Strains

Name	Genotype / Description	Source or Reference
NA1000	CB15N Laboratory strain derived from CB15	Evinger and Agabian, 1977
UJ3638	NA1000 $\Delta tipF$ Markerless in frame deletion of <i>tipF</i>	Huitema et al., 2006
UJ3635	NA1000 $\Delta tipN$ Markerless in frame deletion of <i>tipN</i>	Huitema et al., 2006
PV2025	NA1000 $\Delta tipF$ P _{xyI} - <i>tipF</i>	This Study
PV1928	NA1000 $\Delta tipF$ P _{xyI} - <i>tipFE211A</i>	This Study
PV2152	NA1000 $\Delta tipF$ P _{xyI} - <i>tipFD331A</i>	This Study
PV2151	NA1000 $\Delta tipF$ P _{xyI} - <i>tipFK352A</i>	This Study
ND562	NA1000 $\Delta tipF$ P _{xyI} - <i>tipFE211A/F280S</i>	This Study
ND568	NA1000 $\Delta tipF$ P _{xyI} - <i>tipFE211A/F284L</i>	This Study

ND570	NA1000 $\Delta tipF$ P_{xyI} - <i>tipFD331A/F280S</i>	This Study
ND564	NA1000 $\Delta tipF$ P_{xyI} - <i>tipFD331A/F284L</i>	This Study
ND280	NA1000 $\Delta tipF$ P_{xyI} - <i>tipFF280S</i>	This Study
ND283	NA1000 $\Delta tipF$ + P_{xyI} - <i>tipFF284L</i>	This Study
ND284	NA1000 $\Delta tipF$ + P_{xyI} - <i>tipFADA insert</i> ¹²⁸⁻¹³⁰	This Study
ND282	NA1000 $\Delta tipF$ + P_{xyI} - <i>tipFDTV insert</i> ¹²¹⁻¹²⁴	This Study
ND562	NA1000 P_{van} - <i>tipFE211A/F280S-sEGFP</i>	This Study
ND564	NA1000 P_{van} - <i>tipFD331A/F284L-sEGFP</i>	This Study
ND568	NA1000 P_{van} - <i>tipFE211A/F284L-sEGFP</i>	This Study
ND570	NA1000 P_{van} - <i>tipFD331A/F280S-sEGFP</i>	This Study
ND319	NA1000 $\Delta pflI$ P_{van} - <i>pflI-GFP</i>	This Study
ND424	NA1000 $\Delta tipF\Delta pflI$ P_{van} - <i>pflI-GFP</i>	This Study
ND342	NA1000 $\Delta tipN\Delta pflI$ P_{van} - <i>pflI-GFP</i>	This Study
ND480	NA1000 $\Delta tipN\Delta tipF\Delta pflI$ P_{van} - <i>pflI-GFP</i>	This Study
ND607	NA1000 $\Delta tipF$ P_{van} - <i>fliM-sEGFP</i>	This Study
ND611	NA1000 <i>fliM::Tn5</i> P_{van} - <i>fliM-sEGFP</i>	This Study
ND572	NA1000 $\Delta pflI$ <i>tipF-gfp</i>	This Study

ND573	NA1000 $\Delta tipN \Delta pflil tipF-gfp$	This Study
NR1760	NA1000 $\Delta tipN tipF-gfp$	This Study
ND316	NA1000 $\Delta pflI P_{van-pflI}^{\Delta 4-28}-GFP$	This Study
ND317	NA1000 $\Delta pflI P_{van-pflI}^{\Delta 28-92}-GFP$	This Study
ND318	NA1000 $\Delta pflI P_{van-pflI}^{\Delta 93-142}-GFP$	This Study
ND558	NA1000 $\Delta pflI P_{van-pflI}^{\Delta 142-194}-GFP$	This Study
ND588	NA1000:: <i>tipN-gfp</i> $P_{van-PA5295}$	This Study
ND589	NA1000:: <i>tipN-gfp</i> $P_{van-PA5295AAL}$	This Study
ND590	NA1000:: <i>pflI-venus</i> $P_{van-PA5295}$	This Study
ND591	NA1000:: <i>pflI-venus</i> $P_{van-PA5295AAL}$	This Study
ND578	NA1000:: <i>tipF-gfp</i> $P_{van-PA5295}$	This Study
ND579	NA1000:: <i>tipF-gfp</i> $P_{van-PA5295AAL}$	This Study
ND762	NA1000 <i>pflgE-lacZ/290</i> $P_{xyl-PA5295AAL}$	This Study
ND787	NA1000 <i>pflgE-lacZ/290</i> $P_{xyl-PA5295}$	This Study
ND831	NA1000 $\Delta tipF pflgE-lacZ/290 P_{xyl-PA5295AAL}$	This Study
ND751	NA1000 $\Delta tipF pflgE-lacZ/290 P_{xyl-PA5295}$	This Study
ND839	NA1000 $\Delta tipF vanA::P_{van-tipF-venus pflgE-lacZ/290 P_{xyl-PA5295AAL}$	This Study

ND837	NA1000 $\Delta tipF$ vanA::P _{van} -tipF-venus pflgE-lacZ/290 P _{xyI} -PA5295	This Study
ND843	NA1000 $\Delta tipF$;vanA::P _{van} -tipFE211AF280S-venus pflgE-lacZ/290 P _{xyI} -PA5295AAL	This Study
ND841	NA1000 $\Delta tipF$;vanA::P _{van} -tipFE211AF280S-venus pflgE-lacZ/290 P _{xyI} -PA5295	This Study
ND835	NA1000 $\Delta tipF$;vanA::P _{van} -tipFE211AF284L-venus pflgE-lacZ/290 P _{xyI} -PA5295AAL	This Study
ND833	NA1000 $\Delta tipF$;vanA::P _{van} -tipFE211AF284L-venus pflgE-lacZ/290 P _{xyI} -PA5295	This Study
ND749	NA1000 pfljL-lacZ/290 P _{xyI} -PA5295AAL	This Study
ND777	NA1000 pfljL-lacZ/290 P _{xyI} -PA5295	This Study
ND796	NA1000 $\Delta tipF$ pfljL-lacZ/290 P _{xyI} -PA5295AAL	This Study
ND811	NA1000 $\Delta tipF$ pfljL-lacZ/290 P _{xyI} -PA5295	This Study
ND804	NA1000 $\Delta tipF$;vanA::P _{van} -tipF-venus pfljL-lacZ/290 P _{xyI} -PA5295AAL	This Study
ND802	NA1000 $\Delta tipF$;vanA::P _{van} -tipF-venus pfljL-lacZ/290 P _{xyI} -PA5295	This Study
ND808	NA1000 $\Delta tipF$;vanA::P _{van} -tipFE211AF284L-venus pfljL-lacZ/290 P _{xyI} -PA5295AAL	This Study
ND806	NA1000 $\Delta tipF$;vanA::P _{van} -tipFE211AF280S-venus pfljL-lacZ/290 P _{xyI} -PA5295)	This Study
ND800	NA1000 $\Delta tipF$;vanA::P _{van} -tipFE211AF284L-venus pfljL-lacZ/290 P _{xyI} -PA5295AAL)	This Study
ND798	NA1000 $\Delta tipF$;vanA::P _{van} -tipFE211AF284L-venus pfljL-lacZ/290 P _{xyI} -PA5295).	This Study
UJ6287	NA1000 $\Delta tipF$ P _{van} - PA5295 P _{xyI} -tipF	This Study
UJ6288	NA1000 $\Delta tipF$ P _{van} - PA5295 P _{xyI} -tipFE211A	This Study

UJ6289	NA1000 $\Delta tipF$ P _{van} ⁻ PA5295 P _{xyI} ⁻ tipFE211AF284L	This Study
UJ6292	NA1000 $\Delta tipF$ P _{van} ⁻ PA5295AAL P _{xyI} ⁻ tipF	This Study
UJ6293	NA1000 $\Delta tipF$ P _{van} ⁻ PA5295AAL P _{xyI} ⁻ tipFE211A	This Study
UJ6294	NA1000 $\Delta tipF$ P _{van} ⁻ PA5295 AAL P _{xyI} ⁻ tipFE211AF284L	This Study
UJ 1793	NA1000 $\Delta fliF$ Markerless in frame deletion of <i>fliF</i>	Jenal et al., 1996
LS 2356	NA1000 $\Delta fliG$ Markerless in frame deletion of <i>fliG</i>	Jenal
ND306	NA1000 $\Delta pflI$ Markerless in frame deletion of <i>pflI</i>	This Study
ND359	NA1000 $\Delta tipF \Delta pflI$ Markerless in frame deletion of <i>pflI</i> and <i>tipF</i>	This Study
ND454	NA1000 $\Delta tipN \Delta tipF \Delta pflI$ Markerless in frame deletion of <i>pflI</i> , <i>tipN</i> and <i>tipF</i>	This Study
UJ413	NA1000 <i>fliM</i> ::Tn5 Tn5 insertion in <i>fliM</i>	P. Aldridge
UJ 284	NA1000 $\Delta pleD$	P. Aldridge
UJ5292	pJ69-4A trp1-901 leu2-3,112 ura3-52 his3-200 GAL4 $\Delta GAL80 \Delta LYS2::GAL1-HIS3 GAL2-ADE2$ met2::GAL7-lacZ	James et al., 1996
UJ5649	pJ69-4A UJ5292 containing pGBD-tipF-kan, p426-TEF-ydeH-cm	Jutta Nesper
UJ5646	UJ5292 containing pGBD-tipF-kan, p426-TEF-cm	Jutta Nesper
UJ200	Disruption of the <i>clpX</i> gene by a Strep/SpecR cassette and integration of <i>clpX</i> at the <i>xyI</i> locus in NA1000	Jenal and Fuchs, 1998

Plasmids

Name	Description	Source
PCWR208	pLac290 P _{xyI} - <i>tipF</i>	Huitema et al., 2006
PCWR239	pLac290 P _{xyI} - <i>tipFE211A</i>	Huitema et al., 2006
PCWR261	pLac290 P _{xyI} - <i>tipFD331A</i>	This Study
PCWR262	pLac290 P _{xyI} - <i>tipFK352A</i>	This Study
pND100	pLac290 P _{xyI} - <i>tipFF280S</i>	This Study
pND101	pLac290 P _{xyI} - <i>tipFF284L</i>	This Study
pND102	pLac290 P _{xyI} - <i>tipFADA</i> ²⁸⁻¹³⁰	This Study
pND103	pLac290 P _{xyI} - <i>tipFDTV</i> ¹²¹⁻¹²⁴	This Study
pND85	pLac290 P _{xyI} - <i>tipFE211A/F280S</i>	This Study
pND86	pLac290 P _{xyI} - <i>tipFE211A/F284L</i>	This Study
pND87	pLac290 P _{xyI} - <i>tipFD331A/F280S</i>	This Study
pND88	pLac290 P _{xyI} - <i>tipFD331A/F284L</i>	This Study
pND72	PCWR512 P _{van} - <i>pflI</i> -CTAP	This Study
pND71	PCWR512 P _{van} - <i>tipF</i> -CTAP	This Study
pND75	PCWR512 P _{van} - <i>tipFE211AF284L</i> -CTAP	This Study
pND56	pOK12 Δ <i>pflI</i> ⁴⁻²⁸	This Study
pND57	pOK12 Δ <i>pflI</i> ²⁸⁻⁹²	This Study
pND58	pOK12 Δ <i>pflI</i> ⁹²⁻¹⁴²	This Study
pND59	pOK12 Δ <i>pflI</i> ¹⁴²⁻¹⁹⁴	This Study
pND77	pMT384 P _{van} - <i>pflI</i> - <i>sEGFP</i>	This Study
pND78	pMT384 P _{van} - <i>tipF</i> - <i>sEGFP</i>	This Study
UJ 6444	pET21 p _{lac} ::His ₆ <i>tipF</i> ₁₁₀₋₄₅₂	This Study
UJ 6450	pET21 p _{lac} ::His ₆ <i>tipF</i> ₁₁₀₋₄₅₂ E211A	This Study
UJ 6445	pET21 p _{lac} ::His ₆ <i>tipF</i> ₁₁₀₋₄₅₂ E211A/F284L	This Study
PV1928	pCRW P _{xyI} - <i>tipFE211A</i>	This Study
PV2152	pCRW P _{xyI} - <i>tipFD331A</i>	This Study
PV2151	pCRW P _{xyI} - <i>tipFK352A</i>	This Study
SoA226	pXGFP4 P _{xyI} - <i>fliF</i> - <i>GFP</i>	Soren Abel
pCRW71	pCRW P _{xyI} - <i>fliG</i> - <i>GFP</i>	Huitema et al., 2006
UJ 6287	pRV P _{van} - <i>PA5295</i>	This Study
UJ 6292	pRV P _{van} - <i>PA5295</i> _{AAL}	This Study

pND95	<i>P_{van}-tipFE211A/F280S-sEGFP</i>	This Study
pND96	<i>P_{van}-tipFD331A/F284L-sEGFP</i>	This Study
pND97	<i>P_{van}-tipFE211A/F284L-sEGFP</i>	This Study
pND98	<i>P_{van}-tipFD331A/F280S-sEGFP</i>	This Study

Figure Legends:**Fig.1. Localization of TipN, TipF and PflI to the flagellated pole (A)**

Dynamic protein localization of TipN, TipF and PflI and its coordination with other cell cycle events in *C. crescentus*. TipN (green) localized at the non-flagellated pole recruits newly synthesized TipF (red), which in turn recruits the PflI flagellar positioning protein (yellow). (B) Domain organization of TipN, TipF and PflI. Shown are the predicted transmembrane domains (TM, gray), coiled coil domains (CC, black), and the phosphodiesterase domain (EAL, red) and the proline-rich domain (PR, yellow). (C) TipF and PflI co-localize. The localization of TipF-mCherry and PflI-GFP was analyzed using live-cell fluorescence microscopy in wild-type (WT) cells expressing TipF-mCherry in place of TipF from the *tipF* locus and PflI-GFP from the P_{van} promoter on the medium copy number plasmid, pCWR510. (D) Alignment of the EAL domains from TipF and the c-di-GMP phosphodiesterases CC3396 of *C. crescentus*, VieA of *Vibrio cholerae*, RocR of *Pseudomonas aeruginosa* and Ykul of *Bacillus subtilis*. Key residues that are predicted to be required for phosphodiesterase activity (empty arrowheads) or required for c-di-GMP binding (filled black) are marked. In addition, the residues are indicated that bypass the requirement of E211 or D331 for motility (red triangles), the defining EAL motif and the K332 residue where Asp is normally present (underlined). (E) Motility assay of $\Delta tipF$ mutants harboring plasmids encoding WT, single or double mutant TipF. (DTV)₂ and (ADA)₂ denote the triple duplications of DTV or ADA residues at positions 121-124 or 128-130, respectively. Overnight cultures were spotted on PYE swarm (0.3% soft) agar

plates and incubated for 60 hr at 30°C. Compact swarms indicate the motility defect caused by mutations in the c-di-GMP binding site whereas the suppressive mutations yield diffuse and enlarged swarms.

Fig. 2. TipF is enzymatically inactive but binds c-di-GMP. (A) No c-di-GMP hydrolytic activity is detected in recombinant (soluble) TipF, but in the control PDE YahA. One mM of purified proteins was incubated with c-di-GMP and incubated for 5min and then separated on a ResourceQ column to observe the cleavage product pGpG (left panel). No pGpG was detected after 1 h of incubation with WT or mutant (E211A or E211A/F284L) TipF with c-di-GMP. (B) Isothermal titration calorimetry experiments showing that c-di-GMP binds to the soluble portion of WT TipF, but not to the mutant derivatives E211A or E211A/F284L. The top panels show the raw ITC data curves collected at 25°C in binding buffer (50 mM Tris/HCl, 50 mM NaCl, pH 8.0). The bottom panels show the integrated titration peaks fitted to a one-site binding model (solid line). The average dissociation constant (K_D) of the EAL domain of TipF was estimated at 0.4 (+/- 0.2 μ M), the stoichiometry of binding (n) to 0.35 (+/- 0.1) and the enthalpy of reaction to -2.1 (+/- 0.3 kcal/mol).

Fig. 3. TipF mediates the localization of flagellar proteins FliM, FliG, FliH and PflI to the cell pole. (A) The subcellular localization of FliM-GFP from the P_{van} promoter on a medium copy number plasmid in a *fliM* mutant (*fliM*::Tn5), in a *tipF* mutant ($\Delta tipF$; *fliM*::Tn5) or in a *fliG* mutant ($\Delta fliG$; *fliM*::Tn5) analyzed by live-cell fluorescence microscopy. (B) Localization of PflI-YFP expressed from P_{pflI} at the *pflI* locus in the presence (*pflI-yfp*) or the

absence of TipF ($\Delta tipF$; *pflI-yfp*) or TipN ($\Delta tipN$; *pflI-yfp*). (C, D) Localization of GFP-fusions to the flagellar proteins FliG (C, FliG-GFP) and FliF (D, FliF-GFP) expressed from P_{xyl} at the *xylX* locus in a $\Delta tipF$ mutant. (E) Electron cryo-tomography imaging reveals densities corresponding to the intact flagellum including the MS-ring and the switch complex in or near the inner membrane (IM) of the WT, which are absent in the $\Delta tipF$ mutant. The color-coding of the segmented structures corresponds to the color scheme in (F). Flagellar structures are shown in red in the left panel. The white arrow in the right panel denotes the chemoreceptor arrays. (F) Schematic of the flagellum. The relative position of the MS-ring (FliF), the switch complex (including FliG and FliM), the hook (FlgE) and the filament (flagellins) are indicated, as are the envelope layers: inner (cytoplasmic) membrane (IM), peptidoglycan layer (PG), outer membrane (OM) and S-layer (SL).

Fig. 4. TipF directly interacts with FliG and forms a complex with TipN and PflI. (A) TipF steady-state levels as determined by immunoblotting using polyclonal antibodies to antibodies in lysates from wild-type, $\Delta tipF$, $\Delta tipN$ and *flbD::Tn5*. (B-E) Tandem Affinity Purification (TAP) pull-down of TAP-tagged proteins expressed from P_{van} on a medium copy plasmid, followed by immunoblotting using polyclonal to TipF, PflI, TipN and CtrA. The cell lysates derived from boiled cells shown in the lanes on the left of the panels provide negative and positive controls for the specificity for the antisera. CtrA immunoblots are shown as a control for loading. (B) TipF-TAP and TipF*-TAP (the E211A/F284L mutant is referred to as TipF*) were expressed from the P_{van} promoter on a medium copy number plasmid in $\Delta tipN$ mutants. (C) TipF

is present in PflI-TAP purifications $\Delta tipN \Delta pflI$ double mutant lysates. M, protein marker lane. (D, E) TipN is present in pull-downs of TipF-TAP (D) or PflI-TAP (E) from *flbD::Tn5* lysates. (F) The C-terminus of FliG and the soluble part of TipF interact directly in a yeast two-hybrid (Y2H) assay. Yeast strains that harbor plasmids encoding a C-terminal fragment of FliG(192-340) fused to the GAL4 activation domain (AD) and TipF fused to the GAL4 DNA binding domain (DBD) or the DBD alone were tested for growth on selective media as indicated. The screen was conducted in a yeast strain that ectopically expressed the diguanylate cyclase YdeH from *E. coli*, thereby mimicking a c-di-GMP containing environment. Conditions that promote or inhibit growth are schematically represented (lower panel). The black (branched) arrow denotes promoter activation and thus growth, whereas the grey arrow indicates that the promoter does not fire efficiently and cannot support growth on selective media.

Fig. 5. Localization of TipF and PflI as well as expression of FlgE is c-di-GMP dependent

(A-D) Localization of PflI-YFP (A), TipF-GFP (B), TipN-GFP (C), and YFP tagged TipF-suppressor mutants (D) under normal (PA5295-AAL, +cdG) or c-di-GMP depleted conditions (PA5295-WT, -cdG). PA5295 variants were expressed the P_{xyI} promoter on a medium copy number plasmid in cells expressing the GFP fusion proteins from their respective promoters at the endogenous locus. In (D) TipF-YFP variants were expressed from P_{van} at the *vanA* locus in $\Delta tipF$ cells. (E) Effects of c-di-GMP concentration on transcription of the *flgE* hook gene by b-galactosidase assays of cells (WT,

$\Delta tipF$ or $\Delta tipF$ cells expressing mutant TipF from P_{van} at the *vanA* locus) harboring a P_{flgE} -*lacZ* transcriptional reporter fusion. (F) Effects of c-di-GMP depletion on FlgE steady-state levels in supernatants (Sup.) or cell lysates (Lys.) by immunoblotting using anti-FlgE antibody (α -FlgE). TipF mutants were expressed from the P_{xyl} promoter on a low copy-number plasmid in $\Delta tipF$ cells.

Fig. 6. Suppressor mutations render TipF and PflI localization c-di-GMP independent.

(A-D) Localization of PflI-YFP (A, C) or TipF-GFP mutants (B, D) in $\Delta tipF$ cells harboring plasmids encoding TipF loss of function mutants expressed from the P_{xyl} (A, C) or the P_{van} (B, D) promoter a low copy-number plasmid.

Fig. 7. C-di-GMP levels affect TipF protein stability.

(A - D) Depletion of c-di-GMP by over-expression of a potent PDE reduces TipF steady-state levels. TipF, the c-di-GMP binding mutant E211A or the intragenic suppressor mutant E211A/F284L were expressed from P_{xyl} on a low copy-number plasmid in $\Delta tipF$ cells grown in M2G containing xylose, following a shift to M2G containing vanillate to induce the expression of the PDE PA5295 from *P. aeruginosa* or its active site mutant PA5295-AAL and repress P_{xyl} . Samples were taken every 20 min and protein levels were quantified from the immunoblots and plotted as percentages of the highest value (A and B). The corresponding immunoblots, probed with an anti-TipF polyclonal antiserum, show the levels of the TipF variants during a period of 140 min after vanillate induction (C and D). (E) The dominant negative *clpX*_{ATP}

allele was expressed from plasmid in M2G containing xylose or repressed by growing the cells in M2G. Swarmer cells were isolated and TipF was detected using an anti-TipF antibody and ClpX^{ATP*}::Flag using M2 antibodies. In the presence of WT ClpXP, TipF was not detectable while inactivation of ClpXP by the dominant negative allele encoding ClpX^{ATP*} led to stabilization of TipF. (F) The cell-cycle abundance of TipF resembles that of GcrA. Synchronized WT swarmer cells were followed throughout the cell cycle. CtrA, TipF and GcrA protein levels were determined by immunoblotting using specific polyclonal antisera. (G) GcrA activates *tipF* transcription. The activity of a P_{tipF} -*lacZ* transcriptional reporter was assayed in WT and in a strain (P_{xyf} -*gcrA*) in which GcrA expression is repressible by glucose in the absence of xylose. (H) GcrA binds to the *tipF* promoter as determined by quantitative chromatin-immunoprecipitation (qChIP) experiments using polyclonal antibodies to GcrA. The abundance of the *tipF* and *sciP* promoters was quantified in the immunoprecipitates.

Fig. S1. Secondary structure and activity of WT and mutant. TipF(A) Circular dichroism (CD) spectra of WT, E211A and E211A/F284L TipF. All spectra show the characteristic behavior associated with secondary structures, indicating that the purified proteins are folded. (B and C) FPLC chromatograms showing the lack of phosphodiesterase activity of WT, E211A and E211A/F284L TipF even after 24h.

Fig. S2. TipF promotes FlIF and FlIG localization. The localization pattern

of (A) FilF-GFP or (B) FliG-GFP expressed from P_{xyI} at the *xyIX* locus in WT, $\Delta tipF$, $\Delta fliG$ and $\Delta fliF$ background. The relative positioning along the cell axis and number of foci were quantified. (C) Electron cryotomography image slices revealing the absence of flagellar structure in the $\Delta tipF$ mutant, whereas (D) flagella structures are clearly visible in WT cell poles.

Fig. S3. PflI localization determinants. Live-cell fluorescence microscopy images showing the localization of (A) PflI-GFP expressed from P_{van} on a medium-copy plasmid in $\Delta pflI$, $\Delta pflI \Delta tipF$, and $\Delta pflI \Delta tipF \Delta tipN$ background and (B) the localization TipF-GFP expressed from the endogenous promoter at the *tipF* locus in WT, $\Delta pflI$, $\Delta tipN$, and $\Delta tipN \Delta pflI$ background. (C) Localization of PflI-GFP derivatives harboring a deletion in the transmembrane domain [PflI($\Delta 4-28$)], the coiled-coil region [PflI($\Delta 28-92$)] or one of two adjacent stretches in the proline-rich region [PflI($\Delta 93-142$)] or PflI($\Delta 142-194$)] expressed from P_{van} on a plasmid in $\Delta pflI$ cells.

Fig. S4. Transcription of *tipF* and co-immunoprecipitation PflI with TipF-GFP. (A) $P_{tipF-lacZ}$ activity assayed in WT, $\Delta tipN$, *flbD::Tn5* strains. (B) Co-immunoprecipitation experiment with TipF-GFP expressed from the endogenous promoter at the *tipF* locus. TipF-GFP was precipitated with monoclonal anti-GFP antibodies, the precipitates were then probed for the presence of PflI by immunoblotting using polyclonal antibodies to PflI. The cell lysate lanes from boiled cells shown on the left of the panels provide negative and positive controls for the specificity for the antisera. CtrA

immunoblots are shown as a control for loading. Input designates the solubilized lysates that were used for the immunoprecipitation.

Fig. S5. Effect of TipF suppressor mutations on TipF localization and *fljL* transcription. (A) TipF-YFP variants were expressed from P_{van} at the *vanA* locus in $\Delta tipF$ cells and PA5295-AAL was expressed from the P_{xyI} promoter on a medium copy number plasmid. (B) Effects of c-di-GMP concentration on transcription of the flagellin gene *fljL*. The promoter of *fljL* was fused to *lacZ* and b-galactosidase activity was measured in WT, $\Delta tipF$ or $\Delta tipF$ cells expressing mutant TipF from P_{van} at the *vanA* locus under normal (PA5295-AAL, +cdG) or c-di-GMP depleted conditions (PA5295-WT, -cdG).

Fig. 1

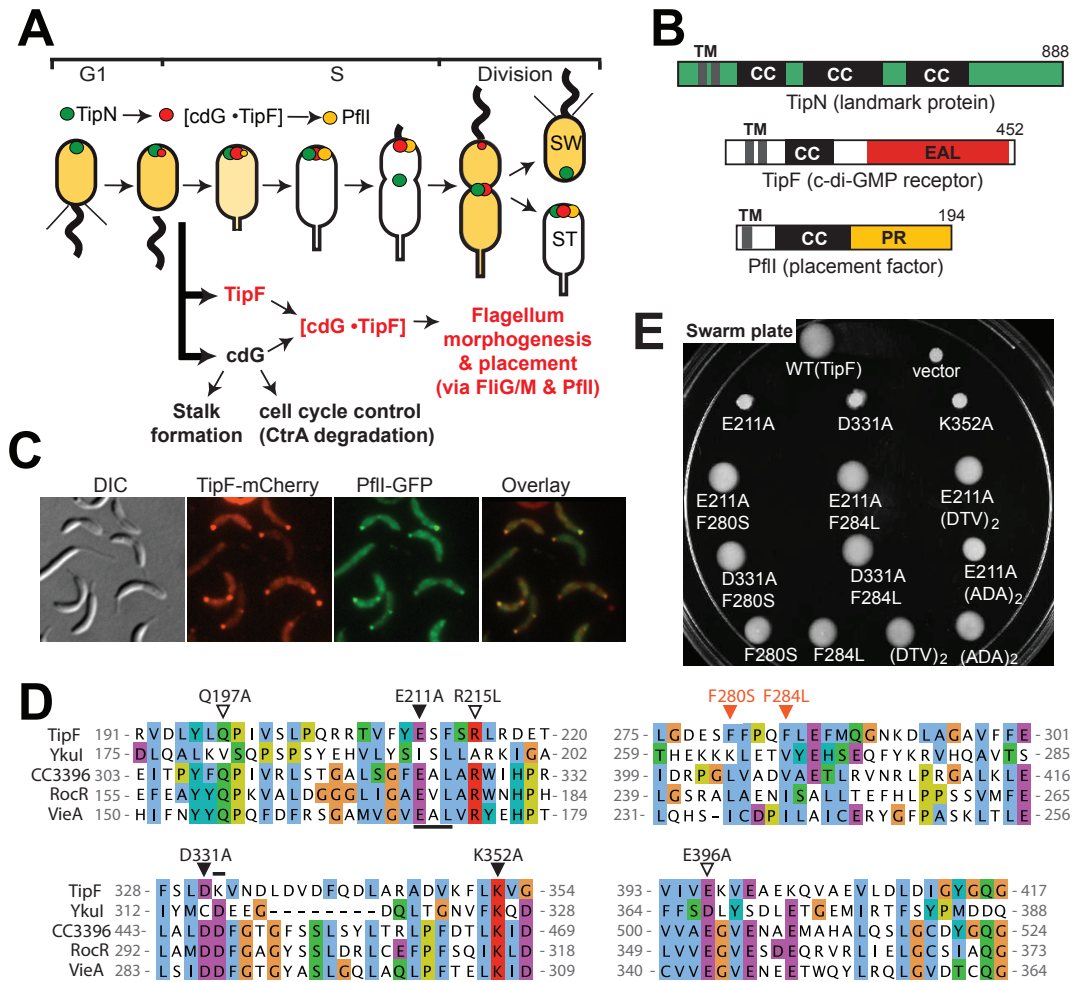


Fig. 2

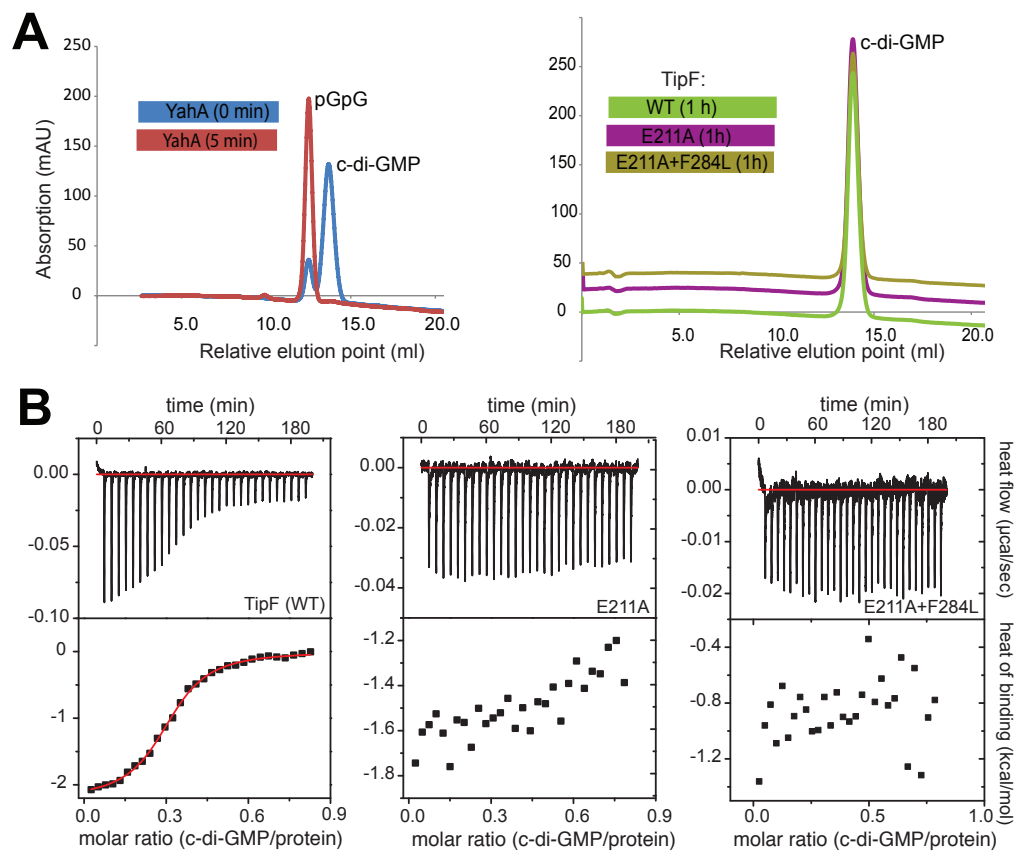


Fig. 3

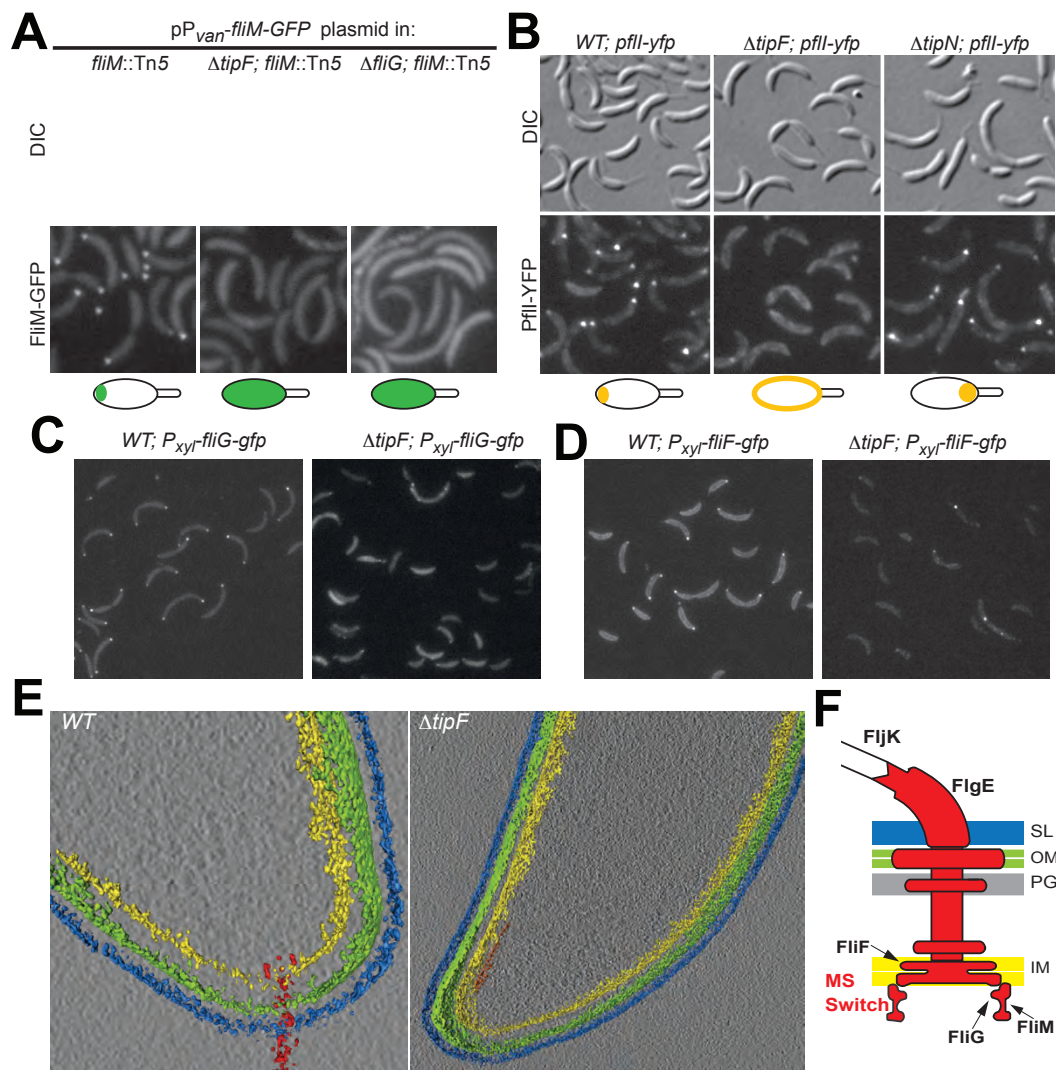


Fig. 4

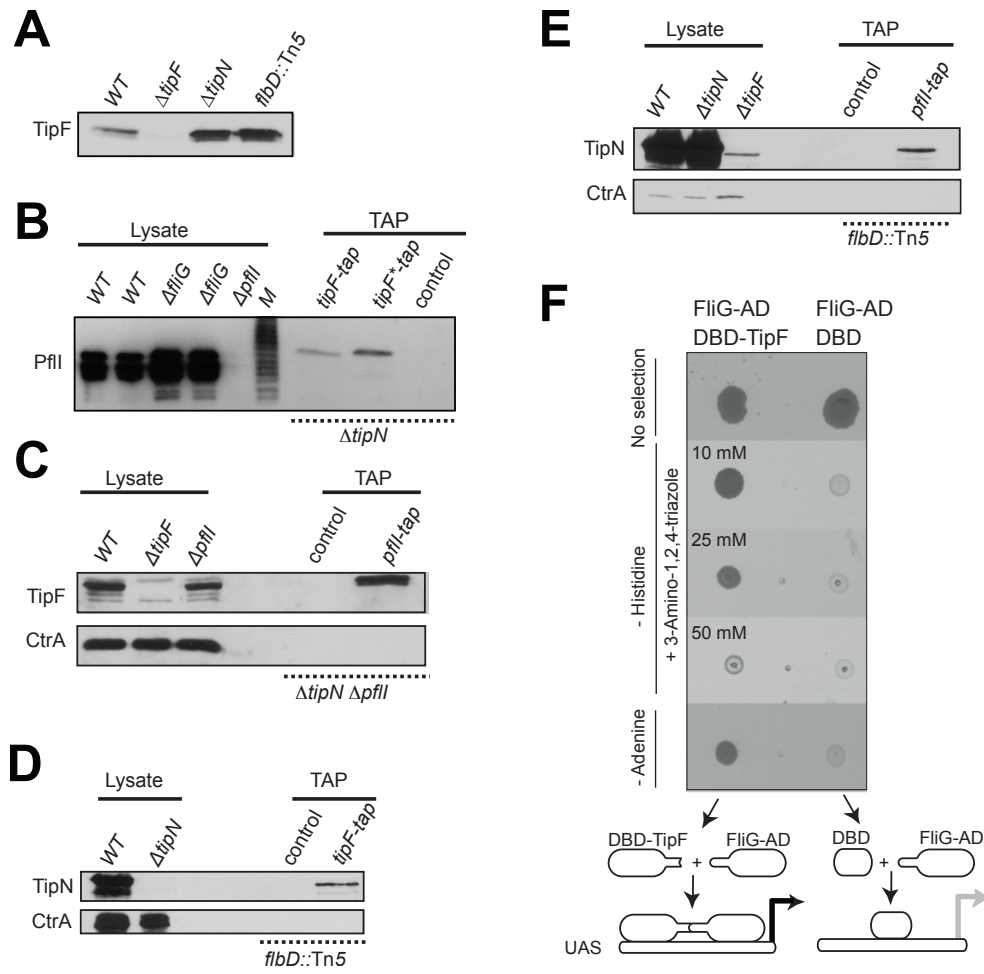


Fig. 5

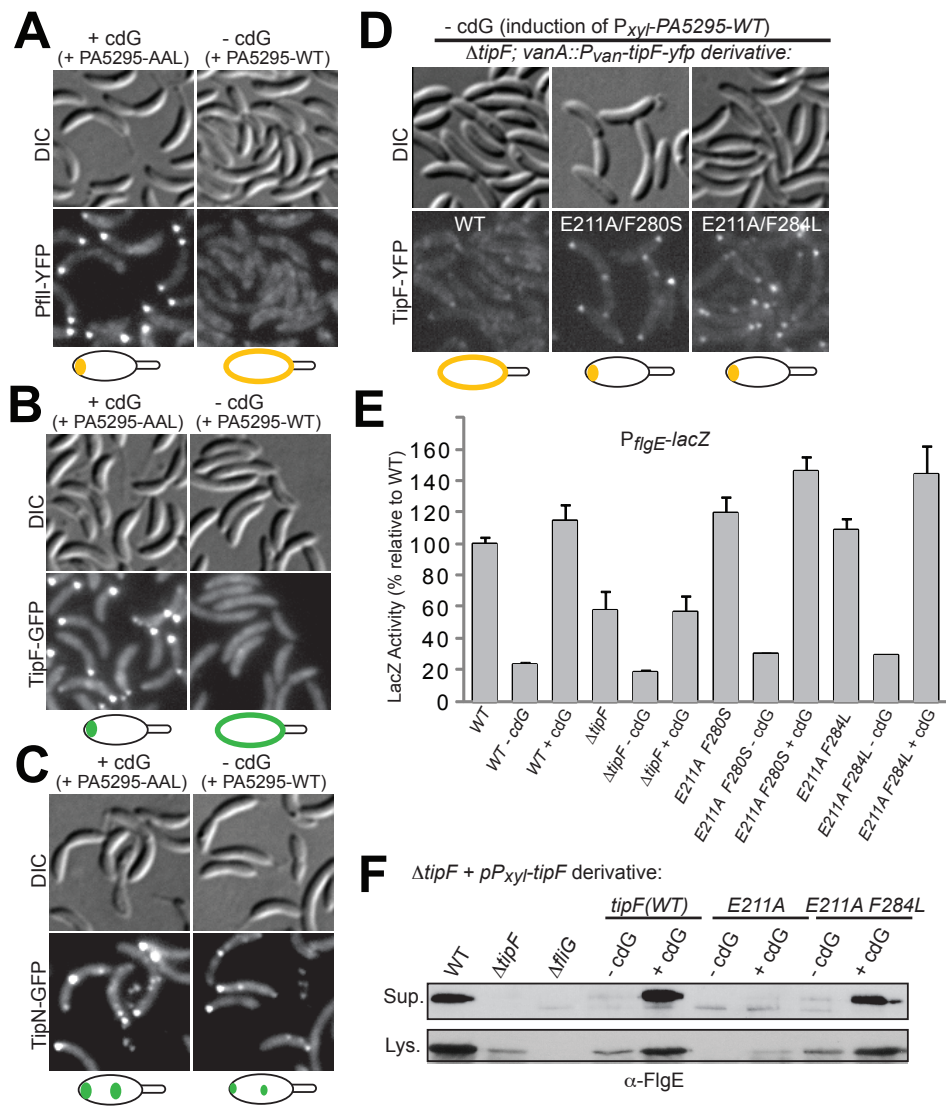


Fig. 6

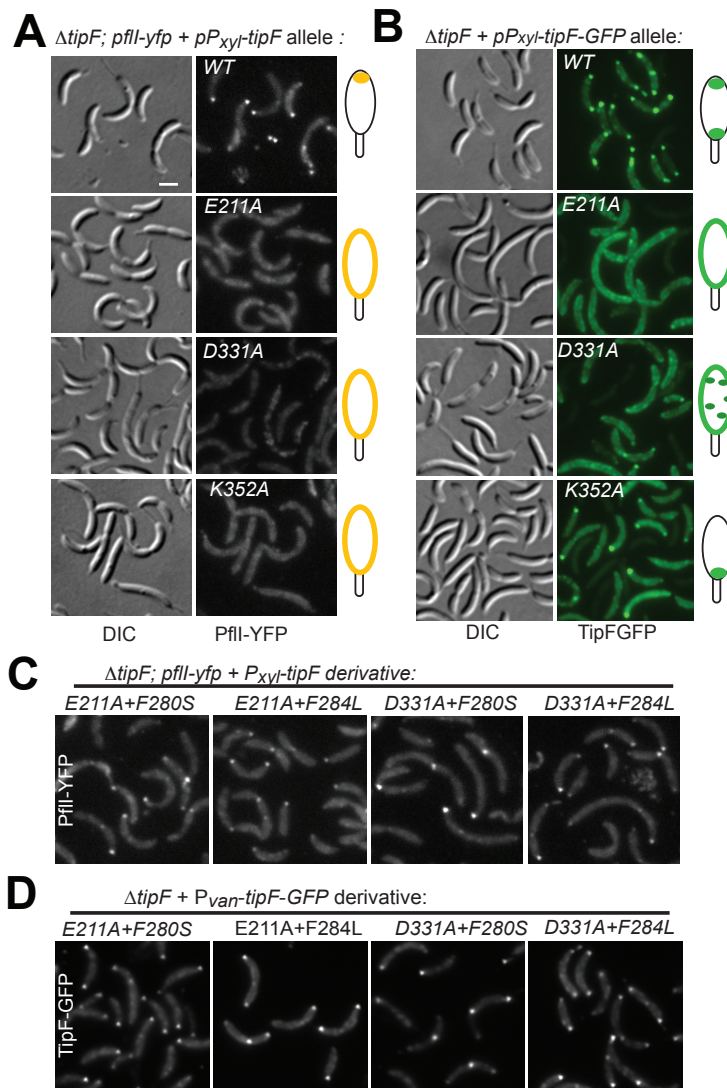


Fig. 7

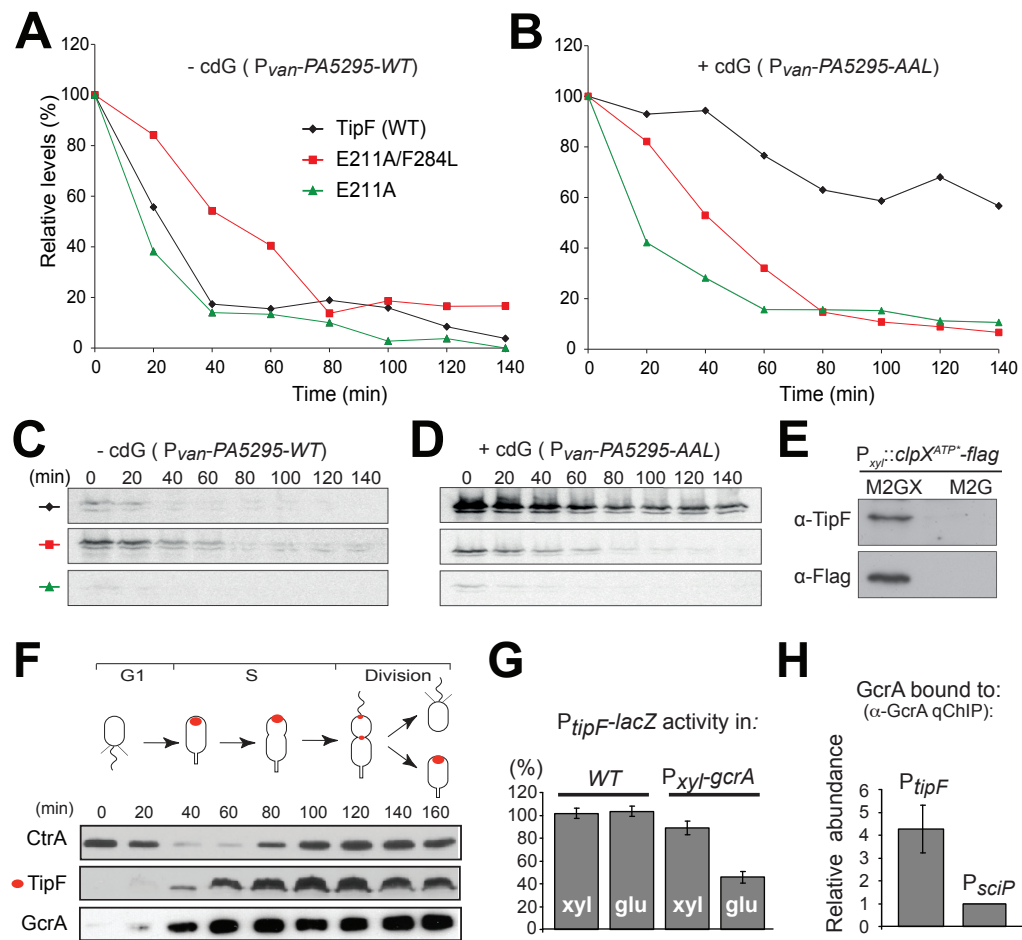


Fig. S1

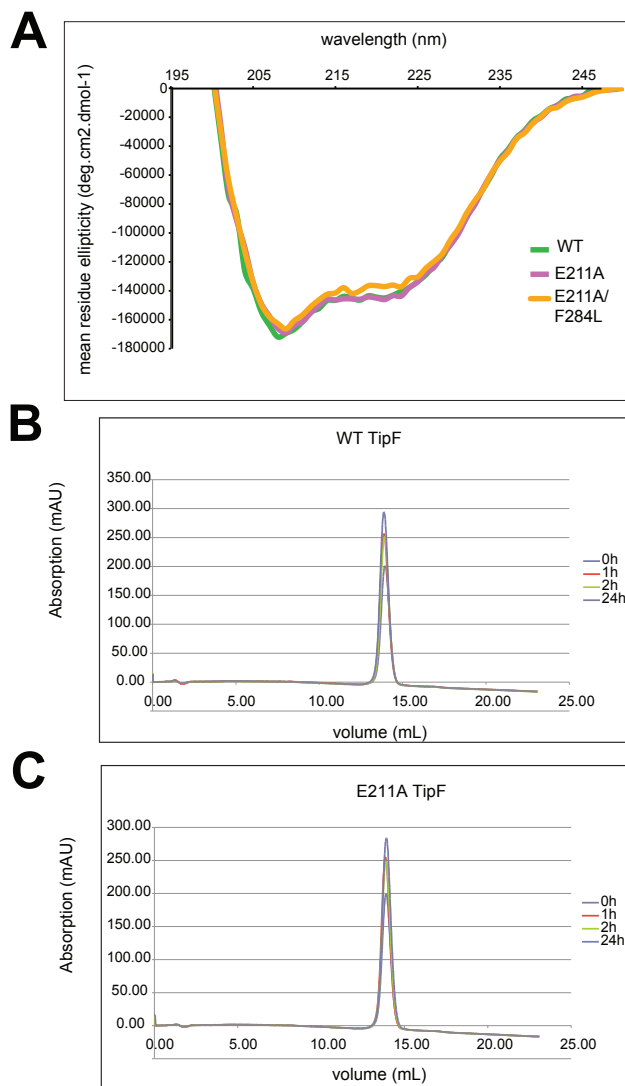


Fig. S2

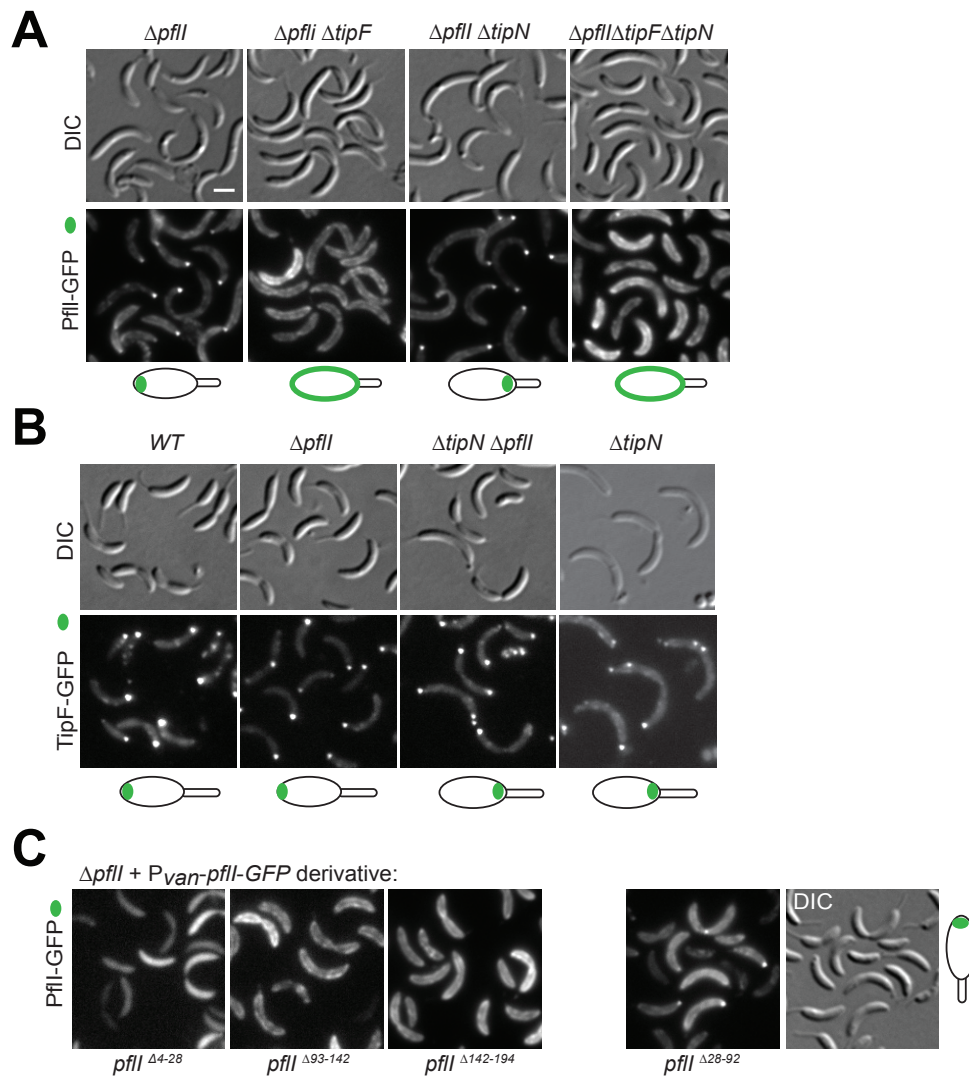


Fig. S3

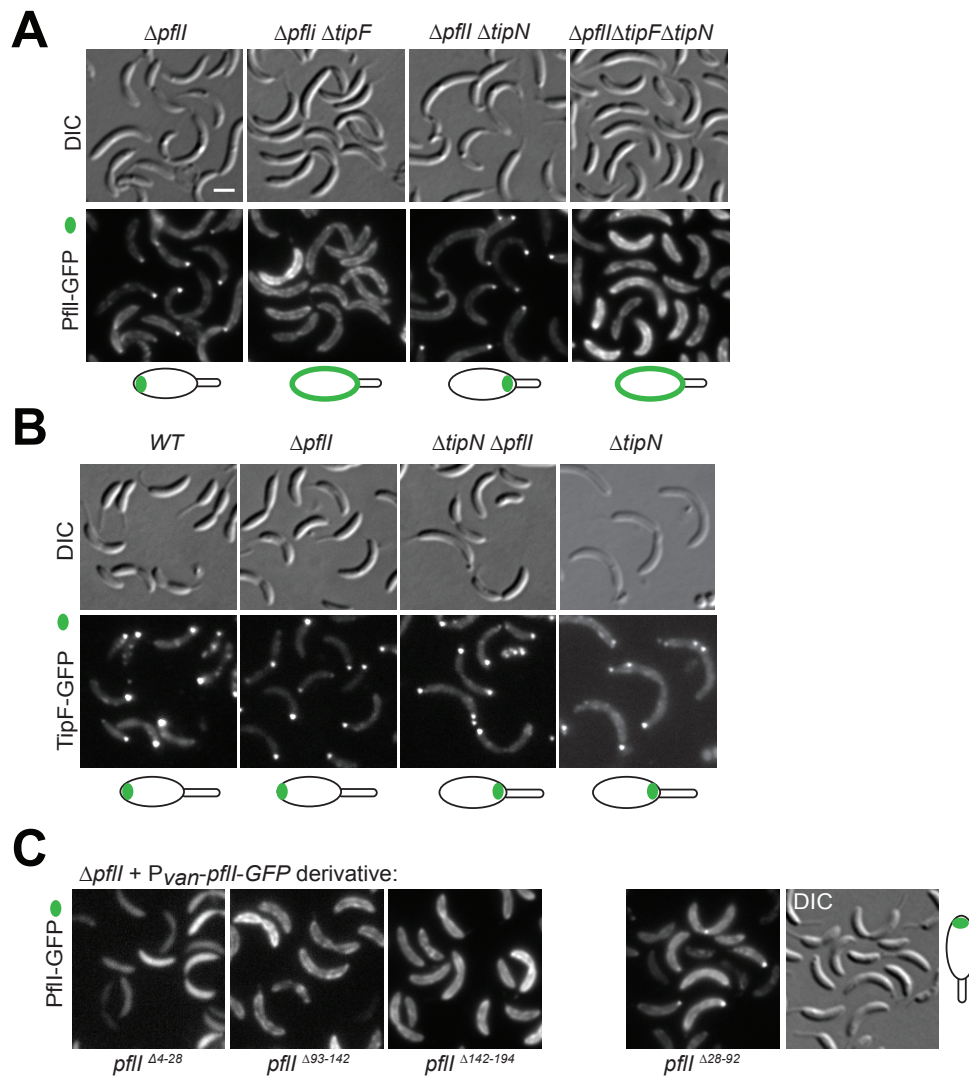


Fig. S4

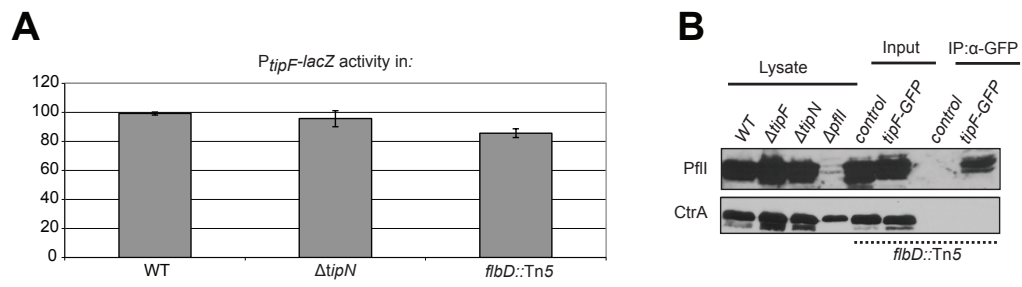
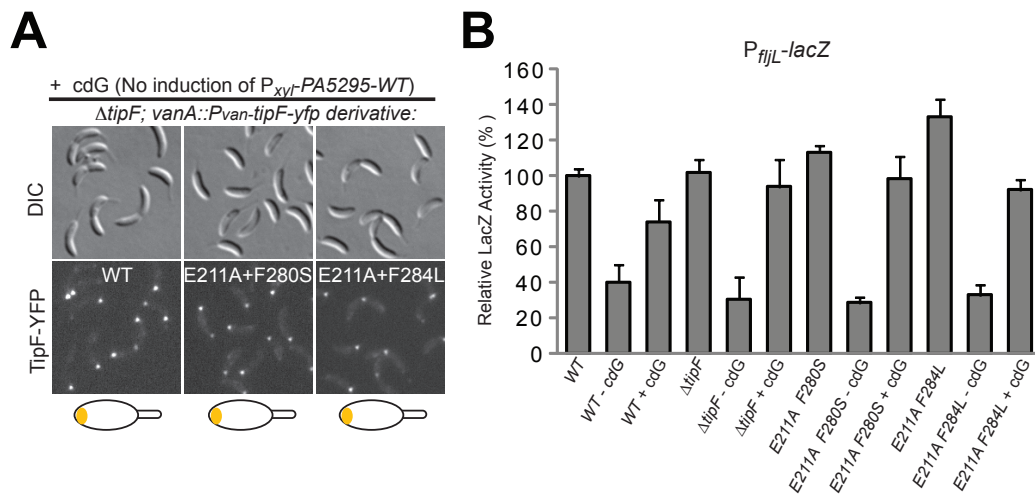


Fig. S5



3.2 Additional results TipF

3.2.1 TipF is cell cycle regulated but its degradation does not depend on known adaptor proteins of the ClpXP degradation pathway

Since TipF is required for flagellum assembly and flagellum biogenesis occurs at a specific time during the cell cycle, we have asked whether TipF is cell cycle controlled. Swarmer cells isolated from NA1000 were allowed to proceed through one cell cycle. Samples were taken every 20 min and subjected to immunoblot analysis using a TipF-specific antiserum. The experiment revealed a unique cell cycle dependent pattern of TipF levels (Fig. 1). TipF is first detectable after 40 min of the cell cycle right on the onset of c-di-GMP accumulation with a main peak at the time points where the flagellum is assembled.

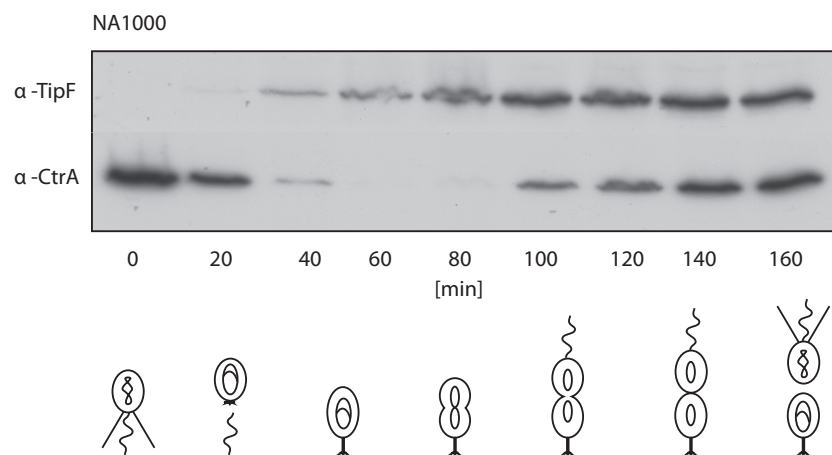


Figure 1: TipF levels are cell cycle regulated. A synchronized culture of *C. crescentus* NA1000 was subjected to immunoblot analysis using anti-TipF antibodies. TipF is appearing after 40 min within the cell cycle. Anti-CtrA immunoblot served as control for the synchronization quality.

The TipF cell cycle dependent pattern suggest that a rapid degradation of TipF occurred within the swarmer cells. This is in agreements with previous observations showing that swarmer cells have low c-di-GMP levels¹¹⁸ and that TipF stability is c-di-GMP mediated (chapter 1). Moreover TipF accumulation right on the swarmer to stalked cell transition is adjunct with c-di-GMP accumulation within the cells¹⁰. Since our data indicates that ClpXP degrades unbound TipF we have asked whether additional factors that are necessary for the ClpXP degradation pathway are required for TipF degradation as well. CpdR is reported to recruit ClpXP and the ClpXP

dependent substrate PdeA to the cell pole and in the absence of CpdR the levels of the ClpXP substrates CtrA and PdeA are stable during the cell cycle^{10,145}. RcdA is in addition needed to recruit the substrate CtrA to the degradation machinery in dependence of PopA and c-di-GMP⁹ (Fig. 2B). In strains carrying either deletions in *cpdR*, *rcdA* or *popA* the levels of TipF show the same characteristic cell cycle accumulation (Fig. 2A) as in wild-type cells, showing that these proteins are not involved in the degradation of TipF.

Specific proteolysis is an important regulation mechanism in *C. crescentus*. ClpXP dependent proteolysis was demonstrated to temporally and spatially regulate key proteins as PdeA¹⁰ and CtrA⁹. We report another key protein to be ClpXP dependent, but in contrast to the substrates described before, TipF degradation neither requires ClpXP localization nor the known adapter proteins. This raises the question how the degradation machinery recognizes TipF and how the machinery discriminates between the bound and the unbound state of TipF but this remains to be a subject of future experiments.

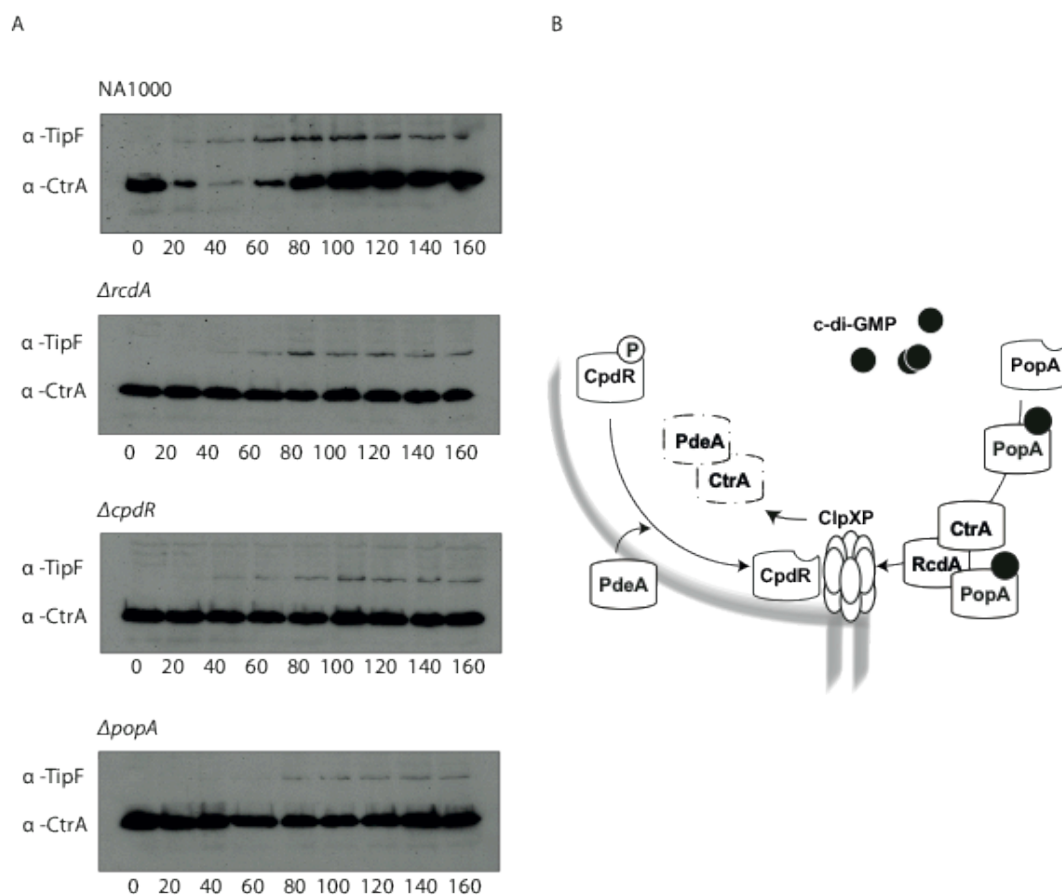


Figure 2: CpdR, RcdA, and PopA are not involved in ClpXP dependent degradation of TipF during the cell cycle. (A) Immunoblots of synchronized cultures of *C. crescentus* NA1000, *cpdR*, *rcdA*, and *popA* deletion strains probed with anti-TipF and anti-CtrA antibodies. (B) Schematic representation of the ClpXP degradation pathway. Shown are the degradation pathway of two known ClpXP substrates, PdeA and CtrA, and the involvement of CpdR, PopA and RcdA in this degradation. CpdR recruits PdeA and the ClpXP protease to the cell pole where the degradation of PdeA and CtrA occurs. CtrA localization to the pole depends on RcdA and PopA. Adapted from^{9,10}.

3.2.2 c-di-GMP independent TipF mutants are stable in a strain lacking c-di-GMP and restore flagellum assembly

Abel and colleagues have constructed a *C. crescentus* strain that lacks all predicted diguanylate cyclases, consequentially this strain cannot synthesize c-di-GMP and all the c-di-GMP related signalling systems are inactivated. The cdG° strain is lacking all characteristic polar organelles of *C. crescentus* including the flagellum (Abel et al., unpublished). Since TipF is required for the biogenesis of the flagellum¹⁴² and as we have shown that TipF is only stable when c-di-GMP is bound, we investigated the stability of TipF and the ability of intragenetic suppressor mutants to restore the assembly of the flagellum and motility in the cdG° background.

RNA sequencing revealed that the mRNA levels of *tipF* in the cdG° and wild-type are identical in the two strains (Abel et al., unpublished). In contrast no TipF protein was detectable in the cdG° strain (Fig. 3A), confirming that the protein is unstable in the absence of c-di-GMP. In addition, over-expression of TipF from a xylose inducible promoter in a cdG° strain containing an additional deletion of *tipF* did not increase the protein levels in the absence of c-di-GMP, while expression of two different TipF intragenetic suppressor mutants, active proteins that cannot bind c-di-GMP (described in Chapter 1.), are detectable in the cdG° strain (Fig. 3B).

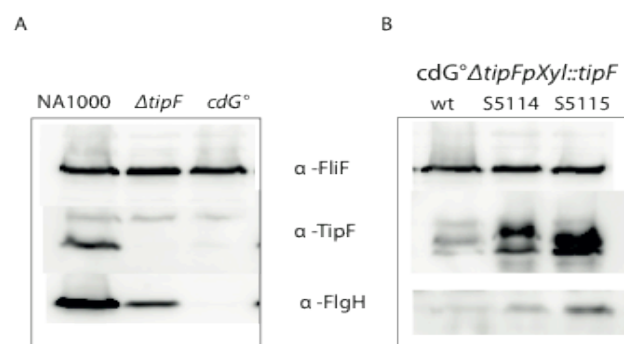


Figure 3: TipF and flagellar protein levels in the absence of c-di-GMP. (A) Cellular extracts of wild-type, cdG° , and $\Delta tipF$ strains were investigated in immunoblot analysis for the levels of TipF, FlgH, and FliF. (B) Cellular levels of TipF, FlgH, and FliF in a $cdG^\circ \Delta tipF$ strain expressing either TipF wild-type protein or the TipF suppressors S5114 (TipF_{E211A/F284L}) and S5115 (TipF_{D331A/F280S}). All immunoblots were probed with anti -TipF, anti-FlgH and anti-FliF antibodies.

We also tested the stability of the selected TipF intragenic suppressors in the $cdG^\circ\Delta tipF$ strain. TipF_{wt} and TipF_{D331A/F284L} were expressed in the $cdG^\circ\Delta tipF$ strain by adding xylose to the cultures, and then shifted to a medium without the inducer and the stability of the proteins were investigated over time (Fig 4). In agreement with our previous findings, the intragenic suppressor was found to be stable for a longer period of time compared to the wild-type protein.

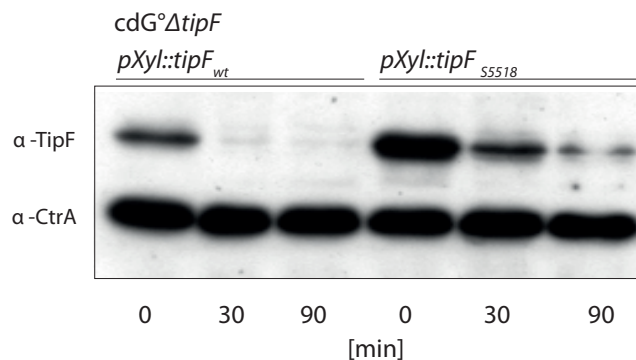


Figure 4: TipF suppressor is stable in the in the cdG° background. Cellular extracts of $cdG^\circ\Delta tipF$ strains expressing the *tipF* alleles encoding for TipF_{wt} and the suppressor S5518 (TipF_{D331A/F284L}) were subjected to immunoblot analysis. Proteins were induced in the presence of xylose for 3h, thereafter the cultures were shifted to a medium without the inducer and samples were taken every 30 min. The blot was probed with anti-TipF antibodies. Anti-CtrA immunoblots served as control.

The $cdG^\circ\Delta tipF$ strain expressing the stabilized suppressor TipF_{E211A/F284L} was also able to regain motility in liquid media (Movie 1). In contrast this strain did not swarm well on semisolid agar plates (Fig. 5A), suggesting additional defects. Therefore the flagellum structure of this strain was resolved by cryo-electron tomography (in cooperation with Misha Kudryashev). The basal body hook complex was intact (Fig. 5B) however the flagellum was misplaced and had only short filaments (Fig. 5C).

We also checked the levels of a selected flagellum protein, and observed that FlgH, the L-ring protein which is missing in the cdG° strain, shows increased but not wt levels in the $cdG^\circ\Delta tipF$ strain expressing the stabilized suppressor TipF_{E211A/F284L} (Fig. 3B). Interestingly, even more FlgH is present in a *tipF* deletion mutant, suggesting that c-di-GMP regulates FlgH in an additional TipF unrelated pathway.

The observation that the TipF suppressor mutant is stable in the absence of c-di-GMP and in turn is sufficient to restore flagellum assembly, indicates that TipF is

sufficient for flagellum assembly and that the interaction of the c-di-GMP signal within the flagellum assembly process is via TipF only. The TipF suppressor cannot restore motility on soft agar plates suggesting additional defects of the cdG° strain not connected to TipF. For instance the flagellum is not correct placed and that is most likely due to the delocalization of TipN, a localization factor that is required for the correct flagellum placement ¹⁴² and is delocalized in a cdG° strain (Abel, unpublished).

The fact that c-di-GMP is required for flagellum assembly demonstrates the complexity of c-di-GMP signaling in *C. crescentus* since c-di-GMP also regulates flagellum ejection ⁷⁶ and inhibits flagellum rotation ³³. This seemingly contradicting activity of c-di-GMP can be explained by the temporal and spatial distribution pattern of c-di-GMP ¹¹⁸ and of the effector molecules, moreover the large variety of binding affinity displayed by c-di-GMP effectors ⁷¹ is a strong indication that different levels of c-di-GMP can induced different cellular response.

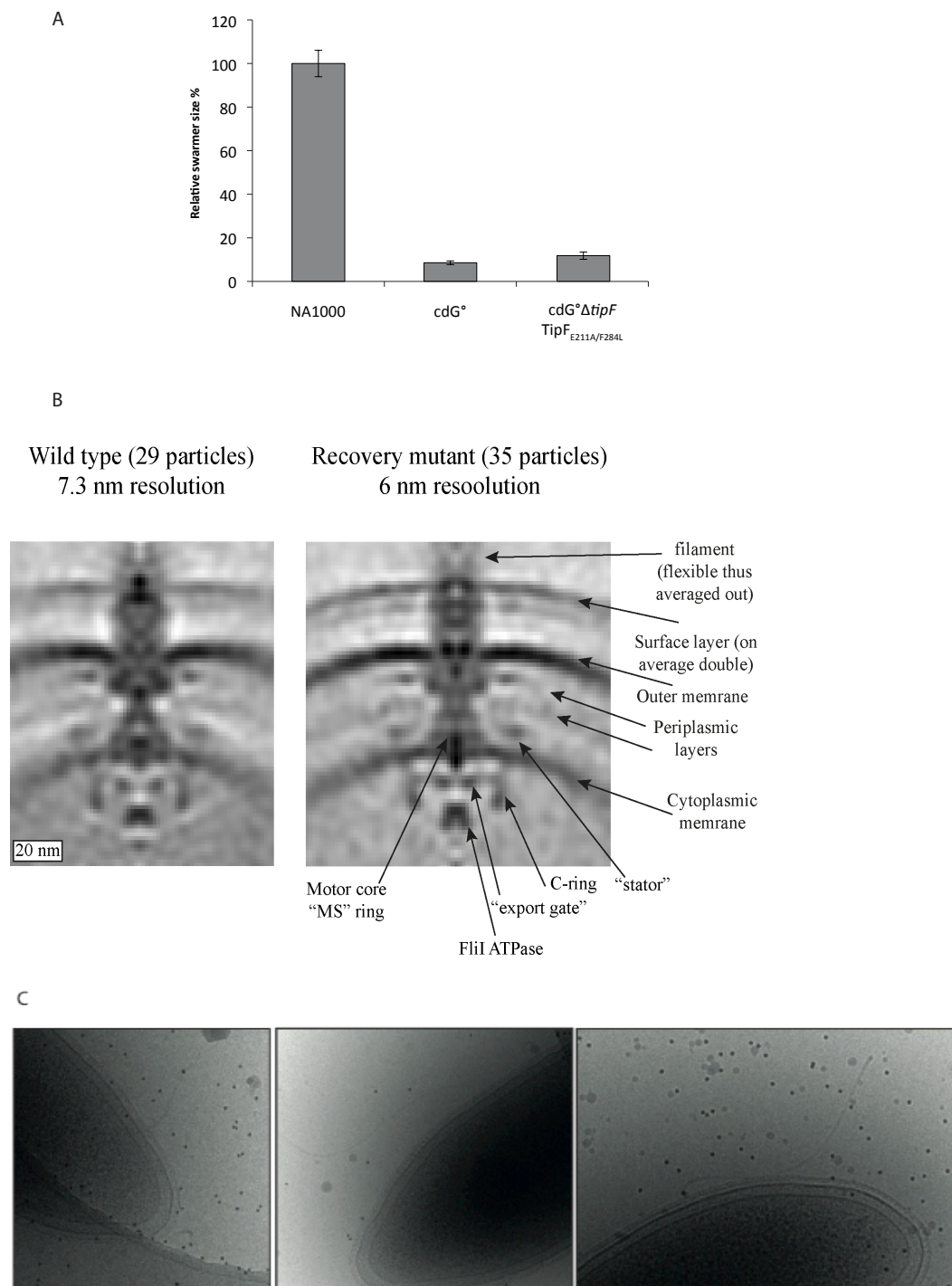


Figure 5: TipF intragenic suppressor restores flagellum assembly in the *cdG°* strain. (A) The *cdG°* mutant displayed severely impaired motility, leading to a swarm size on semi-solid agar plates of only about 10 % compared to NA1000. Expression of TipF_{E211A/F284L} in the *cdG°* strain containing a TipF deletion cannot restore this phenotype. (B) Flagella structures of *C. crescentus* NA1000 and *cdG°ΔtipF* expressing TipF_{E211A/F284L} from a plasmid (Recovery mutant) observed by cryo-electron tomography. Flagellum elements are indicated. (C) *cdG°ΔtipF* expressing TipF_{E211A/F284L} shows flagellum misplacement and filaments protruding from the cell body.

3.2.3 A CtrA mutant is able to partially suppress a deletion of TipF

Intragenic TipF mutants can suppress the motility phenotype of a *tipF* deletion mutant. They were identified by screening for motility in the presence of an active site mutant in the EAL domain (chapter 3.1). In contrast no extragenetic motile suppressor mutants could be identified so far (PV personal communication), indicating that either TipF is the only factor required or that several factors have to be changed in parallel in order to allow swimming on swarm agar plates. Support for the later hypothesis came from the identification of motile suppressors of the *cdG*[°] strain, which were all found to be in *ctrA* (Abel et al., unpublished). CtrA is the master regulator in *C. crescentus* and regulates among other functions the transcription of the flagellar class II genes. One of the identified *ctrA* mutants in the *cdG*[°] strain is *sokA* (Abel et al., unpublished), this allele was described before to suppress *divK*⁸². We have shown that TipF is not detectable in the *cdG*[°] strain, since it is degraded in the absence of bound c-di-GMP (see above). Therefore we analyzed the levels of TipF in the *cdG*[°] *sokA* motile suppressor and indeed TipF was not detectable as in the *cdG*[°] strain (Fig. 6), indicating that assembly of the flagellum can be bypassed in the absence of TipF.

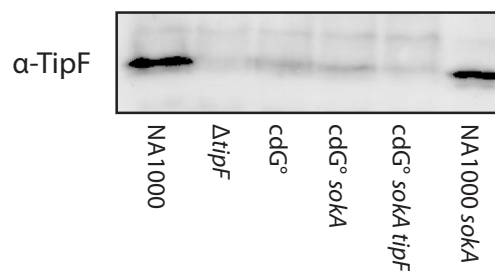


Figure 6: TipF cellular levels. Cellular extracts of wild-type (NA1000), $\Delta tipF$, *cdG*[°], *cdG*[°]*sokA*, *cdG*[°]*sokA**tipF*, and *sokA* strains were investigated in immunoblot analysis for the levels of TipF. The blot was probed with anti-TipF antibodies.

To investigate whether *sokA* can also suppress the motility defect of a *tipF* deletion mutant in the wild-type *C. crescentus*, we analyzed a *sokA* $\Delta tipF$ mutant. This strain was motile in liquid cultures and did slightly restore the motility on semi-solid agar plates (Fig. 7A). Since FliG directly interacts with TipF (chapter 3.1) and is

misslocalized in the absence of TipF¹⁴² we analyzed the localization of FliG-GFP in the *sokAΔtipF* strain. Compared to the *tipF* mutant FliG is localized at higher degree to the pole but not as efficient as in the wild-type or in the *sokA* mutant (Fig 7B), which is in accordance with the results of the motility assay on swarm agar plates.

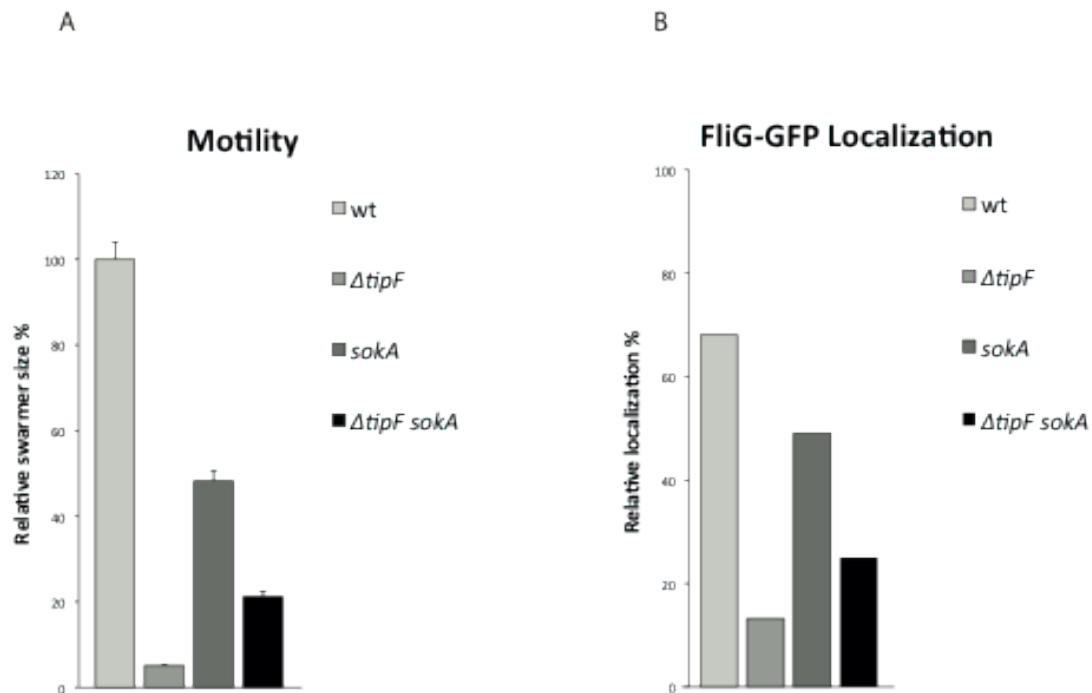


Figure 7: The CtrA mutant SokA partially bypasses necessity of TipF for flagellum assembly and function. (A) The indicated strains were inoculated on PYE swarm agar plates and incubated for 72 hrs at 30°. The swarm-sizes were measured and compared to the wt strain NA1000 (100%). (B) FliG-GFP was expressed in the indicated strains from a plasmid containing *p_{xyI}::fliG-gfp* by adding xylose and the strains were analyzed microscopically. The number of FliG-GFP foci in the indicated strains were counted and compared.

Since a mutation in CtrA is able to partially restore $\Delta tipF$ motility we ask if the activity of CtrA is altered in $\Delta tipF$. Synchronous cultures of wild-type and $\Delta tipF$ (Fig. 8A) were used to monitor the CtrA protein level along the cell cycle. Protein levels of CtrA in the $\Delta tipF$ mutant were found to be identical to the one of the wild-type. In addition we have monitored the protein levels of CcrM and FliF, whose expression is under control of CtrA (Fig. 8B and C). *ccrM* is a DNA methyltransferase, therefore flagella unrelated and FliF builds the flagellar MS ring. We have not noted any changes in appearance timing and level of CcrM and FliF, this suggests that there is

no alteration in the activity of CtrA in $\Delta tipF$ strain.

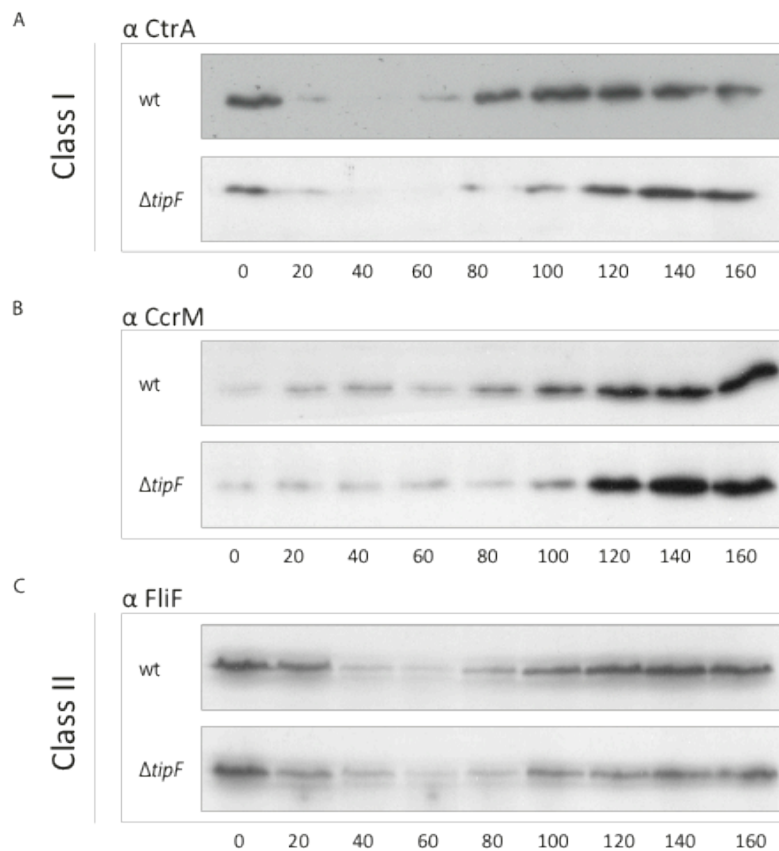


Figure 8: CtrA activity is not altered in a $\Delta tipF$ strain. (A) Synchronized cultures of *C. crescentus* wild-type (NA1000) and $\Delta tipF$ were analyzed by immunoblots with anti-CtrA antibodies. CtrA levels and the cell cycle dependent pattern do not altered in $\Delta tipF$ strain. In addition the protein level and cell cycle dependent pattern of CcrM and FliF (flagellar gene class II) are shown in immonoblot probed with anti-CcrM antibodies (B) and immonoblot probed with anti-FliF antibodies (C), they are comparable to the wild-type strain.

Our results suggest that the assembly of the flagellum has an additional, TipF unrelated, pathway that can be activated by alteration of the CtrA activity through the *sokA* mutation^{82,107}. This indicates that TipF is not the only factor involved in flagellum assembly and that this factor is CtrA regulated. One protein profiling those requirements is PflI. PflI was shown to regulate the positioning of the flagellum¹⁴⁶ in *C. Crescentus*. In addition the transcription of the *fliL* operon, in which *pflI* is located, is CtrA dependent⁸².

We suggest that flagellar assembly and positioning is the integration point of multiple signalling cascades, as each suppressor mutant (SokA or TipF intragenic

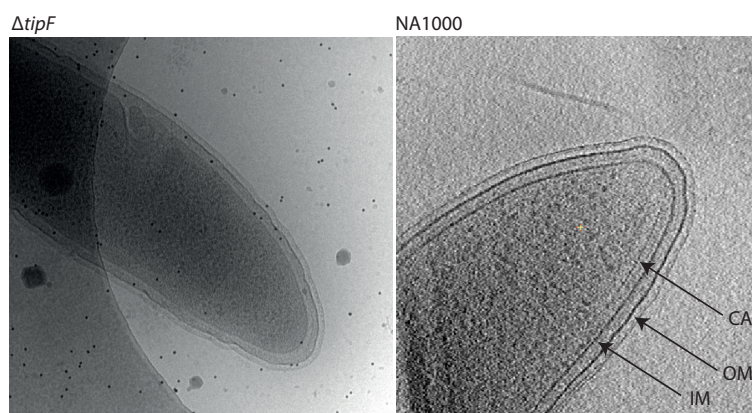
mutation) is able to restore motility to some extent. Next we will test for the involvement of PflI in this process by overexpressing PflI in *tipF* deletion mutant.

3.2.4 The chemotaxis arrays in the *tipF* deletion mutant

Deletion of *tipF* results in several pleiotropic phenotypes, including the loss of flagellum, the reduced attachment ability, and the perturbation of cell division¹⁴². To analyze the morphology of the $\Delta tipF$ strain in more detail, we used cryo-electron tomography and in a number of samples we noted that the chemoreceptor arrays are absent (Fig. 9A). The chemoreceptors, or methyl-accepting chemotaxis proteins (MCPs), form the basis of the signaling apparatus modulating the direction of flagellum rotation¹⁴⁷. To investigate whether TipF might be involved in the localization of MCPs we analyzed McpA, one of 18 MCPs (McpA-R) that are encoded by *C. crescentus*. Immunoblot experiments revealed that McpA is present in the $\Delta tipF$ strain (data not shown). McpA-GFP, expressed from a plasmid under control of the native promoter, was also localized in the *tipF* deletion mutant (Fig. 9B). Only slight differences were noticed, most likely due to the cell elongation of the $\Delta tipF$ mutant.

Our results suggest that TipF is not involved in the localization of McpA. However, we cannot rule out the possibility that McpA-GFP expression results in protein localization due to McpA stabilization and self-assembly properties¹⁴⁸. In a next step, we will investigate the expression level and localization of additional chemotaxis array components in the *tipF* deletion mutant.

A



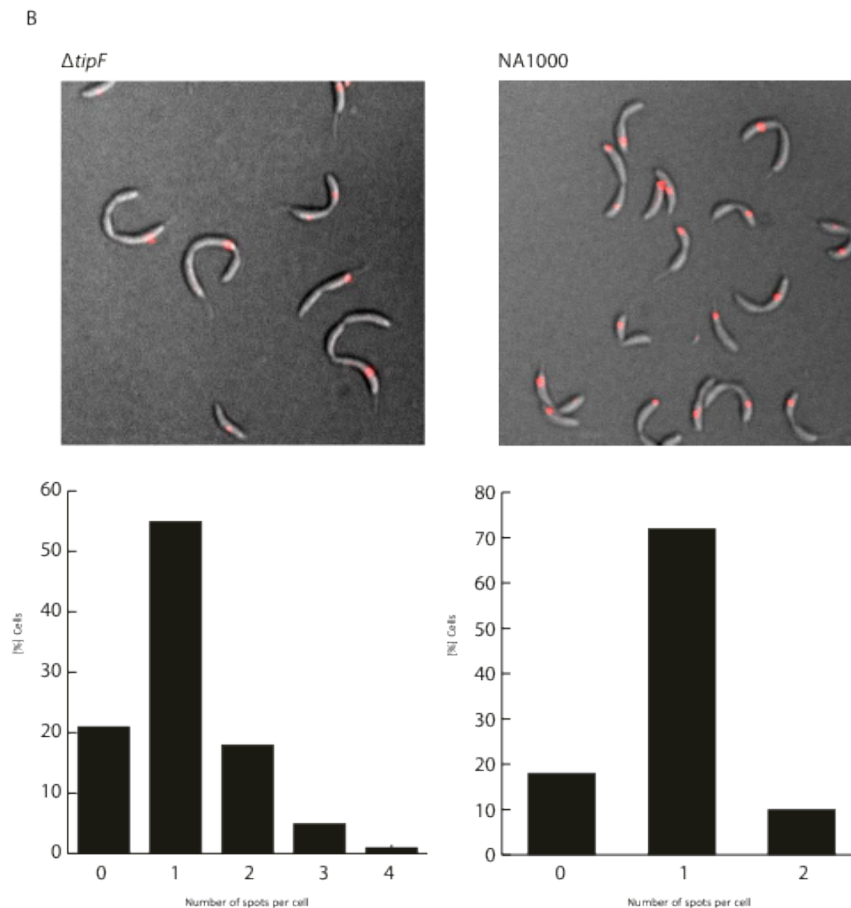


Figure 9: McpA localization is TipF independent. (A) Cryo-electron tomography images showing the chemoreceptor arrays in the NA1000 strain (indicated with an arrow CA-Chemoreceptor array, OM-Outer membrane and IM-Inner membrane) and the absence of those structures in the *tipF* deletion mutant. Indicated with an arrow are the Chemoreceptor array (CA), Outer membrane (OM) and Inner membrane (IM). (B) McpA localization in NA1000 and $\Delta tipF$ strain (top). McpA-GFP was expressed in both strains from a plasmid under control of the native promoter and analyzed by DIC and fluorescence microscopy. The analysis of the amount of spots per cell (bottom) revealed only a slight misplacement of McpA-GFP in the $\Delta tipF$ strain.

3.2.5 Yeast two-hybrid screen for proteins interacting with TipF

So far we have presented several evidences for the involvement of TipF in the assembly of the flagellum. Furthermore, a deletion mutant of *tipF* shows some other phenotypes, like a decrease in attachment (Fig. 10), reduction of pili expression¹⁴² and loss of the chemotaxis array. In order to map the molecular mechanism of those processes we setup a yeast two hybrid screen in an attempt to identify novel direct interacting proteins of TipF. Using the EAL domain of TipF as bait, we screened a genomic prey library of *C. crescentus*. To produce c-di-GMP during the screen we

expressed from the constitutive TEF yeast promoter the diguanylate cyclase YdeH from *E. coli*. In a first screen scoring for growth in the absence of adenine we identified a total of 4 clones. 3 were found to be Gal4-AD fusions to FliG (see also chapter 3.1), two corresponding to aa 192-340 and one to aa 236-340. In a second screen, we identified 5 clones activating HIS3. One had an insert that encodes a C-terminal part of MarR (CC_3112; aa 190-232) and one that codes for the C-terminus of a CelD homolog (CC_2278; aa 304-401). The two prey clones did not interact with the Gal4-DBD itself but were able to activate the reporter gene HIS when the TipF EAL domain was present (Fig. 10).

Not much information is available about the two potential TipF interacting proteins. MarR is annotated as a transcription regulator containing an unorthodox dual wHTH DNA binding domain and no obvious input domain. The CelD homolog (CC_2278) is annotated as Gcn5-related N-acetyltransferase (GNAT). To investigate whether these proteins are involved in similar pathways as TipF, we generated clean deletion mutants in the *C. crescentus* strains CB15 and NA1000. The mutants were analyzed regarding their morphology, ability to swim and to attach to surfaces.

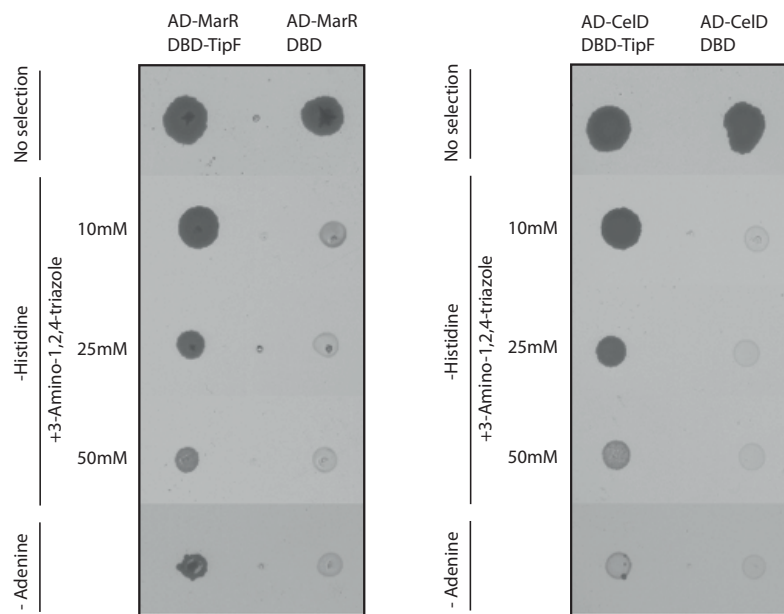


Figure 10: Interaction of TipF with MarR and CeID. The yeast reporter strain PJ69-4A expressing either Gal4-DBD-TipF EAL or Gal4-DBD and Gal4-AD-MarR aa 190-232 or Gal4-DBD-TipF EAL or Gal4-DBD and Gal4-AD-CeID aa 304-401 were assayed for histidine and adenine auxotrophy in the presence of a plasmid expressing YdeH (produces c-di-GMP).

The CC_2278 deletion mutant behaved like the wt strains but showed a subtle attachment defect (Fig. 11) when it was allowed to interact with a polystyrene surface for different periods of time (range from 0.5 hours to 19 hours). The mutant showed reduced attachment in early time points, nevertheless it was able to increase attachment levels when sufficient time was given (Fig. 11). This delayed attachment phenotype suggests that CC_2278 is involved in the temporal regulation of the holdfast. Next we will proof a direct interaction of CC_2278 and TipF by co-immunoprecipitation experiments and then investigate whether TipF is necessary to localize CC_2278. A potential interaction between TipF and CC_2278 is in particular interesting since it could serve as a signal transduction mechanism that regulates the switch between the two lifestyle forms motile and sessile. Several observations were made indicating that the flagellum serves as a mechanoreceptor that mediates an outside inside signal inducing a rapid attachment to the surface once flagellum rotation is inhibited¹⁴⁹. Assuming that CC_2278 is involved in this flagellar mediated signal, its co-localization to the flagellar C-ring (FliG) via TipF could serve the signal

transduction mechanism.

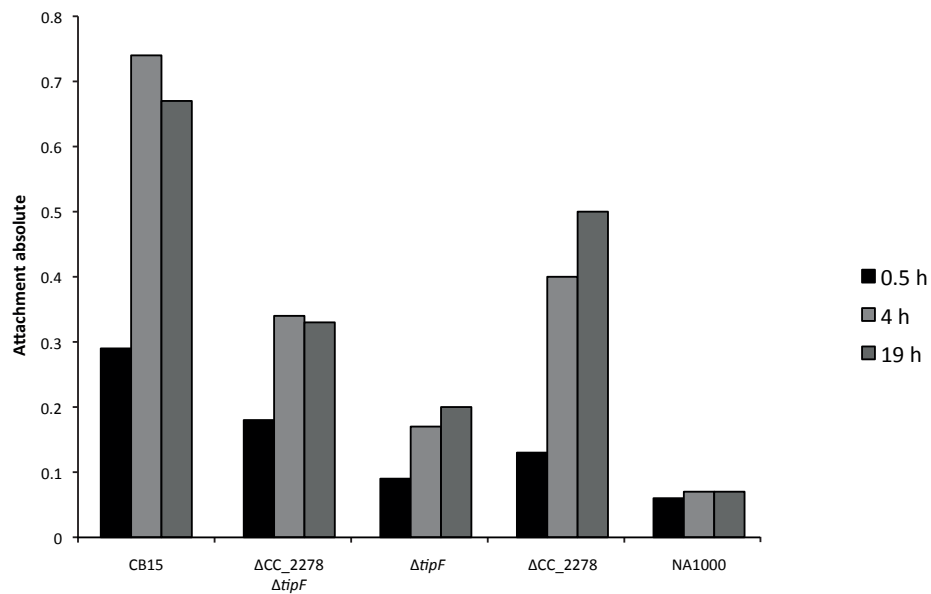


Figure 11: Attachment defect of the CC_2278 deletion mutant. Cells were allowed to attach for 0.5, 4 or 19 hrs and stained with crystal violet. The stain was dissolved and the OD was measured (indicated at the Y axis). The strain NA1000 cannot attach and served as a control.

No obvious link between TipF and MarR could be found so far. In a motility assay on soft agar plates we observed no motility defects of the *marR* deletion strain as the swarm size was similar to the wt NA1000 (Fig. 12A). It did also attach as well as the CB15 wt strain, indicating that pili and the holdfast are present (Fig. 12B). The cellular level of TipF and time of expression were also determined in the *marR* deletion mutant. Immunoblots of samples of synchronized cells revealed that the TipF level and time of appearance remains unaltered in comparison to NA1000 (Fig 12C). The direct interaction between MarR and TipF has still to be proven by independent methods. If the two proteins do interact, further investigations are necessary to find out in which TipF dependent pathway MarR works.

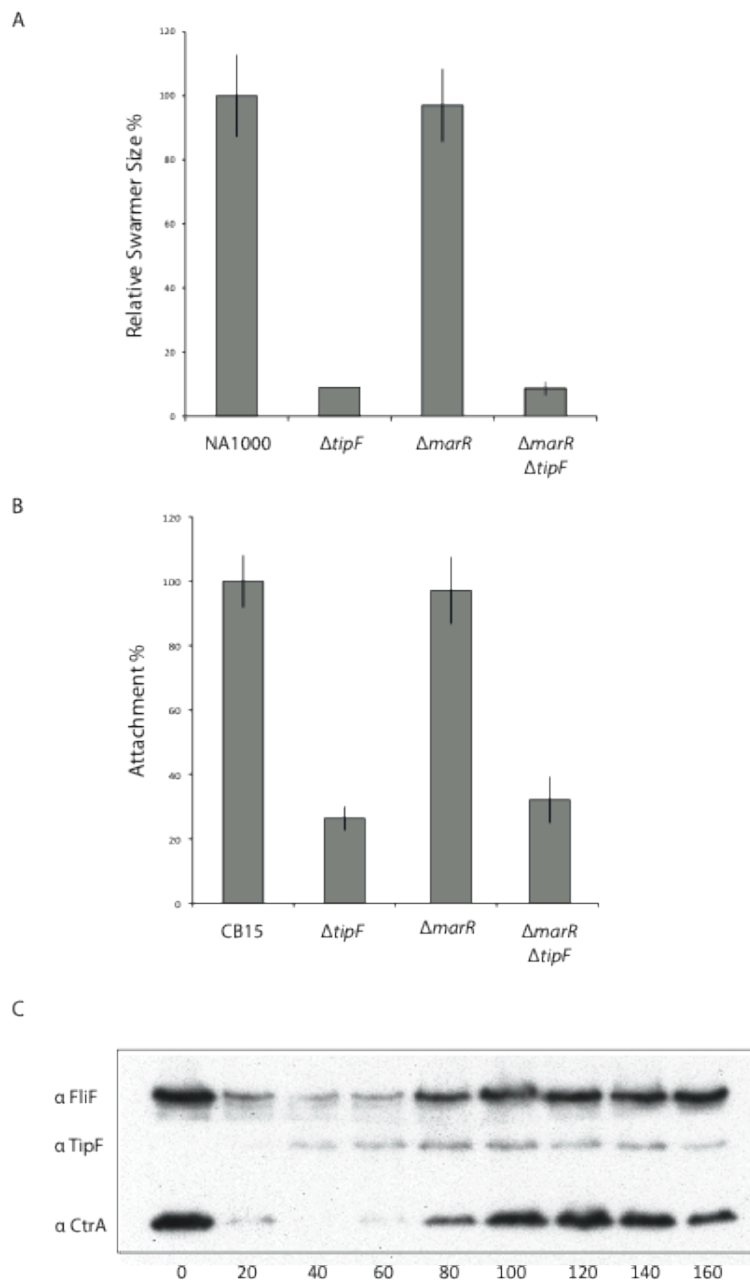


Figure 12: Phenotypes of *marR* deletion mutants. The *marR* deletion mutants were tested for (A) motility (B) attachment and (C) the effect on TipF protein levels through the cell cycle. We have noticed no alteration in all of the measured categories compared to the wild-type.

3.2.6 Material and methods

Growth Conditions

Caulobacter crescentus strains were grown in peptone yeast extract (PYE)¹⁵⁰ or minimal media supplemented with 0.2% glucose or 0.3% D-xylose (M2G or M2X)¹⁵⁰ at 30°C with constant shaking (150 rpm). When selection was required antibiotics in the following concentrations were added: (solid/liquid media in µg/ml): gentamycin (5/0.5), kanamycin (20/5), nalidixic acid (20/not used) and oxytetracycline (5/2.5). For synchronization experiments newborn swarmer cells were isolated by Ludox gradient centrifugation¹⁵¹ and released into fresh minimal medium. When necessary the medium was supplemented with 1 mM Vanillate or 0.3% xylose. For synchronization with inducible constructs, inducer was added to the growth medium 3 h prior to synchrony.

E. coli strains were grown in Luria Broth (LB) at 37 °C. When necessary for selection the following antibiotic concentrations were used: (solid/liquid media in µg/ml) ampicillin (100/50), gentamycin (20/15), kanamycin (50/30) and oxytetracycline (12.5/12.5).

The yeast *Saccharomyces cerevisiae* was grown at 30° either in yeast peptone dextrose containing adenine (YPDA) or synthetic complete (SC) medium¹⁵².

Motility Assays

C. crescentus colonies were spotted onto PYE soft agar plates (0.3% agar) and incubated for 72 h at 30°C. Plates were then scanned (ScanMaker i800 scanner, Microtek, Germany) and analyzed using Photoshop CS3 (Adobe, CA, USA) and ImageJ (NIH, USA) softwares. For all motility experiments the mean of at least three independent colony sizes is shown. Error bar represent standard deviation.

Attachment Assays

C. crescentus strains were grown in PYE in 96-well microtiter plates (Falcon, USA) for 24 h under constant shaking (200 rpm). After crystal violet (0.3% crystal-violet, 5% isopropanol, 5% methanol) staining of the attached biomass it was dissolved with 20% acetic acid and optical density at 600 nm was measured in a photospectrometer (Genesys6, Thermo Spectronic, USA).

Microscopy

DIC and fluorescence microscopy were performed on a DeltaVision Core (Applied Precision, USA)/Olympus IX71 microscope equipped with an UPlanSApo 100x/1.40 Oil objective (Olympus, Japan) and a coolSNAP HQ-2 (Photometrics, USA) CCD camera. Cells were placed on a patch consisting of 1% agarose in water (Sigma, USA). Images were processed ImageJ software (NIH, USA) or Photoshop CS3 (Adobe, USA) software. Bacteria cell and signal localization were analyzed with MicrobeTracker (V0.931) and MATLAB software.

Cryo-electron Tomography was preformed as described in¹⁵³.

Immunoblots

Blots were incubated with the indicated primary antibodies (diluted to the final concentration of 1:10 000) for 1 hr and for an additional hr with HPR-conjugated swine anti-rabbit secondary antibodies (Dako Cytomation, Denmark). Blots were developed with the ECL detection reagent (Western Lightning, Perkin Elmer, USA).

Yeast two-hybrid analysis

Yeast two hybrid screen was performed using the system described in¹⁵⁴. The EAL domain of TipF fused to the Gal4-DBD (DNA binding domain) was expressed in *Saccharomyces cerevisiae* PJ69-4A from plasmid pGBD Kan^R. YdeH, an active DGC that produces c-di-GMP, was expressed in the same strain from plasmid p426-cm-YdeH. For screening, a *C. crescentus* library was transformed into the strain containing the two afore mentioned plasmids. The library contains *C. crescentus* genomic DNA fragments between 500 to 3000 bp, obtained after partial digest of genomic DNA using the enzymes HinPIL, MspI and TaqI, fused to the *gal4-AD* (activator domain) in three reading frames (J. Luciano). Transformants were screened on SD medium lacking leucine, tryptophan, uracil and either adenine or histidine. Prey-plasmids of positive clones were isolated and retransformed in PJ69-4A containing the YdeH expressing plasmid and either the Gal4-DBD-TipF-EAL or the Gal4-DBD only expressing plasmid. Interaction strength and self-activity were tested with these strains on selective medium to check for the activation of reporter genes. Inserts of confirmed interactors were sequenced to ensure in-frame coding sequence with the Gal4-AD.

Strains and plasmids

Strains

Name	Genotype	Description	Source or Reference
NA1000	CB15N	Laboratory strain derived from CB15	Evinger and Agabian, 1977
CB15	CB15	<i>C. crescentus</i> wild type ATCC 19089	Poindexter and Cohen-Bazire, 1964
UJ3638	NA1000 $\Delta tipF$	Markerless in frame deletion of <i>tipF</i>	Huitema et al., 2006
UJ2827	NA1000 $\Delta popA$	Markerless in frame deletion of <i>popA</i>	Duerig et al., 2009
UJ3628	NA1000 <i>rcaA</i> $::hyg$	Disruption of the <i>rcaA</i> gene by a Hyg ^R cassette	Iniesta et al., 2006
UJ4373	NA1000 $\Delta cpdR$	Markerless in frame deletion of <i>cpdR</i>	M. Laub
UJ5065	cdG ^o	Markerless in frame deletion of cc1850, cc0740, cc0857, cc3285, cc2462, cc3094, cc0655, cc0896	M. Nicollier
UJ6463	cdG ^o $\Delta tipF$	Markerless in frame deletion of <i>tipF</i> In UJ5065	S. Abel
UJ6465	cdG ^o $\Delta tipF$ p3064	UJ6463 containing plac290 pXyl:: <i>tipF</i> _{E211A/F284L}	This Study
UJ6466	cdG ^o $\Delta tipF$ p3066	UJ6463 containing plac290 pXyl:: <i>tipF</i> _{E331A/F280L}	This Study
UJ6469	cdG ^o $\Delta tipF$ p264	UJ6463 containing plac290 pXyl:: <i>tipF</i> _{D331A/F284L}	This Study

SoA667	NA1000 <i>cdG</i> [°] <i>sokA</i>	<i>cdG</i> [°] with acquired mutation in <i>ctrA</i> (<i>sokA</i>)	S. Abel
UJ1981	<i>sokA</i>	Mutation in <i>ctrA</i>	Wu et al., 1998
UJ4456	CB15 $\Delta tipF$	Markerless in frame deletion of <i>tipF</i>	S. Abel
UJ5396	NA1000 <i>cdG</i> [°] <i>sokA</i> $\Delta tipF$	Markerless in frame deletion of <i>tipF</i> in SoA667	This Study
UJ6476	NA1000 $\Delta marR$	Markerless in frame deletion of <i>marR</i>	This Study
UJ6477	CB15 $\Delta marR$	Markerless in frame deletion of <i>marR</i>	This Study
UJ6478	NA1000 $\Delta marR$ $\Delta tipF$	Markerless in frame deletion of <i>marR</i> in UJ3638	This Study
UJ6479	CB15 $\Delta marR$ $\Delta tipF$	Markerless in frame deletion of <i>marR</i> in UJ4456	This Study
UJ6474	NA1000 $\Delta celD$ $\Delta tipF$	Markerless in frame deletion of <i>celD</i> UJ3638	This Study
UJ6473	CB15 $\Delta celD$	Markerless in frame deletion of <i>celD</i>	This Study
UJ6473	CB15 $\Delta celD$	Markerless in frame deletion of <i>celD</i>	This Study
UJ6475	CB15 $\Delta celD$ $\Delta tipF$	Markerless in frame deletion of in <i>celD</i> UJ4456	This Study
UJ5292	Yeast pJ69-4A	<i>trp1-901 leu2-3,112 ura3-52 his3-200 GAL4 $\Delta GAL80$ $\Delta LYS2::GAL1-HIS3$ GAL2-ADE2 met2::GAL7-lacZ</i>	James et al., 1996
UJ5649	pJ69-4A	UJ5292 containing pGBD- <i>tipF</i> -kan, p426-TEF- <i>ydeH</i> -cm	This Study
UJ5646	pJ69-4A	UJ5292 containing pGBD- <i>tipF</i> -kan, p426-TEF-cm	This Study

Plasmids

Name	Description	Source or Reference
p208	pLac290 pXyl:: <i>tipF</i> _{WT}	P. Viollier
p3066	pLac290 pXyl:: <i>tipF</i> _{E331A/F280S}	P. Viollier
p3064	pLac290 pXyl:: <i>tipF</i> _{E211A/F284L}	P. Viollier
p264	plac290 pXyl:: <i>tipF</i> _{D331A/F284L}	P. Viollier
pGBD-kan	pGAD with Kan ^R cassette	J. Nesper
pGBD- <i>tipF</i> -kan	pGAD with Kan ^R cassette and <i>tipF</i> -gal4 fusion	J. Nesper
p426-TEF-cm	p426 with Cm ^R cassette	J. Nesper
p426-TEF- <i>ydeH</i> -cm	p426 with Cm ^R cassette <i>pTEF::ydeH</i>	J. Nesper

3.3 The flagellin modification protein FlmA interacts with cyclic diguanosine monophosphate in an unspecific manner

3.3.1 Introduction

The bacterial second messenger cyclic diguanosine monophosphate (c-di-GMP) is a wide spread signal molecule among bacteria. High cellular levels of c-di-GMP are associated with sessile, biofilm associated life forms whereas low cellular levels of c-di-GMP are shown to promote motility and a solitary life form. There is much known about the biosynthesis and degradation mechanisms that govern the intracellular levels of this second messenger. However the processes of signal transduction i.e. how the cellular levels of c-di-GMP induce cellular responses as well as the identity of c-di-GMP effector molecules in particular are mainly unknown. In order to address this subject Christen and colleges have developed a biochemical approach for the identification of putative c-di-GMP binders³³. One of the proteins that they were able to enrich was FlmA.

FlmA (CC_0322) is a 38kD protein encoded in a cluster with other flagellar modification (*flm*) genes. It was reported that the *C. crescentus* gene cluster *flmA-flmH* is involved in motility¹⁵⁵. Mutant strains lacking any of the *flm* genes express a normal hook-basal body structure but are failing to assemble the flagellar filament¹⁵⁶. FlmA contains a C-terminal epimerase domain usually involved in a variety of chemical reactions utilizing nucleotide-sugars as substrates. Moreover, homolog proteins from *Helicobacter pylori* were shown to be involved in the glycosylation of flagellin subunits¹⁵⁷. Both the putative c-di-GMP binding and the proposed association with motility regulation make FlmA a good candidate as a c-di-GMP effector protein. Based on this knowledge we conducted several experiments to test this hypothesis.

3.3.2 Results and Discussion

3.3.2.1 A *flmA* mutant is non-motile and produces a low molecular mass flagellin

We created a clean *flmA* deletion strain and tested it for various phenotypes. The *flmA* mutant displayed severely impaired motility, leading to a colony size on semi-solid agar plates of only about 5 % compared to the wild type (Fig. 1A). In order to pinpoint the cause of this motility defect we tested the *flmA* deletion mutant for its ability to express flagellar elements of class II and III (i.e. the proteins FliM, FliF and FlgH). We observed no change in the expression levels of those proteins (data not shown). We also tested the *flmA* deletion mutant for the expression of flagellin (class IV) and for extracellular flagellin levels (secretion). Both were reduced compared to the wild-type and more importantly we also observed reduction of the molecular mass of the flagellin subunit (Fig. 1B). Similar results were reported earlier^{155,156}.

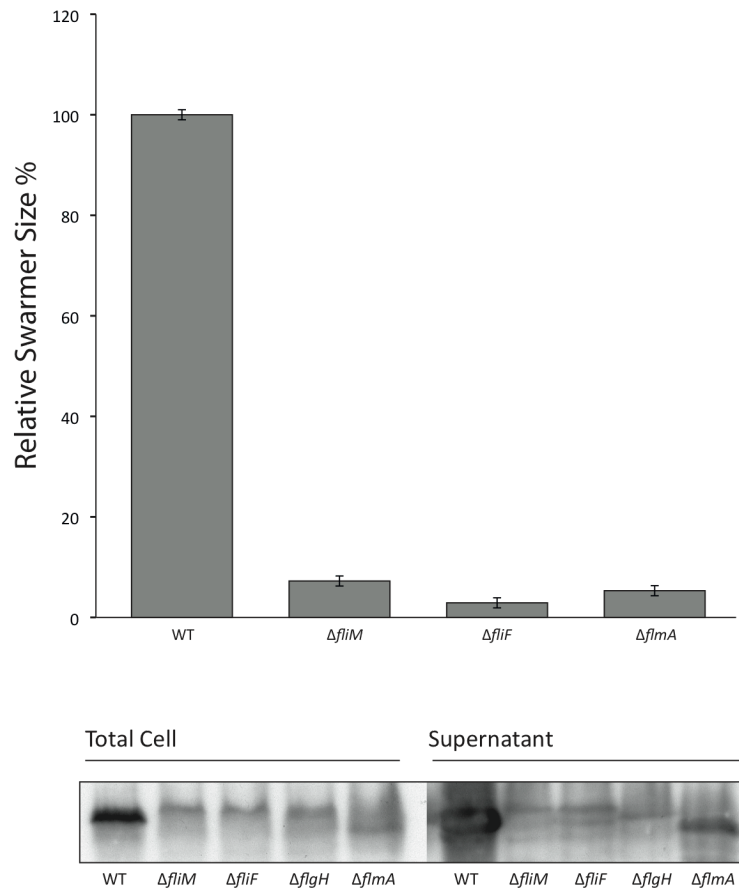


Figure 1: The *flmA* mutant is non-motile and produces a low molecular mass flagellin. (A) Motility assay demonstrating the non-motile phenotype of the *flmA* deletion mutant. The colony diameter on semi-solid agar plates of the *flmA* mutant was compared to wild type. The values for non-motile mutants were included for comparison. (B) The intracellular (total cell) and secreted (supernatant) levels of flagellin analyzed by immunoblots with an anti-Flagellin antibody revealing a reduction in the amount and mass of flagellin in the *flmA* mutant compared to the wild-type. Further flagellar mutants (*fliM*-, *fliF*- and *flgH*-) were included for comparison.

3.3.2.2 FlmA interaction with c-di-GMP

Purified FlmA was analyzed for interaction with c-di-GMP by a UV cross-linking assay with ^{33}P labeled c-di-GMP. An increasing amount of labeled c-di-GMP was added to a constant amount of purified protein and after a short incubation on ice the mixture was exposed to UV radiation. The obtained autoradiographs indicated that the protein interacted with c-di-GMP. Moreover, an apparent saturation was observed and the K_D of the interaction was determined to be $\sim 25\mu\text{M}$ (Fig. 2). Although this

measured kD lays above the affinity range of reported c-di-GMP effectors (50nM-5 μ M), we could not rule out a biological relevance of the interaction between FlmA and c-di-GMP.

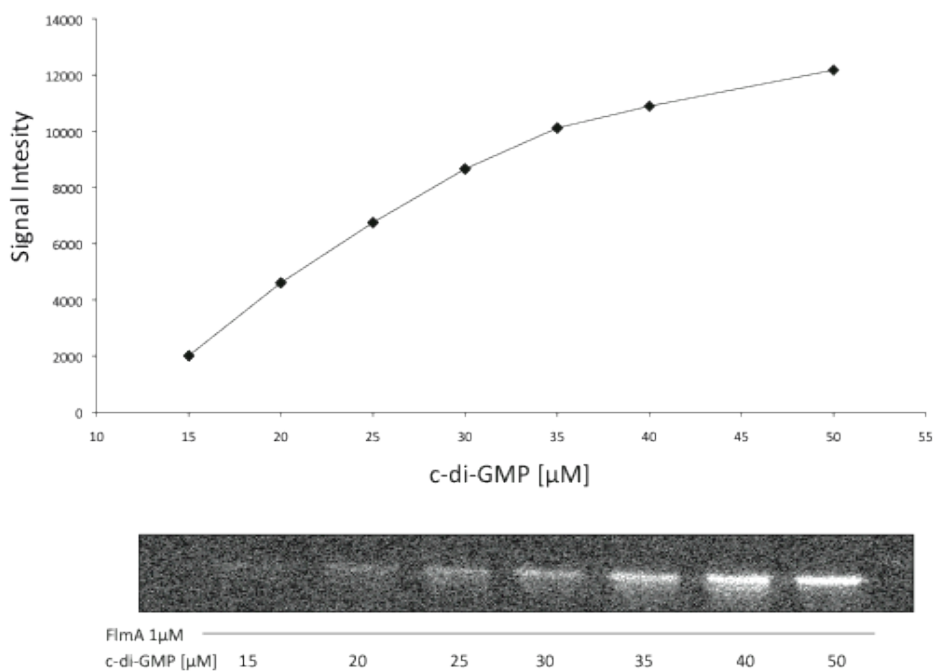


Figure 2: FlmA interaction with ^{33}P labeled c-di-GMP. increasing amount of ^{33}P labeled c-di-GMP was incubated with purified FlmA and exposed to UV radiation, thereafter samples were separated on SDS-PAGE and bound c-di-GMP was visualized by autoradiography. The signal intensity was plotted revealing an apparent saturation.

In order to attain a better characterization of the FlmA interaction with c-di-GMP we conducted isothermal titration calorimetry (ITC). First we performed a control experiment in which instead of c-di-GMP a non-hydrolysable version of GTP (GTP α S) was titrated into FlmA (5 μ M) containing solution (Fig. 3). A constant heat release as a result of the dilution process was observed indicating that the molecules did not interact this experimental setup.

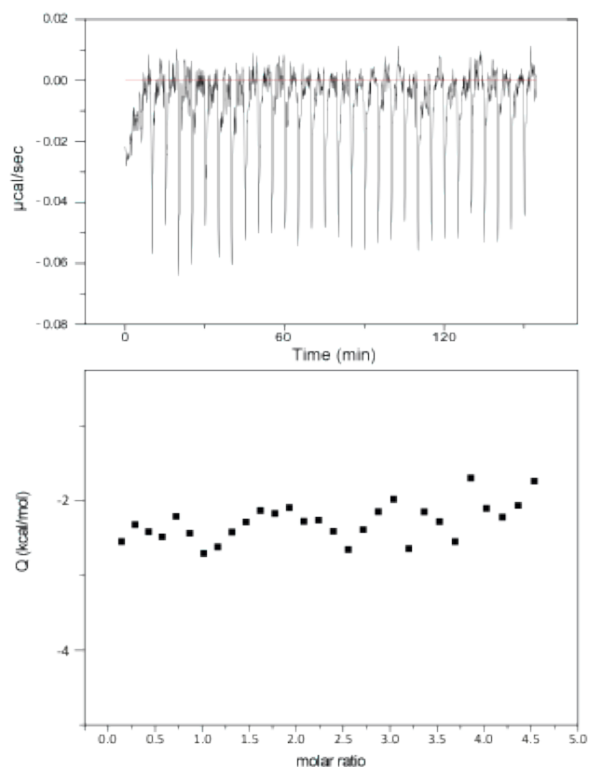


Figure 3: FlmA interaction with GTP α S. Pattern of the heat release during the titration of GTP α S (100 μ M) into a 5 μ M FlmA solution at 15°C (upper panel). The integrated titration peaks are also shown (lower panel). Since the values remained constant we concluded that there is no interaction of GTP α S with the protein in the concentration range tested.

The calorimetric trace obtained when c-di-GMP was titrated into a protein solution with purified FlmA at 15°C showed that each injection caused an exothermic reaction (Fig. 4). A constant decrease in heat release with each injection, as less free protein was available for binding, was also observed. Once the molecular ratio within the cell reached 1:2 (after ~10 injections) all FlmA molecules seemed to be bound and further injections caused no additional heat release besides dilution effects.

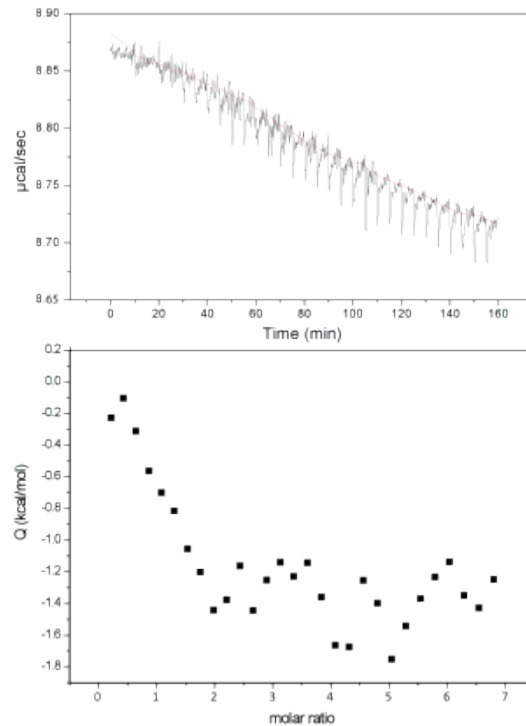


Figure 4: FlmA interaction with c-di-GMP. The titration pattern of d-ci-GMP ($150 \mu\text{M}$) injected into $5 \mu\text{M}$ FlmA at 15°C (upper panel). The integrated titration peaks are shown as well (lower panel). The titration curve shows a constant decrease in heat release until a molar ratio of 1:2. From then on, only constant heat release (dilution effect) is observed.

However these preliminary results were inconclusive due to the low values of heat release and a drifted base line. We therefore conducted an additional measurement in which a higher concentrated solution of c-di-GMP ($350 \mu\text{M}$) was titrated into the FlmA solution ($19.1 \mu\text{M}$) at both 25°C and 15°C (Fig. 5). We noticed that under these conditions a constant heat release per injection step was already reached at a molar ratio of around 1:1, opposing the observations made in the initial experiment. In addition due to the temperature changes we have expected a modification in heat release, as the accessible surface area (ASA) is temperature dependent. However, we did not observe any change in heat release in the measurement made at 15°C in comparison to the measurement made at 25°C (Fig. 5).

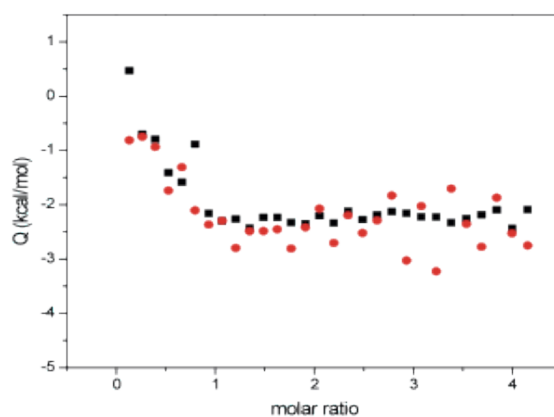


Figure 5: FlmA interaction with c-di-GMP at different temperatures. c-di-GMP (350 μM) was injected into a solution containing 19.1 μM FlmA at 15°C (red circles) and at 25°C (black squares). The integrated titration peaks are shown. Constant heat release is reached at a 1:1 ratio opposing the observation made in the initial experiment (Fig 4).

This led us to believe that the apparent heat releases measured in the initial experiments were not a result of specific interaction. We tested this assumption by performing an experiment in which we titrated c-di-GMP into a solution without protein and we found that the c-di-GMP dilution process had a very similar heat release profile like the one observed when c-di-GMP was titrated into a FlmA solution (Fig. 6). This unusual dilution profile is most probably due to an oligomeric form transition of c-di-GMP as a cause of the decrease of concentration in solution upon titration¹⁵⁸.

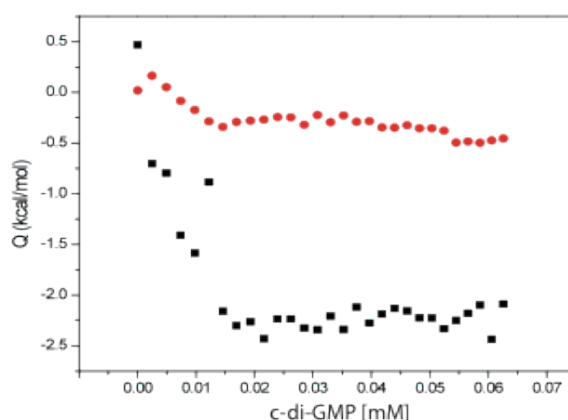


Figure 6: c-di-GMP dilution profile. The integrated titration peaks of the heat release during dilution, obtained from c-di-GMP (350 μM) injection into the buffer (red dots), in comparison to the ones

obtained when c-di-GMP was titrated into FlmA solution (black squares). The constant heat release is reached at the same concentration regardless the presence or absence of the protein.

3.3.2.3 The FlmA interaction to c-di-GMP is unspecific

We conducted a competition experiment in which we measured the ability of small molecules to compete with the c-di-GMP bound to FlmA. In this assay we added a constant amount of ^{33}P labeled c-di-GMP to a constant amount of protein. Thereafter we added the competitor molecules (GTP, GMP, or pGpG) in increasing concentrations. All competitors were able to compete the ^{33}P labeled c-di-GMP (Fig. 7).

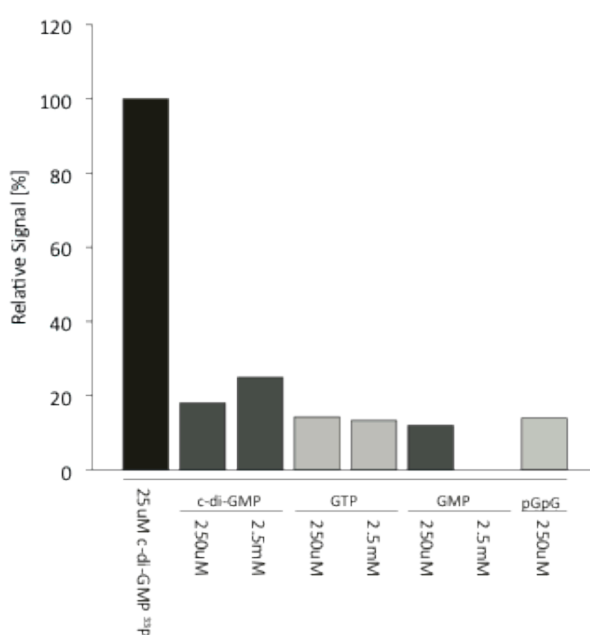


Figure 7: c-di-GMP competition assay. FlmA (1 μM) was incubated with ^{33}P labeled c-di-GMP. Thereafter competitors (unlabeled c-di-GMP, GTP, GMP and pGpG) molecules were added to the indicated final concentrations. Samples were separated on SDS-PAGE and the relative signal intensities obtained from the autoradiograph were plotted.

Taken together our data indicates that FlmA might interact with c-di-GMP however this interaction is unspecific and in a range that is biologically non-relevance. This eliminates the possibility that FlmA acts as c-di-GMP effector protein. It is likely that epimerase domain of FlmA that enables interaction of the protein with nucleotide-sugar substrates is the base of the observed unspecific interaction.

3.3.2.4 Material and methods

Growth Conditions

Caulobacter crescentus strains were grown in peptone yeast extract (PYE)¹⁵⁰ or minimal media supplemented with 0.2% glucose or 0.3% D-xylose (M2G or M2X)¹⁵⁰ at 30°C with constant shaking (150 rpm). When selection was required antibiotics in the following concentrations were added: (solid/liquid media in µg/ml): gentamycin (5/0.5), kanamycin (20/5), nalidixic acid (20/not used) and oxytetracycline (5/2.5). For synchronization experiments newborn swarmer cells were isolated by Ludox gradient centrifugation¹⁵¹ and released into fresh minimal medium. When necessary the medium was supplemented with 1 mM Vanillate or 0.3% xylose. For synchronization with inducible constructs, inducer was added to the growth medium 3 h prior to synchrony.

E. coli strains were grown in Luria Broth (LB) at 37 °C. When necessary for selection the following antibiotic concentrations were used: (solid/liquid media in µg/ml) ampicillin (100/50), gentamycin (20/15), kanamycin (50/30) and oxytetracycline (12.5/12.5).

Motility Assays

C. crescentus colonies were spotted onto PYE soft agar plates (0.3% agar) and incubated for 72 h at 30°C. Plates were then scanned (ScanMaker i800 scanner, Microtek, Germany) and analyzed using Photoshop CS3 (Adobe, CA, USA) and ImageJ (NIH, USA) softwares. For all motility experiments the mean of at least three independent colony sizes is shown. Error bar represent standard deviation.

Attachment Assays

C. crescentus strains were grown in PYE in 96-well microtiter plates (Falcon, USA) for 24 h under constant shaking (200 rpm). After crystal violet (0.3% crystal-violet, 5% isopropanol, 5% methanol) staining of the attached biomass it was dissolved with 20% acetic acid and optical density at 600 nm was measured in a photospectrometer (Genesys6, Thermo Spectronic, USA).

Immunoblots

Primary antibodies were diluted to the final concentration 1:10000 and detected by HRP-conjugated swine anti-rabbit secondary antibodies (Dako Cytomation, Denmark). Western blots were developed with ECL detection reagents (Western Lightning, Perkin Elmer, USA).

Synthesis and Purification of [33P]cyclic-di-GMP

[33P] labelled c-di-GMP was produced enzymatically using α -labelled [33P]GTP as described in³³.

UV Cross-linking of proteins with [33P]c-di-GMP

UV-crosslinking of proteins with radio labelled c-di-GMP was performed as described in³³. Samples were irradiated at 254 nm for 20 min on an ice-cooled, wrapped 96-well aluminium block in an RPR-100 photochemical reactor with a UV lamp RPR-3500 (The Southern New England Ultraviolet

Company). After irradiation, samples were mixed with 2x SDS PAGE sample buffer and heated for 5 min at 95 °C. Labelled Proteins were separated by SDS-PAGE and quantified by autoradiography.

Protein purification

Rosetta BL21pLysS E.coli strain was transformed with respective plasmids and used for protein overexpression after induction of cultures with 0.4 optical density at 600nm with 1mM isopropyl-b-D-thiogalactopyranoside (IPTG) for 4h at RT (LB-broth). After induction the cells were collected by centrifugation. The cell pellets were resuspended in buffer consisting of 20mM Tris-HCl pH7, 250mM NaCl, 5mM imidazole, 10mM MgCl₂, 1% glycerol and Complete mini cocktail of protease inhibitors, EDTA free at the concentrations specified by manufacturer (Roche). The cells were lysed using French press, and the crude extracts were centrifuged at 15,000xg for 40 min at 4⁰C. The cleared lysates were incubated with preequillibrated Profinity IMAC Ni-resin (Bio-Rad) for 1h at 4⁰C and washed consequently with lysis buffer and washing buffer with 20 mM imidazole. The proteins were eluted using 350mM imidazole.

Isothermal titration calorimetry

The interaction of FlmA with cyclic-di-GMP was measured with a VP-ITC isothermal titration calorimeter from MicroCal (Northampton, MA), with the condition specified in the text. All solutions were degassed and equilibrated at desired temperature before using. The delay between the injections was set to 5 min to ensure re-equilibration between injections. Data were evaluated using Origin software (OriginLab) provided by Microcal (Northampton, MA).

Strains and plasmids

Name	Genotype	Description	Source or Reference
CB15	CB15	<i>C. crescentus</i> wild type ATCC 19089	Poindexter and Cohen-Bazire, 1964
NA1000	CB15N	Laboratory strain derived from CB15	Evinger and Agabian, 1977
UJ6480	NA1000 $\Delta flmA$	Markerless in frame deletion of <i>flmA</i>	This Study
UJ1793	NA1000 $\Delta flif$	Markerless in frame deletion of <i>flif</i>	Jenal and Shapiro, 1995
UJ413	NA1000 <i>fliM::Tn5</i>	Disruption of the <i>fliM</i> gene by <i>Tn5</i>	P. Aldridge
UJ3257	NA1000 $\Delta flgH$	markerless in frame deletion of <i>flgH</i>	A. Levi

Plasmids

Name	Description	Source or Reference
pET21 <i>flmA</i>	pET21::His6- <i>flmA</i>	M. Christen

4 Bibliography

1. Weinhouse, H. *et al.* c-di-GMP-binding protein, a new factor regulating cellulose synthesis in *Acetobacter xylinum*. *FEBS Letters* **416**, 207–211 (1997).
2. Ross, P., Weinhouse, H., Aloni, Y. & Michaeli, D. Regulation of cellulose synthesis in *Acetobacter xylinum* by cyclic diguanylic acid. (1987).
3. Hickman, J. W. & Harwood, C. S. Identification of FleQ from *Pseudomonas aeruginosa* as a c-di-GMP-responsive transcription factor. *Molecular microbiology* **69**, 376–89 (2008).
4. Wilksch, J. J. *et al.* MrkH, a novel c-di-GMP-dependent transcriptional activator, controls *Klebsiella pneumoniae* biofilm formation by regulating type 3 fimbriae expression. *PLoS pathogens* **7**, e1002204 (2011).
5. Krasteva, P., Fong, J. & Shikuma, N. *Vibrio cholerae* VpsT regulates matrix production and motility by directly sensing cyclic di-GMP. *Science's* **327**, 866–868 (2010).
6. Sudarsan, N. *et al.* Riboswitches in eubacteria sense the second messenger cyclic di-GMP. *Science (New York, N.Y.)* **321**, 411–3 (2008).
7. Lee, E. R., Baker, J. L., Weinberg, Z., Sudarsan, N. & Breaker, R. R. An allosteric self-splicing ribozyme triggered by a bacterial second messenger. *Science (New York, N.Y.)* **329**, 845–8 (2010).
8. Christen, B. *et al.* Allosteric control of cyclic di-GMP signaling. *The Journal of biological chemistry* **281**, 32015–24 (2006).
9. Duerig, A., Nicollier, M., Schwede, T. & Amiot, N. Second messenger-mediated spatiotemporal control of protein degradation regulates bacterial cell cycle progression. *Genes & Development* **23**, 93 (2009).
10. Abel, S. *et al.* Regulatory Cohesion of Cell Cycle and Cell Differentiation through Interlinked Phosphorylation and Second Messenger Networks. *Molecular Cell* **43**, 550–560 (2011).
11. Hengge, R. Principles of c-di-GMP signalling in bacteria. *Nature reviews. Microbiology* **7**, 263–73 (2009).
12. Jenal, U. & Malone, J. Mechanisms of cyclic-di-GMP signaling in bacteria. *Annual review of genetics* **40**, 385–407 (2006).

13. Povolotsky, T. L. & Hengge, R. "Life-style" control networks in *Escherichia coli*: Signaling by the second messenger c-di-GMP. *Journal of biotechnology* (2011).doi:10.1016/j.jbiotec.2011.12.024
14. Schirmer, T. & Jenal, U. Structural and mechanistic determinants of c-di-GMP signalling. *Nature reviews. Microbiology* **7**, 724–35 (2009).
15. Tal, R. *et al.* Three *cdg* operons control cellular turnover of cyclic di-GMP in *Acetobacter xylinum*: genetic organization and occurrence of conserved domains in isoenzymes. *Journal of bacteriology* **180**, 4416–25 (1998).
16. Paul, R., Weiser, S., Amiot, N. & Chan, C. Cell cycle-dependent dynamic localization of a bacterial response regulator with a novel di-guanylate cyclase output domain. *Genes & Development* **18**, 715–727 (2004).doi:10.1101/gad.289504.The
17. Chan, C. *et al.* Structural basis of activity and allosteric control of diguanylate cyclase. *Proceedings of the National Academy of Sciences of the United States of America* **101**, 17084–9 (2004).
18. Ryjenkov, D. A., Tarutina, M., Moskvin, O. V. & Gomelsky, M. Cyclic Diguanylate Is a Ubiquitous Signaling Molecule in Bacteria : Insights into Biochemistry of the GGDEF Protein Domain †. *Society* **187**, 1792–1798 (2005).
19. Schmidt, A. J., Ryjenkov, D. A. & Gomelsky, M. The Ubiquitous Protein Domain EAL Is a Cyclic Diguanylate-Specific Phosphodiesterase : Enzymatically Active and Inactive EAL Domains The Ubiquitous Protein Domain EAL Is a Cyclic Diguanylate-Specific Phosphodiesterase : Enzymatically Active and Inactive E. *Society* (2005).doi:10.1128/JB.187.14.4774
20. Minasov, G. *et al.* Crystal structures of YkuL and its complex with second messenger cyclic Di-GMP suggest catalytic mechanism of phosphodiester bond cleavage by EAL domains. *The Journal of biological chemistry* **284**, 13174–84 (2009).
21. Rao, F., Yang, Y., Qi, Y. & Liang, Z.-X. Catalytic mechanism of cyclic di-GMP-specific phosphodiesterase: a study of the EAL domain-containing RocR from *Pseudomonas aeruginosa*. *Journal of bacteriology* **190**, 3622–31 (2008).
22. Rao, F. *et al.* The functional role of a conserved loop in EAL domain-based cyclic di-GMP-specific phosphodiesterase. *Journal of bacteriology* **191**, 4722–31 (2009).
23. Pesavento, C. & Hengge, R. Bacterial nucleotide-based second messengers. *Current Opinion in Microbiology* **12**, 170–176 (2009).

24. Tchigvintsev, A. *et al.* Structural insight into the mechanism of c-di-GMP hydrolysis by EAL domain phosphodiesterases. *Journal of molecular biology* **402**, 524–38 (2010).
25. Römling, U. Rationalizing the evolution of EAL domain-based cyclic di-GMP-specific phosphodiesterases. *Journal of bacteriology* **191**, 4697–700 (2009).
26. Ryan, R. P. *et al.* Cell-cell signaling in *Xanthomonas campestris* involves an HD-GYP domain protein that functions in cyclic di-GMP turnover. *Proceedings of the National Academy of Sciences of the United States of America* **103**, 6712–7 (2006).
27. Lovering, A., Capeness, M., Lambert, C. & Hobley, L. The Structure of an Unconventional HD-GYP Protein from *Bdellovibrio* Reveals the Roles of Conserved Residues in this Class of Cyclic-di-GMP Phosphodiesterases. *mBio* (2011).doi:10.1128/mBio.00163-11.Editor
28. Galperin, M. Y., Nikolskaya, a N. & Koonin, E. V. Novel domains of the prokaryotic two-component signal transduction systems. *FEMS microbiology letters* **203**, 11–21 (2001).
29. Seshasayee, A. S. N., Fraser, G. M. & Luscombe, N. M. Comparative genomics of cyclic-di-GMP signalling in bacteria: post-translational regulation and catalytic activity. *Nucleic acids research* **38**, 5970–81 (2010).
30. Mills, E., Pultz, I. S., Kulasekara, H. D. & Miller, S. I. The bacterial second messenger c-di-GMP: mechanisms of signalling. *Cellular microbiology* **13**, 1122–9 (2011).
31. Weber, H., Pesavento, C., Possling, A., Tischendorf, G. & Hengge, R. Cyclic-di-GMP-mediated signalling within the sigma network of *Escherichia coli*. *Molecular microbiology* **62**, 1014–34 (2006).
32. Sommerfeldt, N. *et al.* Gene expression patterns and differential input into curli fimbriae regulation of all GGDEF/EAL domain proteins in *Escherichia coli*. *Microbiology (Reading, England)* **155**, 1318–31 (2009).
33. Christen, M. *et al.* DgrA is a member of a new family of cyclic diguanosine monophosphate receptors and controls flagellar motor function in *Caulobacter crescentus*. *Proceedings of the National Academy of Sciences of the United States of America* **104**, 4112–7 (2007).
34. Paul, R. *et al.* Activation of the diguanylate cyclase PleD by phosphorylation-mediated dimerization. *The Journal of biological chemistry* **282**, 29170–7 (2007).

35. Wassmann, P. *et al.* Structure of BeF₃-modified response regulator PleD: implications for diguanylate cyclase activation, catalysis, and feedback inhibition. *Structure (London, England : 1993)* **15**, 915–27 (2007).
36. Merritt, J. H., Brothers, K. M., Kuchma, S. L. & O'Toole, G. A. SadC reciprocally influences biofilm formation and swarming motility via modulation of exopolysaccharide production and flagellar function. *Journal of bacteriology* **189**, 8154–64 (2007).
37. Ferreira, R. B. R., Antunes, L. C. M., Greenberg, E. P. & McCarter, L. L. *Vibrio parahaemolyticus* ScrC modulates cyclic dimeric GMP regulation of gene expression relevant to growth on surfaces. *Journal of bacteriology* **190**, 851–60 (2008).
38. Hogg, T., Mechold, U., Malke, H., Cashel, M. & Hilgenfeld, R. Conformational Antagonism between Opposing Active Sites in a Bifunctional RelA/SpoT Homolog Modulates (p)ppGpp Metabolism during the Stringent Response. *Cell* **117**, 57–68 (2004).
39. Hengge, R. Cyclic-di-GMP reaches out into the bacterial RNA world. *Science signaling* **3**, pe44 (2010).
40. Navarro, M. V. A. S., De, N., Bae, N., Wang, Q. & Sondermann, H. Structural analysis of the GGDEF-EAL domain-containing c-di-GMP receptor FimX. *Structure (London, England : 1993)* **17**, 1104–16 (2009).
41. Qi, Y. *et al.* Binding of cyclic diguanylate in the non-catalytic EAL domain of FimX induces a long-range conformational change. *The Journal of biological chemistry* **286**, 2910–7 (2011).
42. Kazmierczak, B. I., Lebron, M. B. & Murray, T. S. Analysis of FimX, a phosphodiesterase that governs twitching motility in *Pseudomonas aeruginosa*. *Molecular microbiology* **60**, 1026–43 (2006).
43. Lee, V. T. *et al.* A cyclic-di-GMP receptor required for bacterial exopolysaccharide production. *Molecular microbiology* **65**, 1474–84 (2007).
44. Baraquet, C., Murakami, K., Parsek, M. R. & Harwood, C. S. The FleQ protein from *Pseudomonas aeruginosa* functions as both a repressor and an activator to control gene expression from the *pel* operon promoter in response to c-di-GMP. *Nucleic acids research* 1–12 (2012).doi:10.1093/nar/gks384
45. Whitney, J. C. *et al.* Structure of the cytoplasmic region of PelD, a degenerate diguanylate cyclase receptor that regulates exopolysaccharide production in *Pseudomonas aeruginosa*. *The Journal of biological chemistry* (2012).doi:10.1074/jbc.M112.375378

46. Shikuma, N. J., Fong, J. C. N. & Yildiz, F. H. Cellular Levels and Binding of c-di-GMP Control Subcellular Localization and Activity of the *Vibrio cholerae* Transcriptional Regulator VpsT. *PLoS pathogens* **8**, e1002719 (2012).
47. Tao, F., He, Y.-W., Wu, D.-H., Swarup, S. & Zhang, L.-H. The cyclic nucleotide monophosphate domain of *Xanthomonas campestris* global regulator Clp defines a new class of cyclic di-GMP effectors. *Journal of bacteriology* **192**, 1020–9 (2010).
48. Leduc, J. L. & Roberts, G. P. Cyclic di-GMP allosterically inhibits the CRP-like protein (Clp) of *Xanthomonas axonopodis* pv. *citri*. *Journal of bacteriology* **191**, 7121–2 (2009).
49. He, Y.-W. & Zhang, L.-H. Quorum sensing and virulence regulation in *Xanthomonas campestris*. *FEMS microbiology reviews* **32**, 842–57 (2008).
50. Amikam, D. & Galperin, M. Y. PilZ domain is part of the bacterial c-di-GMP binding protein. *Bioinformatics (Oxford, England)* **22**, 3–6 (2006).
51. Pratt, J. T., Tamayo, R., Tischler, A. D. & Camilli, A. PilZ domain proteins bind cyclic diguanylate and regulate diverse processes in *Vibrio cholerae*. *The Journal of biological chemistry* **282**, 12860–70 (2007).
52. Benach, J. *et al.* The structural basis of cyclic diguanylate signal transduction by PilZ domains. *The EMBO journal* **26**, 5153–66 (2007).
53. Merighi, M., Lee, V. T., Hyodo, M., Hayakawa, Y. & Lory, S. The second messenger bis-(3'-5')-cyclic-GMP and its PilZ domain-containing receptor Alg44 are required for alginate biosynthesis in *Pseudomonas aeruginosa*. *Molecular microbiology* **65**, 876–95 (2007).
54. Paul, K., Nieto, V., Carlquist, W. C., Blair, D. F. & Harshey, R. M. The c-di-GMP binding protein YcgR controls flagellar motor direction and speed to affect chemotaxis by a “backstop brake” mechanism. *Molecular cell* **38**, 128–39 (2010).
55. Boehm, A. *et al.* Second messenger-mediated adjustment of bacterial swimming velocity. *Cell* **141**, 107–16 (2010).
56. Chen, A. G. Y., Sudarsan, N. & Breaker, R. R. Mechanism for gene control by a natural allosteric group I ribozyme. *RNA (New York, N.Y.)* **17**, 1967–72 (2011).
57. Smith, K. D. *et al.* Structural basis of ligand binding by a c-di-GMP riboswitch. *Nature structural & molecular biology* **16**, 1218–1223 (2009).
58. Smith, K. D., Shanahan, C. a, Moore, E. L., Simon, A. C. & Strobel, S. a Structural basis of differential ligand recognition by two classes of bis-(3'-5')-cyclic dimeric guanosine monophosphate-binding riboswitches. *Proceedings of the National Academy of Sciences of the United States of America* **108**, 7757–62 (2011).

59. Carpousis, A. J. The RNA degradosome of *Escherichia coli*: an mRNA-degrading machine assembled on RNase E. *Annual review of microbiology* **61**, 71–87 (2007).
60. Tuckerman, J. R., Gonzalez, G. & Gilles-Gonzalez, M.-A. Cyclic di-GMP activation of polynucleotide phosphorylase signal-dependent RNA processing. *Journal of molecular biology* **407**, 633–9 (2011).
61. Newell, P. D., Boyd, C. D., Sondermann, H. & O'Toole, G. a A c-di-GMP effector system controls cell adhesion by inside-out signaling and surface protein cleavage. *PLoS biology* **9**, e1000587 (2011).
62. Fazli, M. *et al.* The CRP/FNR family protein Bcam1349 is a c-di-GMP effector that regulates biofilm formation in the respiratory pathogen *Burkholderia cenocepacia*. *Molecular microbiology* **82**, 327–41 (2011).
63. Krasteva, P. V. *et al.* *Vibrio cholerae* VpsT regulates matrix production and motility by directly sensing cyclic di-GMP. *Science (New York, N.Y.)* **327**, 866–8 (2010).
64. Shin, J.-S., Ryu, K.-S., Ko, J., Lee, A. & Choi, B.-S. Structural characterization reveals that a PilZ domain protein undergoes substantial conformational change upon binding to cyclic dimeric guanosine monophosphate. *Protein science : a publication of the Protein Society* **20**, 270–7 (2011).
65. Fang, X. & Gomelsky, M. A post-translational, c-di-GMP-dependent mechanism regulating flagellar motility. *Molecular microbiology* **76**, 1295–305 (2010).
66. Ramelot, T. A. *et al.* SHORT COMMUNICATION NMR Structure and Binding Studies Confirm that PA4608 from *Pseudomonas aeruginosa* is a PilZ Domain and a c-di-GMP Binding Protein. *Bioinformatics* **271**, 266–271 (2007).
67. Li, T.-N., Chin, K.-H., Liu, J.-H., Wang, A. H.-J. & Chou, S.-H. XC1028 from *Xanthomonas campestris* adopts a PilZ domain-like structure without a c-di-GMP switch. *Proteins* **75**, 282–8 (2009).
68. Li, T.-N. *et al.* A novel tetrameric PilZ domain structure from xanthomonads. *PloS one* **6**, e22036 (2011).
69. Ko, J. *et al.* Structure of PP4397 reveals the molecular basis for different c-di-GMP binding modes by Pilz domain proteins. *Journal of molecular biology* **398**, 97–110 (2010).
70. Guzzo, C. R., Salinas, R. K., Andrade, M. O. & Farah, C. S. PILZ protein structure and interactions with PILB and the FIMX EAL domain: implications for control of type IV pilus biogenesis. *Journal of molecular biology* **393**, 848–66 (2009).

71. Ryan, R. P., Tolker-Nielsen, T. & Dow, J. M. When the PilZ don't work: effectors for cyclic di-GMP action in bacteria. *Trends in Microbiology* 1–8 (2012).doi:10.1016/j.tim.2012.02.008
72. Merker, R. I. & Smit, J. Characterization of the adhesive holdfast of marine and freshwater caulobacters. *Applied and environmental microbiology* **54**, 2078–85 (1988).
73. Degnen, S. T. & Newton, A. Chromosome replication during development in *Caulobacter crescentus*. *Journal of Molecular Biology* **64**, 671–680 (1972).
74. McAdams, H. H. & Shapiro, L. System-level design of bacterial cell cycle control. *FEBS Letters* **583**, 3984–3991 (2009).
75. Marczyński, G. T. Chromosome methylation and measurement of faithful, once and only once per cell cycle chromosome replication in *Caulobacter crescentus*. *Journal of bacteriology* **181**, 1984–93 (1999).
76. Aldridge, P., Paul, R., Goymer, P., Rainey, P. & Jenal, U. Role of the GGDEF regulator PleD in polar development of *Caulobacter crescentus*. *Molecular microbiology* **47**, 1695–708 (2003).
77. Levi, A. & Jenal, U. Holdfast formation in motile swarmer cells optimizes surface attachment during *Caulobacter crescentus* development. *Journal of bacteriology* **188**, 5315–8 (2006).
78. Jacobs-Wagner, C. Regulatory proteins with a sense of direction: cell cycle signalling network in *Caulobacter*. *Molecular Microbiology* **51**, 7–13 (2003).
79. Quon, K. C., Marczyński, G. T. & Shapiro, L. Cell cycle control by an essential bacterial two-component signal transduction protein. *Cell* **84**, 83–93 (1996).
80. Domian, I. J., Quon, K. C. & Shapiro, L. Cell type-specific phosphorylation and proteolysis of a transcriptional regulator controls the G1-to-S transition in a bacterial cell cycle. *Cell* **90**, 415–24 (1997).
81. Marczyński, G. T. & Shapiro, L. Cell-cycle control of a cloned chromosomal origin of replication from *Caulobacter crescentus*. *Journal of Molecular Biology* **226**, 959–977 (1992).
82. Laub, M. T., Chen, S. L., Shapiro, L. & McAdams, H. H. Genes directly controlled by CtrA, a master regulator of the *Caulobacter* cell cycle. *Proceedings of the National Academy of Sciences of the United States of America* **99**, 4632–7 (2002).
83. Jones, S. E., Ferguson, N. L. & Alley, M. R. New members of the ctrA regulon: the major chemotaxis operon in *Caulobacter* is CtrA dependent. *Microbiology (Reading, England)* **147**, 949–58 (2001).

84. Lenz, P. & Sogaard-Andersen, L. Temporal and spatial oscillations in bacteria. *Nature Reviews Microbiology* **9**, 565–577 (2011).
85. Kelly, a J., Sackett, M. J., Din, N., Quardokus, E. & Brun, Y. V. Cell cycle-dependent transcriptional and proteolytic regulation of FtsZ in *Caulobacter*. *Genes & development* **12**, 880–93 (1998).
86. Jenal, U. The role of proteolysis in the *Caulobacter crescentus* cell cycle and development. *Research in microbiology* **160**, 687–95 (2009).
87. Goley, E. D., Toro, E., McAdams, H. H. & Shapiro, L. Dynamic chromosome organization and protein localization coordinate the regulatory circuitry that drives the bacterial cell cycle. *Cold Spring Harbor symposia on quantitative biology* **74**, 55–64 (2009).
88. Quon, K., Yang, B. & Domian, I. Negative control of bacterial DNA replication by a cell cycle regulatory protein that binds at the chromosome origin. *Proceedings of the* **95**, 120–125 (1998).
89. Zweiger, G. & Shapiro, L. Expression of *Caulobacter dnaA* as a function of the cell cycle. *Journal of bacteriology* **176**, 401–8 (1994).
90. Gorbatyuk, B. & Marczynski, G. T. Regulated degradation of chromosome replication proteins DnaA and CtrA in *Caulobacter crescentus*. *Molecular microbiology* **55**, 1233–45 (2005).
91. Dürig, A. Second messenger mediated spatiotemporal control of cell cycle and development Philosophisch-Naturwissenschaftlichen Fakultät. (2008).
92. Collier, J., Murray, S. R. & Shapiro, L. DnaA couples DNA replication and the expression of two cell cycle master regulators. *The EMBO journal* **25**, 346–56 (2006).
93. Crosson, S., Mcadams, H. & Shapiro, L. genetic oscillator and the regulation of cell cycle progression in *Caulobacter crescentu*. *Cell Cycle* 55–57 (2004).
94. Holtzendorff, J. *et al.* Oscillating global regulators control the genetic circuit driving a bacterial cell cycle. *Science (New York, N.Y.)* **304**, 983–7 (2004).
95. Collier, J., McAdams, H. H. & Shapiro, L. A DNA methylation ratchet governs progression through a bacterial cell cycle. *Proceedings of the National Academy of Sciences of the United States of America* **104**, 17111–6 (2007).
96. Domian, I. J., Reisenauer, a & Shapiro, L. Feedback control of a master bacterial cell-cycle regulator. *Proceedings of the National Academy of Sciences of the United States of America* **96**, 6648–53 (1999).

-
97. Reisenauer, A. & Shapiro, L. DNA methylation affects the cell cycle transcription of the CtrA global regulator in *Caulobacter*. *The EMBO journal* **21**, 4969–77 (2002).
 98. Siam, R. & Marczyński, G. T. Cell cycle regulator phosphorylation stimulates two distinct modes of binding at a chromosome replication origin. *The EMBO journal* **19**, 1138–47 (2000).
 99. Gora, K. G. *et al.* A cell-type-specific protein-protein interaction modulates transcriptional activity of a master regulator in *Caulobacter crescentus*. *Molecular cell* **39**, 455–67 (2010).
 100. Tan, M. H., Kozdon, J. B., Shen, X., Shapiro, L. & McAdams, H. H. An essential transcription factor, SciP, enhances robustness of *Caulobacter* cell cycle regulation. *Proceedings of the National Academy of Sciences of the United States of America* **107**, 18985–90 (2010).
 101. Jacobs, C., Domian, I. J., Maddock, J. R. & Shapiro, L. Cell cycle-dependent polar localization of an essential bacterial histidine kinase that controls DNA replication and cell division. *Cell* **97**, 111–20 (1999).
 102. Paul, R. *et al.* Allosteric regulation of histidine kinases by their cognate response regulator determines cell fate. *Cell* **133**, 452–61 (2008).
 103. Wheeler, R. T. & Shapiro, L. Differential localization of two histidine kinases controlling bacterial cell differentiation. *Molecular cell* **4**, 683–94 (1999).
 104. Matroule, J.-Y., Lam, H., Burnette, D. T. & Jacobs-Wagner, C. Cytokinesis monitoring during development; rapid pole-to-pole shuttling of a signaling protein by localized kinase and phosphatase in *Caulobacter*. *Cell* **118**, 579–90 (2004).
 105. Ohta, N., Lane, T., Ninfa, E. G., Sommer, J. M. & Newton, A. A histidine protein kinase homologue required for regulation of bacterial cell division and differentiation. *Proceedings of the National Academy of Sciences of the United States of America* **89**, 10297–301 (1992).
 106. Hecht, G., Lane, T., Ohta, N. & Sommer, J. An essential single domain response regulator required for normal cell division and differentiation in *Caulobacter crescentus*. *The EMBO* **14**, 3915–3924 (1995).
 107. Wu, J., Ohta, N. & Newton, A. An essential, multicomponent signal transduction pathway required for cell cycle regulation in *Caulobacter*. *Proceedings of the National Academy of Sciences of the United States of America* **95**, 1443–8 (1998).

-
108. Tsokos, C. G., Perchuk, B. S. & Laub, M. T. A dynamic complex of signaling proteins uses polar localization to regulate cell-fate asymmetry in *Caulobacter crescentus*. *Developmental cell* **20**, 329–41 (2011).
 109. Iniesta, A. a, Hillson, N. J. & Shapiro, L. Cell pole-specific activation of a critical bacterial cell cycle kinase. *Proceedings of the National Academy of Sciences of the United States of America* **107**, 7012–7 (2010).
 110. Jenal, U. & Fuchs, T. An essential protease involved in bacterial cell-cycle control. *The EMBO journal* **17**, 5658–69 (1998).
 111. Chien, P., Perchuk, B. S., Laub, M. T., Sauer, R. T. & Baker, T. a Direct and adaptor-mediated substrate recognition by an essential AAA+ protease. *Proceedings of the National Academy of Sciences of the United States of America* **104**, 6590–5 (2007).
 112. Ortega, J., Singh, S. K., Ishikawa, T., Maurizi, M. R. & Steven, a C. Visualization of substrate binding and translocation by the ATP-dependent protease, ClpXP. *Molecular cell* **6**, 1515–21 (2000).
 113. Wang, J., Hartling, J. A. & Flanagan, J. M. ° Resolution The Structure of ClpP at 2 . 3 Å Suggests a Model for ATP-Dependent Proteolysis. *Cell* **91**, 447–456 (1997).
 114. Flynn, J. M., Neher, S. B., Kim, Y. I., Sauer, R. T. & Baker, T. a Proteomic discovery of cellular substrates of the ClpXP protease reveals five classes of ClpX-recognition signals. *Molecular cell* **11**, 671–83 (2003).
 115. McGrath, P. T., Iniesta, A. a, Ryan, K. R., Shapiro, L. & McAdams, H. H. A dynamically localized protease complex and a polar specificity factor control a cell cycle master regulator. *Cell* **124**, 535–47 (2006).
 116. Iniesta, A. A., McGrath, P. T., Reisenauer, A., McAdams, H. H. & Shapiro, L. A phospho-signaling pathway controls the localization and activity of a protease complex critical for bacterial cell cycle progression. *Proceedings of the National Academy of Sciences of the United States of America* **103**, 10935–40 (2006).
 117. Biondi, E. G. *et al.* Regulation of the bacterial cell cycle by an integrated genetic circuit. *Nature* **444**, 899–904 (2006).
 118. Christen, M. *et al.* Asymmetrical distribution of the second messenger c-di-GMP upon bacterial cell division. *Science (New York, N.Y.)* **328**, 1295–7 (2010).
 119. Aldridge, P. & Jenal, U. Cell cycle-dependent degradation of a flagellar motor component requires a novel-type response regulator. *Molecular microbiology* **32**, 379–91 (1999).

120. Sommer, J. M. & Newton, a Turning off flagellum rotation requires the pleiotropic gene pleD: pleA, pleC, and pleD define two morphogenic pathways in *Caulobacter crescentus*. *Journal of bacteriology* **171**, 392–401 (1989).
121. Berg, H. C. The rotary motor of bacterial flagella. *Annual review of biochemistry* **72**, 19–54 (2003).
122. Mot, R. & Vanderleyden, J. The C-terminal sequence conservation between OmpA-related outer membrane proteins and MotB suggests a common function in both Gram-positive and Gram-negative bacteria, possibly in the interaction of these domains with peptidoglycan. *Molecular Microbiology* **12**, 333–334 (1994).
123. Suzuki, H., Yonekura, K. & Namba, K. Structure of the rotor of the bacterial flagellar motor revealed by electron cryomicroscopy and single-particle image analysis. *Journal of molecular biology* **337**, 105–13 (2004).
124. Ueno, T., Oosawa, K. & Aizawa, S. M ring, S ring and proximal rod of the flagellar basal body of *Salmonella typhimurium* are composed of subunits of a single protein, FliF. *Journal of molecular biology* **227**, 672–7 (1992).
125. Lloyd, S. a, Tang, H., Wang, X., Billings, S. & Blair, D. F. Torque generation in the flagellar motor of *Escherichia coli*: evidence of a direct role for FliG but not for FliM or FliN. *Journal of bacteriology* **178**, 223–31 (1996).
126. Park, S.-Y., Lowder, B., Bilwes, A. M., Blair, D. F. & Crane, B. R. Structure of FliM provides insight into assembly of the switch complex in the bacterial flagella motor. *Proceedings of the National Academy of Sciences of the United States of America* **103**, 11886–91 (2006).
127. Macnab, R. M. How bacteria assemble flagella. *Annual review of microbiology* **57**, 77–100 (2003).
128. Homma, M., Komeda, Y., Iino, T. & Macnab, R. M. typhimurium is a flagellar basal body The flaFIX Gene Product of *Salmonella typhimurium* Is a Flagellar Basal Body Component with a Signal Peptide for Export. *Society* **169**, (1987).
129. Jones, C. J., Homma, M. & Macnab, R. M. L-, P-, and M-ring proteins of the flagellar basal body of *Salmonella typhimurium*: gene sequences and deduced protein sequences. *Journal of bacteriology* **171**, 3890–900 (1989).
130. Fujii, T., Kato, T. & Namba, K. Specific arrangement of alpha-helical coiled coils in the core domain of the bacterial flagellar hook for the universal joint function. *Structure (London, England : 1993)* **17**, 1485–93 (2009).

131. Faulds-Pain, A. *et al.* Flagellin redundancy in *Caulobacter crescentus* and its implications for flagellar filament assembly. *Journal of bacteriology* **193**, 2695–707 (2011).
132. Minamino, T. & Namba, K. Self-assembly and type III protein export of the bacterial flagellum. *Journal of molecular microbiology and biotechnology* **7**, 5–17 (2004).
133. Mohr, C. D., Jenal, U. & Shapiro, L. Flagellar assembly in *Caulobacter crescentus* : a basal body P-ring null mutation affects stability of the L-ring protein . These include : Flagellar Assembly in *Caulobacter crescentus* : a Basal Body P-Ring Null Mutation Affects Stability of the L-Ring Pro. *Microbiology* **178**, (1996).
134. England, J. C. & Gober, J. W. Cell cycle control of cell morphogenesis in *Caulobacter*. *Current opinion in microbiology* **4**, 674–80 (2001).
135. Ramakrishnan, G. & Newton, a FlbD of *Caulobacter crescentus* is a homologue of the NtrC (NRI) protein and activates sigma 54-dependent flagellar gene promoters. *Proceedings of the National Academy of Sciences of the United States of America* **87**, 2369–73 (1990).
136. Muir, R. E., Easter, J. & Gober, J. W. The trans-acting flagellar regulatory proteins, FliX and FlbD, play a central role in linking flagellar biogenesis and cytokinesis in *Caulobacter crescentus*. *Microbiology (Reading, England)* **151**, 3699–711 (2005).
137. Muir, R. E., O'Brien, T. M. & Gober, J. W. The *Caulobacter crescentus* flagellar gene, *fliX*, encodes a novel trans-acting factor that couples flagellar assembly to transcription. *Molecular microbiology* **39**, 1623–37 (2001).
138. Xu, Z., Dutton, R. J. & Gober, J. W. Direct interaction of FliX and FlbD is required for their regulatory activity in *Caulobacter crescentus*. *BMC microbiology* **11**, 89 (2011).
139. Mangan, E. K. *et al.* FlbT couples flagellum assembly to gene expression in *Caulobacter crescentus*. *Journal of bacteriology* **181**, 6160–70 (1999).
140. Anderson, P. E. & Gober, J. W. FlbT, the post-transcriptional regulator of flagellin synthesis in *Caulobacter crescentus*, interacts with the 5' untranslated region of flagellin mRNA. *Molecular microbiology* **38**, 41–52 (2000).
141. Kanbe, M., Shibata, S., Umino, Y., Jenal, U. & Aizawa, S.-I. Protease susceptibility of the *Caulobacter crescentus* flagellar hook-basal body: a possible mechanism of flagellar ejection during cell differentiation. *Microbiology (Reading, England)* **151**, 433–8 (2005).

142. Huitema, E., Pritchard, S., Matteson, D., Radhakrishnan, S. K. & Viollier, P. H. Bacterial birth scar proteins mark future flagellum assembly site. *Cell* **124**, 1025–37 (2006).
143. Lam, H., Schofield, W. B. & Jacobs-Wagner, C. A landmark protein essential for establishing and perpetuating the polarity of a bacterial cell. *Cell* **124**, 1011–23 (2006).
144. Davis, N. J. & Viollier, P. H. Probing flagellar promoter occupancy in wild-type and mutant *Caulobacter crescentus* by chromatin immunoprecipitation. *FEMS microbiology letters* **319**, 146–52 (2011).
145. Iniesta, A. a & Shapiro, L. A bacterial control circuit integrates polar localization and proteolysis of key regulatory proteins with a phospho-signaling cascade. *Proceedings of the National Academy of Sciences of the United States of America* **105**, 16602–7 (2008).
146. Obuchowski, P. PflI, a protein involved in flagellar positioning in *Caulobacter crescentus*. *Journal of bacteriology* **190**, 1718–29 (2008).
147. Blair, D. F. How Bacteria Sense and Swim. *Annual Review of Microbiology* **49**, 489–520 (1995).
148. Briegel, A. *et al.* Location and architecture of the *Caulobacter crescentus* chemoreceptor array. *Molecular microbiology* **69**, 30–41 (2008).
149. Anderson, J. K., Smith, T. G. & Hoover, T. R. Sense and sensibility : flagellum-mediated gene regulation. **18**, 1–17 (2011).
150. Ely, B. Genetics of *Caulobacter crescentus*. *Bacterial Genetic Systems Volume 204*, 372–384 (1991).
151. Jenal, U. & Shapiro, L. Cell cycle-controlled proteolysis of a flagellar motor protein that is asymmetrically distributed in the *Caulobacter* predivisional cell. *The EMBO journal* **15**, 2393–406 (1996).
152. Gietz, R. D., Triggs-Raine, B., Robbins, a, Graham, K. C. & Woods, R. a Identification of proteins that interact with a protein of interest: applications of the yeast two-hybrid system. *Molecular and cellular biochemistry* **172**, 67–79 (1997).
153. Kudryashev, M., Cyrklaff, M., Wallich, R., Baumeister, W. & Frischknecht, F. Distinct in situ structures of the *Borrelia* flagellar motor. *Journal of Structural Biology* **169**, 54–61 (2010).
154. James, P., Halladay, J. & Craig, E. A. Genomic Libraries and a Host Strain Designed for Highly Efficient Two-Hybrid Selection in Yeast. *Genetics* **144**, 1425–1436 (1996).

155. Leclerc, G., Wang, S. P. & Ely, B. A new class of *Caulobacter crescentus* flagellar genes. *Journal of bacteriology* **180**, 5010–9 (1998).
156. Johnson, R. C., Ferber, D. M. & Ely, B. Synthesis and assembly of flagellar components by *Caulobacter crescentus* motility mutants. *Journal of bacteriology* **154**, 1137–44 (1983).
157. Schirm, M. *et al.* Structural, genetic and functional characterization of the flagellin glycosylation process in *Helicobacter pylori*. *Molecular Microbiology* **48**, 1579–1592 (2003).
158. Gentner, M., Allan, M. G., Zaehring, F., Schirmer, T. & Grzesiek, S. Oligomer formation of the bacterial second messenger c-di-GMP: reaction rates and equilibrium constants indicate a monomeric state at physiological concentrations. *Journal of the American Chemical Society* **134**, 1019–29 (2012).

5 Appendices

5.1 De- and repolarization mechanism of flagellar morphogenesis during a bacterial cell cycle

Downloaded from genesdev.cshlp.org on December 15, 2014 - Published by Cold Spring Harbor Laboratory Press

De- and repolarization mechanism of flagellar morphogenesis during a bacterial cell cycle

Nicole J. Davis,^{1,5} Yaniv Cohen,^{2,5,6} Stefano Sanselicio,^{3,6} Coralie Fumeaux,³ Shogo Ozaki,² Jennifer Luciano,² Ricardo C. Guerrero-Ferreira,⁴ Elizabeth R. Wright,⁴ Urs Jenal,^{2,7} and Patrick. H. Viollier^{1,3,7}

¹Department of Molecular Biology and Microbiology, School of Medicine, Case Western Reserve University, Cleveland, Ohio 44106, USA; ²Biozentrum of the University of Basel, 4056 Basel, Switzerland; ³Department Microbiology and Molecular Medicine, Institute of Genetics and Genomics in Geneva (iGE3), Faculty of Medicine/Centre Médical Universitaire, University of Geneva, 1211 Genève 4, Switzerland; ⁴Division of Pediatric Infectious Diseases, Department of Pediatrics, Emory University School of Medicine, Children's Healthcare of Atlanta, Atlanta, Georgia 30322, USA

Eukaryotic morphogenesis is seeded with the establishment and subsequent amplification of polarity cues at key times during the cell cycle, often using (cyclic) nucleotide signals. We discovered that flagellum de- and repolarization in the model prokaryote *Caulobacter crescentus* is precisely orchestrated through at least three spatiotemporal mechanisms integrated at TipF. We show that TipF is a cell cycle-regulated receptor for the second messenger—bis-(3'-5')-cyclic dimeric guanosine monophosphate (c-di-GMP)—that perceives and transduces this signal through the degenerate c-di-GMP phosphodiesterase (EAL) domain to nucleate polar flagellum biogenesis. Once c-di-GMP levels rise at the G1 → S transition, TipF is activated, stabilized, and polarized, enabling the recruitment of downstream effectors, including flagellar switch proteins and the PflI positioning factor, at a preselected pole harboring the TipN landmark. These c-di-GMP-dependent events are coordinated with the onset of *tipF* transcription in early S phase and together enable the correct establishment and robust amplification of TipF-dependent polarization early in the cell cycle. Importantly, these mechanisms also govern the timely removal of TipF at cell division coincident with the drop in c-di-GMP levels, thereby resetting the flagellar polarization state in the next cell cycle after a preprogrammed period during which motility must be suspended.

[*Keywords:* asymmetric division; c-di-GMP; *Caulobacter*; cell cycle; flagellum; morphogenesis; polarity]

Supplemental material is available for this article.

Received May 22, 2013; revised version accepted August 23, 2013.

Cell polarity is fundamental to intracellular organization and morphogenesis in all forms of life, yet little is known about how polarity-dependent cues are implemented, reinforced, and removed during the bacterial cell cycle. Eukaryotic cells interpret (cyclic) nucleotide signals to regulate polarity-dependent processes via effectors such as kinases and/or GTPases dictated in response to spatiotemporal cues provided by prepositioned "landmark" proteins and cell cycle regulators (Slaughter et al. 2009; Charest and Firtel 2010; St Johnston and Ahringer 2010; Amato et al. 2011; Ji and Tulin 2012). Here we unearth a polarized cyclic nucleotide signaling pathway cued by bis-(3'-5')-cyclic dimeric guanosine monophosphate

(c-di-GMP) that first triggers and reinforces and later resets flagellar polarity during a bacterial cell cycle.

The Gram-negative α -proteobacterium *Caulobacter crescentus* (henceforth, *Caulobacter*) is an ideal model system to study how polarization is coordinated with cell cycle progression. At the predivisional cell stage, *Caulobacter* is overtly polarized, bearing a cylindrical extension of the cell envelope (the stalk) at the old pole and a newly assembled flagellum whose rotation is activated at cytokinesis at the opposite pole (Tsokos and Laub 2012). Cytokinesis yields a motile swarmer cell that resides in a G1-like, nonreplicative state and a dividing stalked cell engaged in S phase (Fig. 1A). Two master transcriptional regulators of the cell cycle, CtrA and GcrA, reinforce the transcriptional program at sequential stages of the cell cycle (Quon et al. 1996; Laub et al. 2000; Holtzendorff et al. 2004). CtrA is present in G1 phase, proteolytically removed during the G1 → S transition, and reappears later in S phase (Figs. 1A, 7D [below]). In

⁵These authors contributed equally to this work.

⁶These authors contributed equally to this work.

⁷Corresponding authors

E-mail patrick.viollier@unige.ch

E-mail urs.jenal@unibas.ch

Article is online at <http://www.genesdev.org/cgi/doi/10.1101/gad.222679.113>.

Davis et al.

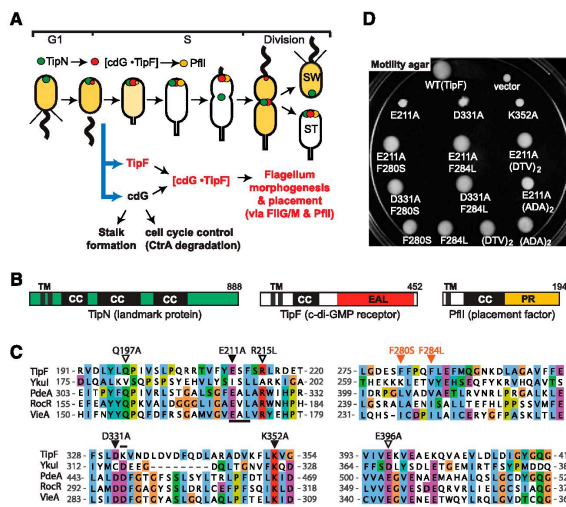


Figure 1. Localization of TipN, TipF, and PflI to the flagellated pole. (A) Dynamic protein localization of TipN, TipF, and PflI and its coordination with other cell cycle events in *C. crescentus*. TipN (green) localized at the nonflagellated pole recruits newly synthesized TipF (red), which in turn recruits the PflI flagellar positioning protein (yellow). Thick blue arrows indicate the synthesis of TipF (by GcrA) and c-di-GMP. (B) Domain organization of TipN, TipF, and PflI. Shown are the predicted transmembrane domains (TM; gray), coiled-coil domains (CC; black), PDE domain (EAL; red), and proline-rich domain (PR; yellow). (C) Alignment of the EAL domains from TipF and the c-di-GMP PDEs PdeA of *C. crescentus*, VieA of *Vibrio cholerae*, RocR of *Pseudomonas aeruginosa*, and YkuI of *Bacillus subtilis*. Key residues that are predicted to be required for PDE activity (empty arrowheads) or required for c-di-GMP binding (filled black) are marked. Residues that bypass the requirement of E211 or D331 for motility (red triangles), the defining EAL motif, and the K332 residue of the conserved Asp-Asp loop (underlined) are indicated. (D) Motility assay of $\Delta tipF$ mutants harboring plasmids encoding wild-type (WT) or single- or double-mutant

TipF. DTV and ADA denote the triple duplications of DTV or ADA residues at positions 121–124 or 128–130, respectively. Overnight cultures were spotted on PYE swarm agar plates and incubated for 60 h at 30°C. Compact swarms indicate the motility defect caused by mutations in the c-di-GMP-binding site, whereas the suppressive mutations yield diffuse and enlarged swarms.

contrast, GcrA accumulates during the G1 → S transition, inducing the synthesis of CtrA along with polarity and other cell cycle proteins (McAdams and Shapiro 2011), and is then eliminated from G1 progeny cells along with c-di-GMP (Paul et al. 2008; Christen et al. 2010).

During the G1 → S transition, the flagellum is shed to permit cells to immobilize to surfaces using an adhesive polar structure. The flagellum is then resynthesized at the new pole in late S phase following this preprogrammed nonmotile period. CtrA induces the synthesis of early flagellar structural constituents, including the FliF MS ring protein and two components of the switch complex (FliG and FliM) [see Fig. 3A, below]. The newly synthesized flagellar parts are assembled from the inside of the cell outward, first with an organizational platform in the inner membrane (the MS ring) to which the switch complex on the cytoplasmic side of the membrane is tethered (Chevance and Hughes 2008; Brown et al. 2011). The assembly of subsequent structures follows suit, ultimately ending with the elaboration of the external parts, such as the hook and the flagellar filament.

Superimposed on these temporal patterns are spatial cues that guide flagellar proteins to the appropriate site of assembly at the new cell pole opposite the stalk (Fig. 1A). The new cell pole harbors TipN, a polytopic coiled-coil protein that is deposited at the new pole as it is generated during cytokinesis (Huitema et al. 2006; Lam et al. 2006). At cytokinesis, TipN redistributes to the division plane from the poles, ensuring that cell polarity cues are avail-

able for the flagellar polarization in the next cell cycle. Indeed, flagella are mispositioned in the absence of *tipN*, indicating that TipN is required for the proper placement, but not the assembly, of the flagellum (Huitema et al. 2006; Lam et al. 2006). A flagellar misplacement defect has also been observed in mutants lacking the PflI positioning factor, a bitopic membrane protein with a proline-rich domain at the C terminus facing the cytoplasm that is localized to the future flagellated pole before the synthesis of early flagellar components (Obuchowski and Jacobs-Wagner 2008). While the spatial relationship between TipN and PflI remains unexplored, TipN recruits TipF, a polytopic membrane protein that positively regulates flagellum biogenesis (Huitema et al. 2006). In the absence of TipN, TipF localizes to sites of misplaced flagella, raising the possibility that mislocalized TipF is responsible for the flagellar misplacement phenotype of a *tipN* mutant. This is supported by the observation that *tipF* deletion mutants lack external flagellar structures such as the hook and filament (Huitema et al. 2006).

TipF features a C-terminal and cytoplasmic EAL [also known as DUF2] domain that, in related proteins, confers c-di-GMP-specific phosphodiesterase (PDE) activity (Hengge 2009; Schirmer and Jenal 2009; Boyd and O'Toole 2012). The levels of c-di-GMP are modulated by diguanylate cyclases (DGCs) that synthesize c-di-GMP from GTP and PDEs that hydrolyze c-di-GMP into linear pGpG. In *Caulobacter*, multiple DGCs and PDEs determine c-di-GMP levels during the cell cycle to promote develop-

Mechanism of flagellum de- and repolarization

ment and cell cycle progression (Paul et al. 2004, 2008; Abel et al. 2011). c-di-GMP levels are low in G1 cells but peak at the G1 → S transition and decline thereafter (Paul et al. 2008; Christen et al. 2010). While c-di-GMP binds to various receptor proteins to curb flagellar rotation (Wolfe and Visick 2008; Boehm et al. 2010; Fang and Gomelsky 2010; Paul et al. 2010), the spatiotemporal mechanism underlying c-di-GMP-induced flagellum morphogenesis has not been resolved.

Here we show that c-di-GMP controls the activation, polarization, and stabilization of the flagellar regulator TipF (Huitema et al. 2006). We found that TipF is a receptor for c-di-GMP that peaks at the G1 → S transition and show that TipF•c-di-GMP seeds polar flagellar assembly by recruiting the PflI placement factor (Obuchowski and Jacobs-Wagner 2008) and components of the flagellar switch into a complex with TipN, a landmark protein that is prepositioned at the newborn pole (Huitema et al. 2006; Lam et al. 2006). Importantly, we found that c-di-GMP-induced stabilization and polarization of TipF is amplified with the coordinated transcription of the *tipF* gene and thus is tuned to other c-di-GMP-dependent developmental events that occur at the G1 → S transition (Paul et al. 2004, 2008; Duerig et al. 2009).

Results

c-di-GMP binds and activates TipF

Initial hints into the mechanism of TipF-mediated flagellum biogenesis came from comparisons of the TipF primary structure with known PDEs. TipF features a Lys at position 332 instead of an Asp in related proteins (Fig.

1C), and a Glu-Ser-Phe (ESF, residues 211–213) triplet replaces the defining Glu-Ala-Leu (EAL) motif. The highly conserved Asp331–Asp332 motif is a hallmark of active PDEs, with both residues being involved in coordinating the two metal ions in the catalytic center (Barends et al. 2009). To explore whether the sequence conservation reflects a functional requirement for the residues at these positions, we engineered alanine mutations at several conserved positions implicated or not in coordinating the cofactor (Mg^{2+} or Mn^{2+}), the substrate, and/or the nucleophile (E211A, D331A, and K352A) (Fig. 1C, filled triangles). Neither of these mutant proteins could support TipF function (motility on 0.3% soft agar plates) when expressed in a $\Delta tipF$ background from P_{xyI} on a low-copy plasmid, indicating that these residues play a key role in TipF function (Fig. 1D).

To test whether TipF is an active PDE, we purified the soluble hexa-histidine (His₆)-tagged form of TipF lacking the first 115 residues, including the two predicted membrane-spanning segments, and the E211A mutant derivative from *Escherichia coli*. Circular dichroism (CD) spectra suggested that the secondary structures of purified TipF wild type and E211A mutant were unchanged (Supplemental Fig. S1A). We then assayed both proteins for PDE activity by high-pressure liquid chromatography (HPLC) analysis with the c-di-GMP substrate (Fig. 2A). No cleavage of c-di-GMP to the linear form pGpG was observed with either wild-type TipF or the E211A mutant (Fig. 2A, right panel) even after extended incubation times of up to 24 h (Supplemental Fig. S1B,C). In contrast, the control PDE YahA from *E. coli* converted all of the c-di-GMP to pGpG in <5 min (Fig. 2A, left panel).

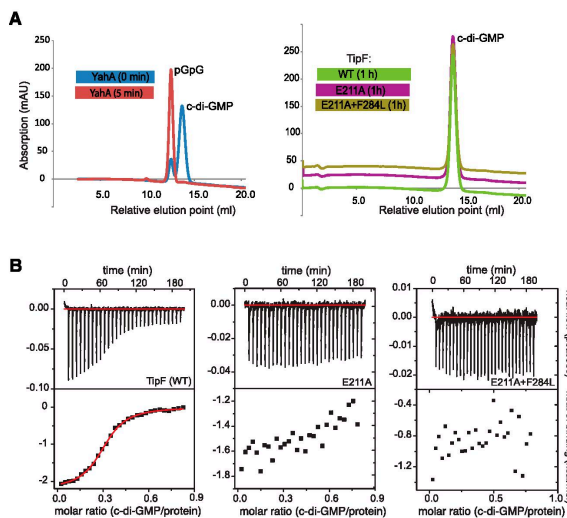


Figure 2. TipF is enzymatically inactive but binds c-di-GMP. (A) c-di-GMP hydrolytic activity is not detected in recombinant (soluble) TipF but is in the control PDE YahA. (Left panel) Purified proteins (1 μ M) were incubated with c-di-GMP for 5 min and then separated on a ResourceQ column to observe the cleavage product pGpG. No pGpG was detected after 1 h of incubation with wild-type (WT) or mutant (E211A or E211A/F284L) TipF with c-di-GMP. (Right panel) TipF with c-di-GMP. (B) ITC experiments showing that c-di-GMP binds to the soluble portion of wild-type TipF but not to the mutant derivatives E211A or E211A/F284L. The top panels show the raw ITC data curves collected at 25°C in binding buffer [50 mM Tris/HCl, 50 mM NaCl at pH 8.0]. The bottom panels show the integrated titration peaks fitted to a one-site binding model (solid line). The average dissociation constant (K_D) of TipF to c-di-GMP was estimated at 0.4 (± 0.2 μ M), the stoichiometry of binding (n) was estimated at 0.35 (± 0.1), and the enthalpy of reaction was estimated at -2.1 (± 0.3 kcal/mol).

Davis et al.

In the absence of detectable PDE activity, we asked whether wild-type TipF or the E211A mutant can bind c-di-GMP using an isothermal titration calorimetry (ITC)-based binding assay (Fig. 2B). Successive injections of 10 μ L of a 118 μ M solution of c-di-GMP solution into the ITC reaction chamber containing 32.5 μ M wild-type TipF was accompanied by the characteristic heat release, reflecting specific and high-affinity binding of c-di-GMP (Fig. 2B, left panel). The resulting integrated titration peaks were fitted to a sigmoidal enthalpy curve, and a dissociation constant (K_D) of 0.4 (± 0.2 μ M) for c-di-GMP was derived for wild-type TipF. In contrast, only background (nonspecific) heat release was observed when an equimolar amount of TipF (E211A) was injected into the chamber (Fig. 2B, middle panel [note the different scales in the panels]). Together, these results demonstrate that TipF does not have PDE activity under the conditions tested and that wild-type TipF, but not the E211A derivative, binds c-di-GMP with high affinity. On the basis of these results, we hypothesize that c-di-GMP binding is necessary for TipF to signal motility and that the E211A mutant is nonfunctional because it can no longer bind and be activated by c-di-GMP. In support of this view, we found that depleting *Caulobacter* cells of c-di-GMP phenocopies the localization and flagellar assembly defect caused by the absence of TipF or the “c-di-GMP-blind” E211A mutant (Fig. 6E, below).

If TipF is activated without hydrolyzing c-di-GMP, then mutations that are known to specifically cripple catalytic activity of PDEs, but not c-di-GMP binding, should not affect TipF function. To test this prediction, we engineered mutants Q197A, R215L, and E396A (Fig. 1C, open triangles) and found that the mutant proteins R215L and E396A confer motility in $\Delta tipF$ cells indistinguishable from that of wild-type TipF, while Q197A also supported motility but with reduced efficiency (data not shown). Taken together, we conclude that TipF binds c-di-GMP and that binding is required for flagellar functions.

TipF acts early in polar flagellum assembly

Since previous transmission electron micrographs showed the external structures, the flagellar hook, and the filament (Fig. 3A) to be missing from $\Delta tipF$ cells (Huitema et al. 2006), we wondered whether the assembly of internal flagellar (sub)structures also requires TipF. To this end, we conducted electron cryotomography (ECT) of wild-type and $\Delta tipF$ cells by ECT (Fig. 3B; Supplemental Fig. S2A,B; see the Supplemental Movies), a high-resolution imaging method that preserves cellular structures in their native (cryogenically vitrified) state and reveals them owing to the natural contrast from electron density. We subjected two-dimensional (2D) projections of three-

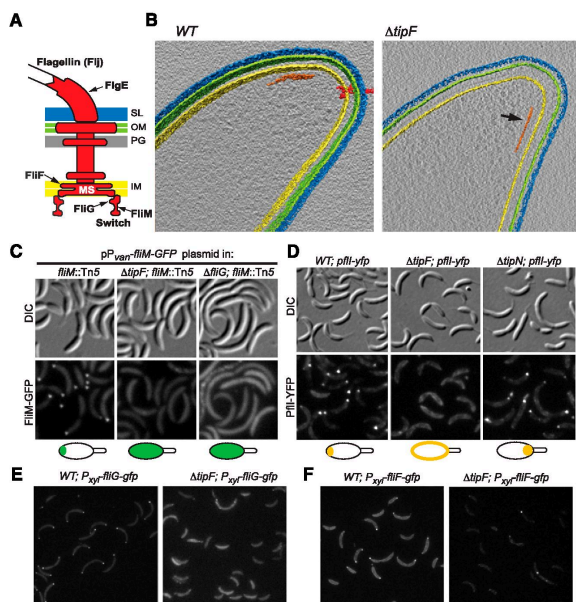


Figure 3. TipF mediates the localization of flagellar proteins FlIM, FlIG, FlIF, and PflI to the cell pole. (A) Schematic of the flagellum. The relative position of the MS ring (FlIF), the switch complex (including FlIG and FlIM), the hook (FlgE), and the filament (flagellins) are indicated, as are the envelope layers: inner (cytoplasmic) membrane (IM), peptidoglycan layer (PG), outer membrane (OM), and S layer (SL). (B) ECT imaging reveals density correspondences to the intact flagellum, including the MS ring and the switch complex in or near the inner membrane of the wild type (WT) that are absent in the $\Delta tipF$ mutant. The color-coding of the segmented structures corresponds to the color scheme in A. Flagellar structures (red) are shown in the left panel and in the segmentation of wild type. The black arrow points to the chemoreceptor array (orange) in $\Delta tipF$ cells that is also present in wild type. Bars, 200 nm. (C) The subcellular localization of FlIM-GFP from the P_{var} promoter on a medium copy number plasmid in a *fliM* mutant (*fliM::Tn5*), a *tipF* mutant ($\Delta tipF$; *fliM::Tn5*), or a *fliG* mutant derivative ($\Delta fliG$; *fliM::Tn5*) analyzed by live-cell fluorescence microscopy. (D) Localization of PflI-YFP expressed from P_{pflI} at the *pflI* locus in the presence (*pflI-yfp*) or absence of TipF ($\Delta tipF$; *pflI-yfp*) or TipN ($\Delta tipN$; *pflI-yfp*). (DIC) Differential interference contrast images. (E, F) Localization of FliG-GFP (E) and FliF-GFP (F) expressed from P_{xyf} at the *xyfX* locus in a $\Delta tipF$ mutant.

dimensional (3D) tomograms to segmentation algorithms to reveal the densities of the flagellar MS ring and switch complex at the cytoplasmic membrane at the poles of wild-type cells but could not detect these structures at $\Delta tipF$ poles (Fig. 3A,B). The fact that chemoreceptor arrays that normally assemble at the same pole (Alley et al. 1992) and at the same time as the flagellum were seen in $\Delta tipF$ cells confirms that the correct site was imaged (Fig. 3B, right panel).

Live-cell fluorescence imaging was used next to underscore the ECT results. To this end, we localized the FliM switch protein (Fig. 3C) as a C-terminal protein fusion to GFP (FliM-GFP) expressed from P_{van} in $fliM::Tn5$ cells harboring or not harboring a $\Delta fliG$ or $\Delta tipF$ in-frame deletion. FliM is predicted to interact with the FliG switch protein that is tethered to the inner membrane via the FliF MS ring protein (Fig. 3A, Chevance and Hughes 2008). Consistent with this notion, FliM-GFP is diffuse in the cytoplasm of $\Delta fliG$; $fliM::Tn5$ cells but is sequestered to the flagellated pole (opposite the stalk) in $fliM::Tn5$ cells (Fig. 3C). Moreover, FliM-GFP is delocalized in $\Delta tipF$; $fliM::Tn5$ cells (Fig. 3C). Consistent with the dependence of polar localization of FliM on FliG, we confirmed that a derivative of the FliG switch protein fused C-terminally to GFP (FliG-GFP) also depends on TipF for polar localization (Fig. 3E; Supplemental Fig. S2C).

Since two switch proteins (FliG and FliM) are no longer polarized in the absence of TipF, we asked whether the MS ring protein FliF localizes in a TipF-dependent fashion using a partially functional FliF-GFP fusion expressed in the presence of endogenous FliF from the xylose-inducible promoter at the chromosomal *xyfX* locus. Akin to FliG-GFP, only few polar FliF-GFP foci were seen in $\Delta tipF$ cells (Fig. 3F; Supplemental Fig. S2B), providing further evidence that neither the MS ring nor the switch complex assembles in $\Delta tipF$ cells. Interestingly, we found that FliF-GFP required FliG to be sequestered to the pole (Supplemental Fig. S2D), suggesting that the mislocalization of FliF-GFP seen in $\Delta tipF$ cells is a secondary effect of FliG dispersion. In support of this notion, we identified FliG as an interaction partner of soluble TipF in a yeast two-hybrid assay, suggesting that TipF and FliG interact (see below).

Based on the result that FliF and FliG are dispensable for polar localization of TipF (data not shown), we conclude that TipF acts at the earliest known (nucleation) step in flagellum biogenesis, switch, and MS ring formation, respectively.

The PflI flagellar positioning factor is recruited into a polar complex by TipF

PflI is required for proper positioning of the flagellum and is recruited to the future flagellum assembly site before flagellar structural proteins are expressed by an unknown mechanism (Obuchowski and Jacobs-Wagner 2008). Like TipF, PflI is still polar in the absence of the MS ring protein FliF, raising the possibility that PflI localization is dependent on TipF. In support of this, we found TipF-mCherry to

colocalize with PflI-GFP (PflI fused C-terminally to GFP) (Supplemental Fig. S3C) and observed that PflI-YFP or PflI-GFP are delocalized in $\Delta tipF$ cells (Fig. 3D; Supplemental Fig. S3A, respectively). Conversely, PflI does not noticeably affect TipF localization, as indicated by the apparent normal localization of TipF-GFP (expressed in lieu of endogenous TipF from the *tipF* locus) in $\Delta pflI$ compared with wild-type cells (Supplemental Fig. S3B).

Since TipF is recruited to this site by the TipN landmark protein (Supplemental Fig. S3B), we predicted that PflI localization should also be dependent on TipN. Indeed, PflI-YFP or PflI-GFP foci are mispositioned near or within the stalk in $\Delta tipN$ cells, a pattern resembling the misplacement of TipF-GFP in the absence of TipN (Fig. 3D; Supplemental Fig. S3A,B). The formation of these (mis-localized) PflI foci in $\Delta tipN$ cells is still TipF-dependent, as indicated by the dispersion of PflI-GFP in the envelope of $\Delta tipF$; $\Delta tipN$ cells (Supplemental Fig. S3A). A similar dispersion of PflI-GFP occurs when the C-terminal proline-rich domain of PflI is deleted (residues 93–142 or 142–194) (Fig. 1B; Supplemental Fig. S3D), suggesting that this domain responds to the presence of TipF. In contrast, the $\Delta pflI$ mutation does not seem to change the mislocalization of TipF-GFP in $\Delta tipN$ cells (Supplemental Fig. S3B). Thus, flagellar assembly and recruitment events at the newborn pole proceed in the order TipN > TipF > [(PflI)/FliF/G/M].

To test whether this localization dependency is reflected in physical interactions among the proteins, we conducted pull-down experiments from extracts derived from cells harboring an empty vector control or a plasmid expressing either a TipF or PflI derivative with a C-terminal TAP (tandem affinity purification) tag (see the Materials and Methods) from the P_{van} promoter. Owing to the instability of TipF (described below), we conducted the pull-down experiments in mutant backgrounds ($\Delta tipN$ and $fliB::Tn5$, when appropriate) in which TipF abundance is increased (Fig. 4A). This likely results from a post-transcriptional mechanism, as *tipF* transcription is unchanged in a *tipN* and *fliB* mutant (Supplemental Fig. S4A). Immunoblotting of TipF-TAP and PflI-TAP pull-down samples with antibodies to PflI (Fig. 4B) or TipF (Fig. 4C) provided evidence that TipF and PflI interact (directly or indirectly), but the pull down is inefficient. In contrast, coimmunoprecipitation of PflI with TipF-GFP using monoclonal antibodies to GFP was efficient (Supplemental Fig. S4B,C,D). Moreover, immunoblotting of the TipF-TAP (Fig. 4D) and PflI-TAP (Fig. 4E) pull-down samples with polyclonal antibodies to TipN provided evidence that TipN is in a complex with TipF and PflI.

Finally, using an unbiased approach for interaction partners of TipF, we conducted a yeast two-hybrid screen using soluble TipF (lacking transmembrane segments, residues 1–90) as bait to probe a prey library of *Caulobacter* genomic fragments. Two positive clones, each encoding Gal4-AD fusions to a C-terminal fragment of FliG (FliG_C)—residues 192–340 and residues 237–340 (Fig. 4F,G)—emerged from this screen. This result shows that FliG can directly interact with the soluble part of TipF and accounts for the localization dependency seen in vivo.

Davis et al.

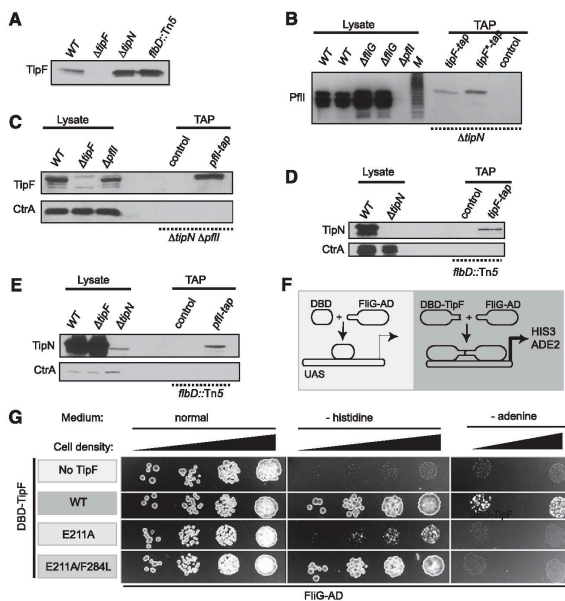


Figure 4. TipF directly interacts with FliG and forms a complex with TipN and PflI. (A) TipF steady-state levels as determined by immunoblotting using polyclonal antibodies to TipF in lysates from wild-type, $\Delta tipF$, $\Delta tipN$, and $flbD::Tn5$. (B–E) TAP pull-down of TAP-tagged proteins expressed from P_{van} on a medium copy plasmid followed by immunoblotting using polyclonal antibodies to TipF, PflI, TipN, and CtrA. The cell lysates derived from boiled cells shown in the lanes at the left of the panels provide negative and positive controls for the specificity of the antisera. CtrA immunoblots are shown as a control for loading. (B) TipF-TAP and TipF*·TAP (the E211A/F284L mutant is referred to as TipF*) were expressed from the P_{van} promoter on a medium copy number plasmid in $\Delta tipN$ mutants. (M) Protein marker lane. (C) TipF is present in PflI-TAP purifications of $\Delta tipN \Delta pflI$ double-mutant lysates. (D,E) TipN is present in pull-downs of TipF-TAP (D) or PflI-TAP (E) from $flbD::Tn5$ lysates. (F) Schematic showing the yeast two-hybrid (Y2H) assay using the C terminus of FliG (residues 237–340) as prey and the soluble part of TipF (residues 92–452) as bait to induce transcriptional activation of HIS3 and ADE2 (dark-gray box) as readout of the interaction. In the presence of DNA-binding domain (DBD)-TipF [TipF fused to the GAL4 DBD], transcriptional activation is seen, but not when DBD is used without a TipF fusion (light-gray box). (G) Growth of the yeast strains

expressing the DBD-only (i.e., without TipF), wild-type, and mutant DBD-TipF variants along with FliG-AD (activation domain) on normal medium and selective medium lacking histidine (–histidine) or adenine (–adenine). The latter condition is more stringent. Gray scales from dark to light indicate the level of interaction corresponding to the growth readout on selective medium. Dark gray represents the strongest interaction as seen for wild-type DBD-TipF with FliG-AD.

Collectively, our results show that TipF interacts directly with FliG_C and assembles a flagellar organizational center comprising FliG, FliN, PflI, and TipN at the new pole.

c-di-GMP induces TipF polarization and signaling

If TipF is activated upon binding c-di-GMP, then cells expressing TipF variants that are unable to interact with c-di-GMP or cells depleted for c-di-GMP should also be unable to localize PflI. Neither the E211A derivative nor the D331A or K352A mutants were able to direct PflI into polar assemblies (Fig. 5A). Moreover, these inactive TipF mutants were themselves no longer sequestered to the pole (Fig. 5B). Furthermore, the $tipF(E211A)$ mutation phenocopies the flagellar assembly defect of the $\Delta tipF$ deletion, as reflected in the absence of the FlgE hook protein (see Fig. 6F).

To test whether c-di-GMP depletion mimics the effects of the [c-di-GMP-binding defective] E211A mutant, we heterologously expressed the potent *Pseudomonas aeruginosa* PDE PA5295 in strains carrying the $pflI-yfp$ reporter and imaged the resulting cells. Expression of PA5295, but not the catalytically inactive mutant PA5295-AAL [carrying an analogous mutation to TipF(E211A) at position E328], was previously shown to reduce c-di-GMP levels beyond detection (Duerig et al. 2009). We found that induction of

PA5295 (depletion of c-di-GMP) dispersed PflI-YFP from the pole (Fig. 6A). Consistent with these results, we observed that c-di-GMP depletion completely delocalized TipF-GFP from the pole (Fig. 6B), while TipN-GFP was still polar under these conditions (Fig. 6C). c-di-GMP depletion also prevented FlgE expression, akin to the $\Delta tipF$ or $tipF(E211A)$ mutation (Fig. 6F). Interestingly, however, c-di-GMP depletion had a much stronger effect on transcription of the $flgE$ gene than the $\Delta tipF$ or $tipF(E211A)$ mutation (Fig. 6E), indicating that c-di-GMP modulates another step in flagellum biogenesis independently of TipF.

We conclude that c-di-GMP binding is a critical step in TipF activation and polarization. Interfering with this activating step by either introducing mutations in TipF that prevent c-di-GMP binding or depleting cells of c-di-GMP locks TipF in a conformational state that prevents its activation and polarization, the recruitment of PflI, and flagellar assembly at the newborn pole.

Bypassing the requirement of c-di-GMP for TipF signaling

To illuminate how c-di-GMP activates and polarizes TipF, we isolated intragenic suppressor mutations that restore

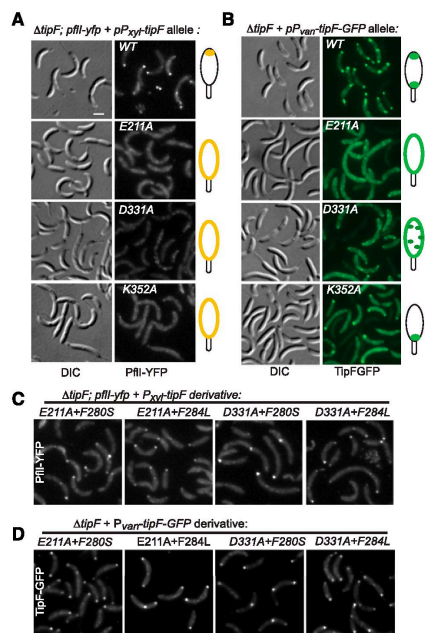


Figure 5. Suppressor mutations render TipF and PflI localization c-di-GMP-independent. (A–D) Localization of PflI-YFP (A,C) or TipF-GFP (B,D) mutants in $\Delta tipF$ cells harboring plasmids encoding TipF loss-of-function mutants expressed from the P_{xyt} (A,C) or the P_{varn} (B,D) promoter a low copy number plasmid. (DIC) Differential interference contrast images. Note that TipF(K352A)-GFP can cluster at the stalked pole but not at the newborn pole and that the ectopic signals at the stalked pole of wild-type (WT) TipF-GFP are due to (constitutive) expression of TipF from P_{varn} on the low-copy plasmid compared with constructs expressing TipF-GFP or YFP from the chromosome (cf. B vs. Fig. 6B and Supplemental Fig. S3B).

motility to *tipF(E211A)* or *tipF(D331A)* cells. The suppressor alleles carry either a missense mutation in one of two proximal codons (F280S or F284L) within the c-di-GMP-binding (EAL) domain or a duplication of a codon triplet (either ADA or DTV, residues 121–124 or 128–130, respectively) within the coiled-coil motif preceding the EAL domain (Fig. 1C,D). Importantly, the F280S or F284L missense mutations suppress either the *tipF(E211A)* or *tipF(D331A)* allele. As F280S or F284L are not allele-specific mutations, we considered the possibility that they also mitigate the localization defects of the D331A and E211A mutants. Indeed, C-terminal GFP fusions of the four double mutants [E211A/F280S, E211A/F284L, D331A/F280S, and D331A/F284L] revealed the proteins to be polarized and able to recruit PflI-YFP to the new pole (Fig. 5C,D).

If the suppressor mutations lock TipF in an activated state, then they might allow TipF to remain polarized under conditions of c-di-GMP depletion. We tested this idea by localizing YFP-tagged derivatives of wild-type, E211A/F280S, and E211A/F284L versions of TipF expressed in $\Delta tipF$ cells. While all three fusion proteins were polarized in the presence of c-di-GMP (Supplemental Fig. S5A), depletion of c-di-GMP dispersed wild-type TipF-YFP, but polar foci of the E211A/F280S and E211A/F284L versions persisted (Fig. 6D). Biochemical and biophysical analyses showed that the E211A/F284L double mutant is still unable to bind or hydrolyze c-di-GMP in vitro (Fig. 2A,B) and that the secondary structure is preserved (Supplemental Fig. S1). Interaction studies of wild-type and mutant TipF by yeast two-hybrid (Fig. 4G) and coimmunoprecipitation (Supplemental Fig. S4C,D) assays showed that TipF(E211A) associates poorly with FlhG and PflI, but the suppressor mutations attenuated this effect of the E211A mutation.

To test whether these c-di-GMP bypass mutants can also support motility in the absence of c-di-GMP, we tested whether cells harboring suppressor mutations could swim in broth after depletion of c-di-GMP. As this was not the case (data not shown), we wondered whether c-di-GMP also promotes flagellar assembly or function at a later, TipF-independent step. We examined this possibility using the accumulation of the FlgE hook protein as a convenient proxy for defects in flagellar gene expression that can arise when assembly is blocked. Immunoblotting (Fig. 6F) revealed that FlgE steady-state levels (cell-associated and the hook accumulating in the supernatant) are reduced in c-di-GMP-depleted cells even in the presence of the E211A/F280S and E211A/F284L TipF versions. Transcription of *flgE* (probed using a $P_{flgE-lacZ}$ transcriptional reporter) attained only 30% \pm 1% (E211A/F280S) and 30% \pm 1% (E211A/F284L) of wild-type activity and was much below the activity level observed for the $\Delta tipF$ single mutant (57% \pm 1% of wild type) (Fig. 6E). Moreover, $P_{flgE-lacZ}$ reporter activity is further reduced (to 21% of wild type) when c-di-GMP is depleted in $\Delta tipF$ cells, indicating that this c-di-GMP control step is required for efficient *flgE* transcription. A similar c-di-GMP-dependent effect was seen on transcription of the *fljL* flagellin gene using the $P_{fljL-lacZ}$ transcriptional reporter (Supplemental Fig. S5B). In this case, however, c-di-GMP depletion reduces *fljL* transcription in $\Delta tipF$ cells from near-full wild-type levels (*fljL* transcription is not affected by $\Delta tipF$ mutation) to 32% \pm 2%.

We conclude that TipF localization can be partially uncoupled from c-di-GMP control by the F280S and F284L suppressor mutations, but c-di-GMP influences at least one additional event in flagellum assembly, gene expression, localization, and/or (possibly affects) TipN polarization.

TipF abundance coincides with and depends on the cell cycle burst in c-di-GMP

Monitoring the steady-state levels of wild-type TipF and TipF(E211A) by immunoblotting suggested that (untagged)

Davis et al.

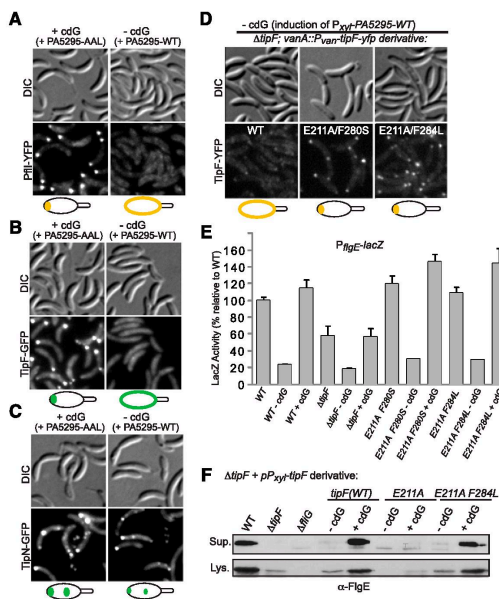


Figure 6. Localization of TipF and PflI as well as expression of FlgE is c-di-GMP-dependent. (A–D) Localization of PflI-YFP (A), TipF-GFP (B), TipN-GFP (C), and YFP-tagged TipF suppressor mutants (D) under normal (PA5295-AAL, +cdG) or c-di-GMP-depleted (PA5295-WT, –cdG) conditions. PA5295 variants were expressed from the *P_{xyI}* promoter on a medium copy number plasmid in cells expressing the GFP fusion proteins from their respective promoters at the endogenous locus. In D, TipF-YFP variants were expressed from *P_{van}* at the *vanA* locus in $\Delta tipF$ cells. (DIC) Differential interference contrast images. (E) Effects of c-di-GMP concentration on transcription of the *flgE* hook gene by β -galactosidase assays of cells (wild-type [WT], $\Delta tipF$, or $\Delta tipF$ cells expressing mutant TipF from *P_{van}* at the *vanA* locus) harboring a *P_{flgE}-lacZ* transcriptional reporter fusion. (F) Effects of c-di-GMP depletion on FlgE steady-state levels in supernatants (Sup.) or cell lysates (Lys.), determined by immunoblotting using anti-FlgE antibody (α -FlgE). TipF mutants were expressed from the *P_{xyI}* promoter on a low copy number plasmid in $\Delta tipF$ cells.

TipF is stabilized upon binding c-di-GMP (Fig. 7A,B). The abundance of wild-type TipF expressed from *P_{xyI}* (i.e., using the transcriptional and translational regulatory signals of the *xytX* gene) in $\Delta tipF$ cells is significantly higher than that of the E211A version, suggesting that TipF is regulated at the level of stability by c-di-GMP. Indeed, half-life measurements of (untagged) wild-type TipF and TipF(E211A) under normal (Fig. 7B) or c-di-GMP-depleted (Fig. 7A) conditions (as described above) approximated the half-life of wild-type TipF at >2 h in the presence of c-di-GMP and <20 min in its absence. In contrast, for the E211A version, the half-life values were ~10–20 min irrespective of the presence or absence of c-di-GMP, demonstrating that the E211A protein is not further destabilized upon c-di-GMP depletion (Fig. 7A,B). Remarkably, the half-life (~40 min) of the E211A/F284L variant was higher than that of the E211A single mutant but lower than that of wild-type TipF. Again, the half-life of this mutant was largely insensitive to the presence or absence of c-di-GMP, consistent with the persistence of E211A/F284L at the pole in the absence of c-di-GMP (see above). Thus, when c-di-GMP is depleted, TipF is unable to adopt an active conformation and is destabilized. These events can be uncoupled from c-di-GMP with a mutation of F284L, which not only activates the E211A mutant form constitutively, but, at the same time, partially protects it from proteolysis in vivo.

In the search for a candidate protease that destabilizes TipF in vivo, we tested strains with mutations in all ATP-dependent proteases and found that ClpX, the ATP-dependent chaperone component of the ClpXP protease, controls the cell cycle-dependent accumulation of endogenous (untagged) TipF expressed from its native chromosomal location (Fig. 7C). Immunoblotting revealed TipF to be absent from G1-phase cells, induced during the G1 → S transition (40 min), and diminished at the time of division (Fig. 7D). Poisoning ClpXP activity by expression of a dominant-negative [catalytically inactive] ClpX variant (ClpX*) (Osteras et al. 1999) from *P_{xyI}*, allows TipF accumulation in G1 cells (Fig. 7C), presumably because the normal turnover of TipF in G1 phase is blocked. Since a precipitous drop in c-di-GMP levels occurs in G1 cells (Paul et al. 2008; Christen et al. 2010) and TipF stability is clearly influenced by c-di-GMP abundance/binding, our results are consistent with the notion that the trough in c-di-GMP facilitates the turnover and thus the removal of TipF-dependent polarization during the cell cycle. In support of this view, fusion of GFP to the C terminus of TipF causes the aberrant accumulation of TipF in G1 phase (Fig. 7D) and allows TipF steady-state levels in unsynchronized populations to be maintained in the absence of c-di-GMP (Supplemental Fig. S6A,B). Similarly, comparison of the steady-state levels between untagged wild-type and TipF(E211A/F280S) expressed from

Mechanism of flagellum de- and repolarization

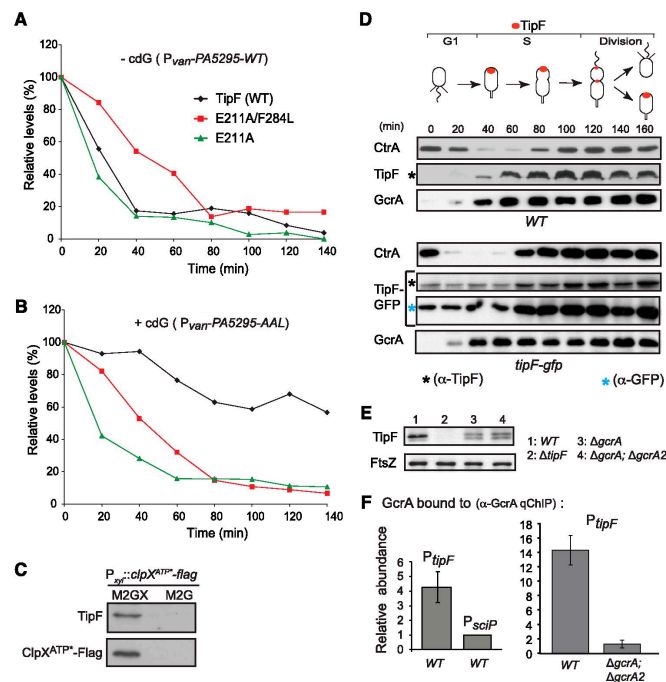


Figure 7. c-di-GMP levels affect TipF protein stability. *(A,B)* Depletion of c-di-GMP by overexpression of a potent PDE reduces TipF steady-state levels. TipF, the c-di-GMP-binding mutant E211A, or the intragenic suppressor mutant E211A/F284L was expressed from *P_{xyf}* in *ΔtipF* cells grown in M2G containing xylose following a shift to M2G containing vanillate to induce the expression of the PDE PA5295 from *P. aeruginosa* or its active site mutant, PA5295-AAL, and repress *P_{xyf}*. Samples were taken every 20 min, and protein levels were quantified from the immunoblots and plotted as percentages of the highest value. *(C)* The dominant-negative *clpX^{ATP}* allele was expressed from plasmid in M2G containing xylose [M2GX] or repressed by growing the cells in M2G. Swarmer cells were isolated, and TipF was detected using a polyclonal anti-TipF antibody and ClpX^{ATP}::Flag using monoclonal anti-M2 antibodies. In the presence of wild-type (WT) ClpXP, TipF was not detectable, while inactivation of ClpXP by the dominant-negative allele encoding ClpX^{ATP} led to stabilization of TipF. *(D)* The cell cycle abundance of TipF resembles that of GcrA. Synchronized wild-type or *tipF-gfp* (in which endogenous *tipF* is replaced by *tipF-gfp*) swarmer cells were released in fresh medium, and CtrA, TipF, TipF-GFP, and/or GcrA steady-state levels were determined by immunoblotting using antibodies to TipF (black asterisk), GFP (blue asterisk), CtrA, or GcrA at different times during cell cycle progression. *(E)* TipF and FtsZ (control) steady-state levels in wild-type and mutant cells, as determined by immunoblotting using antibodies to TipF and FtsZ. *(F)* GcrA binds to the *tipF* promoter, as determined by qChIP experiments using polyclonal antibodies to GcrA. The abundance of the *tipF* and *scfP* promoters was quantified in the immunoprecipitates (*left* panel) and *tipF* (*right* panel) in wild-type and *ΔgcrA*, *ΔgcrA2* double-mutant cells.

the xylose-inducible *P_{xyf}* promoter on a low-copy plasmid revealed that the stabilized E211A/F280S variant is more abundant than wild-type TipF in G1-phase cells (Supplemental Fig. S6C). Together, these findings support the model that the fluctuation of c-di-GMP during the cell cycle (i.e., its concentration trough in G1 cells) helps restrict TipF abundance to S phase.

Additionally, the cell cycle abundance pattern of TipF is reinforced by timely synthesis, as is evident from the immunoblotting experiments in Figure 7D showing the

increase of TipF during the cell cycle. Strikingly, the cell cycle pattern of TipF mirrors that of GcrA, a master transcriptional regulator that is required for the accumulation of a myriad of cell cycle-regulated transcripts, including *tipF*, at the G1 → S transition (Holtzendorff et al. 2004). Consistent with the hypothesis that GcrA directly activates transcription of the TipF-encoding gene at the G1 → S transition, we observed that GcrA is required for efficient TipF protein accumulation (Fig. 7E), and quantitative chromatin immunoprecipitation (qChIP)

Davis et al.

analysis using polyclonal antibodies to GcrA revealed that GcrA binds the *tipF* promoter, but not the *sciP* promoter, in vivo in a GcrA-dependent manner (Fig. 7F). The induction of TipF expression at the transcriptional level by GcrA and the concordant surge in c-di-GMP levels at the G1 → S transition ensure that TipF is active and ready to prime flagellum biosynthesis at the newborn pole, while a drop in c-di-GMP in the incipient G1 daughter cells results in the removal of TipF, thus resetting the flagellar polarity cascade for the next cell cycle.

Discussion

The establishment, amplification, and propagation of polarity cues during the cell cycle are hallmarks of all polarized cells, from bacterial to metazoan origin. Here we elucidate a mechanism that not only implements but also serves to subsequently reset a polarity pathway during the cell cycle in response to cyclic nucleotide signaling. While nucleotide-based signals direct critical events in the establishment and/or reinforcement of polarity cues in eukaryotes (Slaughter et al. 2009; Charest and Firtel 2010; St Johnston and Ahringer 2010; Amato et al. 2011; Ji and Tulin 2012), the underlying mechanisms are not well understood in bacterial systems. Using polar flagellum morphogenesis as a proxy to unravel how and when polarity cues are instated by cyclic nucleotide signaling during the *Caulobacter* cell cycle, we found that the presence of c-di-GMP activates and amplifies the TipF-dependent flagellar polarization pathway, while its removal promotes the elimination of TipF from G1 cells and provides a (possible checkpoint-like) mechanism, allowing the re-establishment of the flagellar polarization pathway to be coordinated with other developmental events at the G1 → S transition.

At least four regulatory factors (TipN, GcrA, ClpX, and c-di-GMP) impart spatiotemporal control on TipF through interwoven mechanisms acting at different levels. c-di-GMP adopts a central position in this regulatory web, implementing its effects by directly binding TipF (Fig. 2). The induction of TipF at the G1 → S transition is reinforced by two concurrent mechanisms: its synthesis triggered by the GcrA master regulator and its stabilization by c-di-GMP (Fig. 1A). Both mechanisms ensure that TipF accumulation is coordinated to other critical morphogenetic events that are activated at the same time. GcrA promotes the expression of genes encoding determinants for polarity (PodJ), controlling morphogenesis of pili, division (MipZ, a division inhibitor), and asymmetry (PleC, a histidine kinase/phosphatase) (Viollier et al. 2002; Holtzendorff et al. 2004; Thanbichler and Shapiro 2006). The concurrent accumulation of c-di-GMP protects TipF from ClpXP-dependent proteolysis and thus reinforces the surge of TipF while also promoting the degradation of CtrA at the G1 → S transition via the PopA effector and stalk biogenesis by an unknown mechanism (Paul et al. 2004, 2008; Duerig et al. 2009; Abel et al. 2011). Importantly, c-di-GMP binding is required not only to activate and polarize TipF, but also for the TipF-dependent recruitment of flagellar assembly factors and regulators such

as PflI, FliG, and FliM to the new pole. The underlying conformational rearrangements that likely occur when TipF binds c-di-GMP can be blocked by mutational destruction of the c-di-GMP-binding site or when c-di-GMP is depleted from cells. While these manipulations abrogate TipF polarization and function, we isolated compensatory missense mutations in the c-di-GMP-binding domain that reverse these effects and also allow TipF localization under conditions of c-di-GMP depletion. The same motility suppressor screen was answered by triplet codon duplications in a predicted coiled-coil-rich region that precedes the c-di-GMP-binding domain (Fig. 1B). Helical wheel analysis of these mutant proteins predicts that the α -helicity is maintained by the duplication while causing a shift of the hydrophobic region that could cause structural rearrangements. This rearrangement likely also underlies the interaction of TipF•c-di-GMP with TipN. During the late stages of constriction of the preceding cell cycle, the TipN landmark signal is deposited at the newborn pole to ensure correct interpretation of the polarity axis in the progeny (Huitema et al. 2006; Lam et al. 2006). Because of this spatial cue, the subsequent events triggered by c-di-GMP at the G1 → S transition are executed at the correct subcellular site (i.e., the newborn pole) (Fig. 1A). In support of this, our pull-down experiments revealed TipN to be part of this flagellar organizational complex that includes TipF, Pfl, and at least one flagellar switch component (Fig. 2A).

The flagellar switch complex is best known as a target to regulate flagellar rotation but fulfills a fundamental role in flagellar assembly (Irikura et al. 1993; Chevance and Hughes 2008; Davis and Viollier 2011). Indeed the FliG switch protein interacts with the FliF MS ring protein and the MotA stator protein along with other switch proteins. This central position of FliG in flagellar assembly and function has been exploited to regulate motility in response to specific developmental states or nutritional and systemic cues (Ryjenkov et al. 2006; Blair et al. 2008; Paul et al. 2011; Zarbiv et al. 2012). Despite the dual role of FliG, no mechanism has been described to regulate flagellar assembly through FliG. TipF is the first representative of this class, as the soluble portion of TipF (encompassing the predicted coiled-coil and EAL domains) interacts directly with the C-terminal portion (FliG_C). The role of c-di-GMP in flagellar assembly likely goes beyond the TipF–FliG interaction, as indicated by the existence of an apparent TipF-independent, but c-di-GMP-dependent, flagellar assembly step (Fig. 6E,F).

The FlhF GTPase of *vibriosis*, *pseudomonads*, and *Campylobacter jejuni* may function akin to the TipF and c-di-GMP-dependent flagellar polarization pathway (Pandza et al. 2000; Salvetti et al. 2007; Balaban et al. 2009; Kusumoto et al. 2009). FlhF is polarized and recruits the MS ring protein FliF to the polar site of flagellation in *Vibrio cholerae* (Green et al. 2009). However, despite the pervasive polar flagellation found across bacterial lineages, FlhF polarization, activation, and function are poorly understood. Interestingly, the *Myxococcus xanthus* Ras-like GTPases MglA and SofG are used to direct motility pro-

Mechanism of flagellum de- and repolarization

teins required for flagellum-independent (gliding) motility to the pole (Leonardy et al. 2010; Zhang et al. 2010; Bulyha et al. 2013). Moreover, a member of the ParA/MinD family of ATPases positions the chemosensory apparatus at the pole in *V. cholera* (Ringgaard et al. 2011; Yamaichi et al. 2012), and a related protein ensures the medial placement of the chemosensory apparatus in *Rhodobacter sphaeroides* (Thompson et al. 2006), but the temporal relationships with the cell cycle are unexplored in these systems.

c-di-GMP-mediated spatiotemporal control of polar morphogenesis extends far beyond the α -proteobacterial lineage. In the γ -proteobacterium *P. aeruginosa*, an imbalance in c-di-GMP abundance is observed in the two progeny compartments of a dividing cell, with the trough in c-di-GMP levels occurring in the daughter compartment bearing the polar flagellum (Christen et al. 2010). FimX, an EAL-GGDEF domain hybrid protein from *P. aeruginosa*, is polarly localized and promotes the assembly of retracting type IV (polar) pili (Tfp) for twitching motility. Importantly, FimX influences the positioning of Tfp and uses an EAL domain to bind c-di-GMP and induce (long-range) conformational change in the adjacent domain (Huang et al. 2003). However, it is unknown how FimX scouts the pole, how it signals Tfp assembly, and how its localization is coordinated with cell cycle progression. We show that spatiotemporal cues from pre-existing spatial landmarks, the c-di-GMP second messenger, and the cell cycle transcriptional program are integrated at Tfp to orchestrate the periodic removal and re-establishment of a polarity pathway controlling morphogenesis during the cell cycle. Thus, small nucleotide-induced polarization pulses that drive morphogenesis at key times in the cell cycle appear to have been invented more than once during evolution from prokaryotic to metazoan cells and may thus even function akin in eukaryotic organelles.

Materials and methods

Coimmunoprecipitation

Cells (50 mL) were grown to mid-log phase in the presence of 50 mM vanillate inducer, harvested, washed three times in buffer I (50 mM sodium phosphate at pH 7.4, 50 mM NaCl, 1 mM EDTA), and resuspended in buffer II (50 mM sodium phosphate at pH 7.4, 50 mM NaCl, 0.5% n-dodecyl- β -D-maltoside, two protease inhibitor tablets [Complete EDTA-free, Roche]) containing 1 \times Ready-Lyse lysis solution (Epicentre), 2 mM MgCl₂, 1 mM EDTA, and 30 U of DNase I (Roche). The solution was incubated for 20 min at room temperature and subsequently centrifuged at 10,000g for 3 min at 4°C to remove cellular debris. The supernatant was precleared with 50 μ L of Proteinase-G agarose beads (Roche). To the precleared solution, mouse monoclonal anti-GFP antibodies (1:300 dilution; Living Colors A.V. monoclonal antibody [JL-8], Clontech,) was added and incubated for 90 min at 4°C. The antibody-protein complexes were trapped with Proteinase-G agarose beads washed once with buffer I containing 0.5% n-dodecyl- β -D-maltoside, twice with 1% immunoprecipitation buffer [Protein G immunoprecipitation kit, Sigma-Aldrich], and once with 0.1% immunoprecipitation buffer to remove salts and finally resuspended in 70 μ L of 1 \times Laemmli sample buffer. After boiling and centrifugation, precipitated pro-

teins were identified by immunoblotting using polyclonal antibodies to PflI or CtrA.

TAP

The TAP procedure was based on that described by Rigaut et al. (1999). Briefly, cells (1 L) were grown to mid-log phase in the presence of 50 mM vanillate for 3 h and harvested by centrifugation at 6000g for 10 min. The cells were then washed in buffer I (50 mM sodium phosphate at pH 7.4, 50 mM NaCl, 1 mM EDTA) and lysed for 15 min at room temperature in 500 μ L of buffer II (buffer I + 10% n-dodecyl- β -D-maltoside, two protease inhibitor tablets [Complete EDTA-free, Roche], 1 \times Ready-Lyse lysozyme [Epicentre], 500 U of DNase I [Roche], 2 mM MgCl₂, 1 mM EDTA). The volume of the solution was brought up to 10 mL with buffer I and incubated for 15 min at room temperature. Cellular debris was removed by centrifugation at 7000g for 15 min at 4°C, and the salt concentration of the supernatant was adjusted by adding 10 μ L of 1 M Tris per milliliter sample, 20 μ L of 5 M NaCl per milliliter sample, and 25 μ L of 10% n-dodecyl- β -D-maltoside per milliliter sample. The supernatant was incubated for 2 h at 4°C with IgG Sepharose beads (GE Healthcare Biosciences) that had been washed once with IPP150 buffer (10 mM Tris-HCl at pH 8, 150 mM NaCl, 0.25% n-dodecyl- β -D-maltoside). After incubation, the beads were washed at 4°C three times with IPP150 buffer and once with TEV cleavage buffer (10 mM Tris-HCl at pH 8, 150 mM NaCl, 0.25% n-dodecyl- β -D-maltoside, 0.5 mM EDTA, 1 mM DTT). The beads were then incubated overnight at 4°C with 1 mL of TEV solution (TEV cleavage buffer with 100 U of TEV protease per milliliter [Promega]) to release the tagged complex. CaCl₂ (3 μ M) was added to the solution and incubated for 1 h at 4°C with calmodulin beads (GE Healthcare Biosciences) that had been washed once with calmodulin-binding buffer (10 mM β -mercaptoethanol, 10 mM Tris-HCl at pH 8, 150 mM NaCl, 1 mM magnesium acetate, 1 mM imidazole, 2 mM CaCl₂, 0.25% n-dodecyl- β -D-maltoside). After incubation, the beads were washed three times with calmodulin-binding buffer and eluted with IPP150 calmodulin elution buffer (calmodulin-binding buffer substituted with 2 mM EGTA instead of CaCl₂). The eluate was then concentrated with Biomax centrifugal filter tubes (Millipore).

Protein overexpression and purification for PDE assay and ITC analyses

E. coli BL21 cells carrying the respective wild-type and mutant Tfp overexpression plasmids were grown in LB medium, and expression was induced by adding isopropyl 1-thio- β -D-galactopyranoside at A600 = 0.4 to a final concentration of 1 μ M. Cells were centrifuged and resuspended in buffer containing 20 mM Tris-HCl (pH 7), 250 mM NaCl, 5 mM imidazole, 10 mM MgCl₂, 1% glycerol, and Complete minicocktail of EDTA-free protease inhibitors at the concentrations specified by the manufacturer (Roche). Cells were lysed by passage through a French pressure cell, and the suspension was clarified by centrifugation at 15,000g for 40 min. The supernatant was incubated with pre-equilibrated Profinity IMAC Ni-resin (Bio-Rad) for 1 h at 4°C. The resins were washed, and the proteins were eluted with 350 mM imidazole. The eluate was loaded on a HiLoad 16/60 Superdex 75 prep-grade gel filtration column (GE Healthcare; FPLC system: AEKTA Purifier, Amersham Biosciences) for the next purification step using 50 mM Tris-HCl (pH 8) and 50 mM NaCl buffer. The monomer fractions were collected and concentrated (Amicon Ultra 10,000-MW centrifugal filters, Millipore) for further assays. The protein concentrations were determined using the Bradford assay (Bio-Rad).

Davis et al.

PDE assay

Wild-type and mutant TipF were purified as His6-tagged variants using standard conditions [see the Supplemental Material] and tested for c-di-GMP PDE activity. As a control, PDE class A YahA from *E. coli* was used. For each protein, a 10 μ M final concentration was incubated with 100 μ M c-di-GMP (synthesized enzymatically and purified via FPLC reverse-phase chromatography) in 50 mM Tris-HCl (pH 8), 50 mM NaCl, 5 mM MgCl₂, and 1 mM DTT at room temperature. Samples were taken at time points 0 h, 1 h, 2 h, and overnight. The reactions were stopped by heating for 5 min at 99°C, diluted with 5 mM NH₄HCO₃ (pH 8), filtered (0.22 μ M), and analyzed on a Resource Q ion-exchange chromatography column (GE Healthcare).

ITC

The interaction of TipF with c-di-GMP was measured with a VP-ITC isothermal titration calorimeter from MicroCal, with TipF (32.5 μ M) in the calorimeter cell and c-di-GMP (118 μ M) in the injection syringe (buffer: 50 mM Tris/HCl, 50 mM NaCl at pH 8 at 25°C). All solutions were degassed and equilibrated at the desired temperature (25°C or 35°C) before using. The delay between the injections was set to 5 min to ensure re-equilibration between injections. Data were evaluated using Origin software (OriginLab).

Cryo-electron microscopy sample preparation

C. crescentus grown in PYE medium were flash-frozen (plunge-frozen) onto glow-discharged, 200 mesh, Quantifoil copper grids (Quantifoil) in liquid ethane using a Vitrobot Mark II system (FEI). BSA-treated colloidal gold (10 nm) was applied to the grids and air-dried before sample application and plunge-freezing.

Cryo-electron microscopy data collection

Cryo-electron tomography data collection was performed with an FEI Tecnai G² F30 at the University of Minnesota Characterization Facility. Images were acquired with a Gatan 4 k \times 4 k Ultrascan charged-couple device (CCD camera) with a pixel size of 0.372 nm (at 31,000 \times) or 0.495 nm (at 23,000 \times) on the specimen. A total electron dose of 150 electrons per squared angstrom (e⁻/Å²) was used to collect a full-tilt series ranging from -65° to +65° (131 images). Data were collected at a defocus of 8.0 μ m under focus (first CTF 0; 1/4 nm⁻¹). Images were acquired automatically with 1° tilt steps using the predictive University of California at San Francisco tomography package (Zheng et al. 2007).

Cryo-electron image processing and analysis

Tomographic reconstructions were generated using IMOD (Kremer et al. 1996). The Amira visualization software package [Visage Imaging Systems, Inc.] was used for volume rendering and material labeling (segmentation). A visualization and segmentation toolbox (Pruggnaller et al. 2008) developed specifically for 3D electron microscopy data analysis in Amira was used to achieve a more objective segmentation of the data by avoiding manual contouring (entirely subjective tracing of edges or features). After contrast inversion, slices were filtered using a 3D Gaussian smoothing with a kernel size of 3 \times 3 \times 3. Subsequently, the IslandLabel module was applied to binarize the data with a threshold and tag connected regions of the binary image with a label.

Construction of strains and plasmids, immunoblotting, yeast two-hybrid analyses, and fluorescence microscopy

Descriptions of the construction of strains and plasmids, immunoblotting, yeast two-hybrid analyses, and fluorescence microscopy can be found in the Supplemental Material.

Acknowledgments

We thank Lucy Shapiro and Jim Gober for providing antibodies. Funding support is from Swiss National Science Foundation (no. 127287 to P.H.V. and no. 130469 to U.J.), National Institutes of Health (GM104540 to E.R.W.), and Human Frontier Science Program (RGP0051/2010 to P.H.V. and E.R.W.).

References

- Abel S, Chien P, Wassmann P, Schirmer T, Kaever V, Laub MT, Baker TA, Jenal U. 2011. Regulatory cohesion of cell cycle and cell differentiation through interlinked phosphorylation and second messenger networks. *Mol Cell* **43**: 550–560.
- Alley MR, Maddock JR, Shapiro L. 1992. Polar localization of a bacterial chemoreceptor. *Genes Dev* **6**: 825–836.
- Amato S, Liu X, Zheng B, Cantley L, Rakic P, Man HY. 2011. AMP-activated protein kinase regulates neuronal polarization by interfering with PI 3-kinase localization. *Science* **332**: 247–251.
- Balaban M, Joslin SN, Hendrixson DR. 2009. FlhF and its GTPase activity are required for distinct processes in flagellar gene regulation and biosynthesis in *Campylobacter jejuni*. *J Bacteriol* **191**: 6602–6611.
- Barends TR, Hartmann E, Griese JJ, Beitlich T, Kirienko NV, Ryjenkov DA, Reinstein J, Shoeman RL, Gomelsky M, Schlichting I. 2009. Structure and mechanism of a bacterial light-regulated cyclic nucleotide phosphodiesterase. *Nature* **459**: 1015–1018.
- Blair KM, Turner L, Winkelman JT, Berg HC, Kearns DB. 2008. A molecular clutch disables flagella in the *Bacillus subtilis* biofilm. *Science* **320**: 1636–1638.
- Boehm A, Kaiser M, Li H, Spangler C, Kasper CA, Ackermann M, Kaever V, Sourjik V, Roth V, Jenal U. 2010. Second messenger-mediated adjustment of bacterial swimming velocity. *Cell* **141**: 107–116.
- Boyd CD, O'Toole GA. 2012. Second messenger regulation of biofilm formation: Breakthroughs in understanding c-di-GMP effector systems. *Annu Rev Cell Dev Biol* **28**: 439–462.
- Brown MT, Delalez NJ, Armitage JP. 2011. Protein dynamics and mechanisms controlling the rotational behaviour of the bacterial flagellar motor. *Curr Opin Microbiol* **14**: 734–740.
- Bulyha I, Lindow S, Lin L, Bolte K, Wuichet K, Kahnt J, van der Does C, Thanbichler M, Sogaard-Andersen L. 2013. Two small GTPases act in concert with the bactofilin cytoskeleton to regulate dynamic bacterial cell polarity. *Dev Cell* **25**: 119–131.
- Charest PC, Firtel RA. 2010. 'TORCing' neutrophil chemotaxis. *Dev Cell* **19**: 795–796.
- Cheavance FF, Hughes KT. 2008. Coordinating assembly of a bacterial macromolecular machine. *Nat Rev Microbiol* **6**: 455–465.
- Christen M, Kulasekara HD, Christen B, Kulasekara BR, Hoffman LR, Miller SI. 2010. Asymmetrical distribution of the second messenger c-di-GMP upon bacterial cell division. *Science* **328**: 1295–1297.

Mechanism of flagellum de- and repolarization

- Davis NJ, Viollier PH. 2011. Probing flagellar promoter occupancy in wild-type and mutant *Caulobacter crescentus* by chromatin immunoprecipitation. *FEMS Microbiol Lett* **319**: 146–152.
- Duerig A, Abel S, Folcher M, Nicollier M, Schwede T, Amiot N, Giese B, Jenal U. 2009. Second messenger-mediated spatiotemporal control of protein degradation regulates bacterial cell cycle progression. *Genes Dev* **23**: 93–104.
- Fang X, Gomelsky M. 2010. A post-translational, c-di-GMP-dependent mechanism regulating flagellar motility. *Mol Microbiol* **76**: 1295–1305.
- Green JC, Kahramanoglu C, Rahman A, Pender AM, Charbonnel N, Fraser GM. 2009. Recruitment of the earliest component of the bacterial flagellum to the old cell division pole by a membrane-associated signal recognition particle family GTP-binding protein. *J Mol Biol* **391**: 679–690.
- Hengge R. 2009. Principles of c-di-GMP signalling in bacteria. *Nat Rev Microbiol* **7**: 263–273.
- Holtzendorff J, Hung D, Brende P, Reisenauer A, Viollier PH, McAdams HH, Shapiro L. 2004. Oscillating global regulators control the genetic circuit driving a bacterial cell cycle. *Science* **304**: 983–987.
- Huang B, Whitchurch CB, Mattick JS. 2003. FimX, a multidomain protein connecting environmental signals to twitching motility in *Pseudomonas aeruginosa*. *J Bacteriol* **185**: 7068–7076.
- Hutema E, Pritchard S, Matteson D, Radhakrishnan SK, Viollier PH. 2006. Bacterial birth scar proteins mark future flagellum assembly site. *Cell* **124**: 1025–1037.
- Irikura VM, Kihara M, Yamaguchi S, Sockett H, Macnab RM. 1993. *Salmonella typhimurium* *fliC* and *fliN* mutations causing defects in assembly, rotation, and switching of the flagellar motor. *J Bacteriol* **175**: 802–810.
- Ji Y, Tulin AV. 2012. Poly(ADP-ribose) controls DE-cadherin-dependent stem cell maintenance and oocyte localization. *Nat Commun* **3**: 760.
- Kremer JR, Mastrorade DN, McIntosh JR. 1996. Computer visualization of three-dimensional image data using IMOD. *J Struct Biol* **116**: 71–76.
- Kusumoto A, Nishioka N, Kojima S, Homma M. 2009. Mutational analysis of the GTP-binding motif of FlhF which regulates the number and placement of the polar flagellum in *Vibrio alginolyticus*. *J Biochem* **146**: 643–650.
- Lam H, Schofield WB, Jacobs-Wagner C. 2006. A landmark protein essential for establishing and perpetuating the polarity of a bacterial cell. *Cell* **124**: 1011–1023.
- Laub MT, McAdams HH, Feldblyum T, Fraser CM, Shapiro L. 2000. Global analysis of the genetic network controlling a bacterial cell cycle. *Science* **290**: 2144–2148.
- Leonardy S, Miertzschke M, Bulyha I, Sperling E, Wittinghofer A, Sogaard-Andersen L. 2010. Regulation of dynamic polarity switching in bacteria by a Ras-like G-protein and its cognate GAP. *EMBO J* **29**: 2276–2289.
- McAdams HH, Shapiro L. 2011. The architecture and conservation pattern of whole-cell control circuitry. *J Mol Biol* **409**: 28–35.
- Obuchowski PL, Jacobs-Wagner C. 2008. Pfl, a protein involved in flagellar positioning in *Caulobacter crescentus*. *J Bacteriol* **190**: 1718–1729.
- Osteras M, Stotz A, Schmid Nuoffer S, Jenal U. 1999. Identification and transcriptional control of the genes encoding the *Caulobacter crescentus* ClpXP protease. *J Bacteriol* **181**: 3039–3050.
- Pandza S, Baetens M, Park CH, Au T, Keyhan M, Matin A. 2000. The G-protein FlhF has a role in polar flagellar placement and general stress response induction in *Pseudomonas putida*. *Mol Microbiol* **36**: 414–423.
- Paul R, Weiser S, Amiot NC, Chan C, Schirmer T, Giese B, Jenal U. 2004. Cell cycle-dependent dynamic localization of a bacterial response regulator with a novel di-guanylate cyclase output domain. *Genes Dev* **18**: 715–727.
- Paul R, Jaeger T, Abel S, Wiederkehr J, Folcher M, Biondi EG, Laub MT, Jenal U. 2008. Allosteric regulation of histidine kinases by their cognate response regulator determines cell fate. *Cell* **133**: 452–461.
- Paul K, Nieto V, Carlquist WC, Blair DF, Harshey RM. 2010. The c-di-GMP binding protein YcgR controls flagellar motor direction and speed to affect chemotaxis by a ‘backstop brake’ mechanism. *Mol Cell* **38**: 128–139.
- Paul K, Carlquist WC, Blair DF. 2011. Adjusting the spokes of the flagellar motor with the DNA-binding protein H-NS. *J Bacteriol* **193**: 5914–5922.
- Pruggnaller S, Mayr M, Frangakis AS. 2008. A visualization and segmentation toolbox for electron microscopy. *J Struct Biol* **164**: 161–165.
- Quon KC, Marczynski GT, Shapiro L. 1996. Cell cycle control by an essential bacterial two-component signal transduction protein. *Cell* **84**: 83–93.
- Rigaut G, Shevchenko A, Rutz B, Wilm M, Mann M, Seraphin B. 1999. A generic protein purification method for protein complex characterization and proteome exploration. *Nat Biotechnol* **17**: 1030–1032.
- Ringgaard S, Schirmer K, Davis BM, Waldor MK. 2011. A family of ParaA-like ATPases promotes cell pole maturation by facilitating polar localization of chemotaxis proteins. *Genes Dev* **25**: 1544–1555.
- Ryjenkov DA, Simm R, Romling U, Gomelsky M. 2006. The PilZ domain is a receptor for the second messenger c-di-GMP: The PilZ domain protein YcgR controls motility in enterobacteria. *J Biol Chem* **281**: 30310–30314.
- Salvetti S, Ghelardi E, Celandroni F, Ceragioli M, Giannessi F, Senesi S. 2007. FlhF, a signal recognition particle-like GTPase, is involved in the regulation of flagellar arrangement, motility behaviour and protein secretion in *Bacillus cereus*. *Microbiology* **153**: 2541–2552.
- Schirmer T, Jenal U. 2009. Structural and mechanistic determinants of c-di-GMP signalling. *Nat Rev Microbiol* **7**: 724–735.
- Slaughter BD, Smith SE, Li R. 2009. Symmetry breaking in the life cycle of the budding yeast. *Cold Spring Harb Perspect Biol* **1**: a003384.
- St Johnston D, Ahringer J. 2010. Cell polarity in eggs and epithelia: Parallels and diversity. *Cell* **141**: 757–774.
- Thanbichler M, Shapiro L. 2006. MipZ, a spatial regulator coordinating chromosome segregation with cell division in *Caulobacter*. *Cell* **126**: 147–162.
- Thompson SR, Wadhams GH, Armitage JP. 2006. The positioning of cytoplasmic protein clusters in bacteria. *Proc Natl Acad Sci* **103**: 8209–8214.
- Tsokos CG, Laub MT. 2012. Polarity and cell fate asymmetry in *Caulobacter crescentus*. *Curr Opin Microbiol* **15**: 744–750.
- Viollier PH, Sternheim N, Shapiro L. 2002. A dynamically localized histidine kinase controls the asymmetric distribution of polar pili proteins. *EMBO J* **21**: 4420–4428.
- Wolfe AJ, Visick KL. 2008. Get the message out: Cyclic-di-GMP regulates multiple levels of flagellum-based motility. *J Bacteriol* **190**: 463–475.
- Yamaichi Y, Bruckner R, Ringgaard S, Moll A, Cameron DE, Briegel A, Jensen GJ, Davis BM, Waldor MK. 2012. A multidomain hub anchors the chromosome segregation and chemotactic machinery to the bacterial pole. *Genes Dev* **26**: 2348–2360.

Davis et al.

- Zariv G, Li H, Wolf A, Cecchini G, Caplan SR, Sourjik V, Eisenbach M. 2012. Energy complexes are apparently associated with the switch-motor complex of bacterial flagella. *J Mol Biol* **416**: 192–207.
- Zhang Y, Franco M, Ducret A, Mignot T. 2010. A bacterial Ras-like small GTP-binding protein and its cognate GAP establish a dynamic spatial polarity axis to control directed motility. *PLoS Biol* **8**: e1000430.
- Zheng SQ, Keszthelyi B, Branlund E, Lyle JM, Braunfeld MB, Sedat JW, Agard DA. 2007. UCSF tomography: An integrated software suite for real-time electron microscopic tomographic data collection, alignment, and reconstruction. *J Struct Biol* **157**: 138–147.

Erratum

Genes & Development 27: 2049–2062 (2013)

De- and repolarization mechanism of flagellar morphogenesis during a bacterial cell cycle

Nicole J. Davis, Yaniv Cohen, Stefano Sanselicio, Coralie Fumeaux, Shogo Ozaki, Jennifer Luciano, Ricardo C. Guerrero-Ferreira, Elizabeth R. Wright, Urs Jenal, and Patrick.H. Viollier

In the above-mentioned article, Nicole J. Davis and Yaniv Cohen contributed equally. The authors acknowledge there should not be a second notation of equal contribution between Yaniv Cohen and Stefano Sanselicio.

5.2 Acknowledgements

I would like to thank Prof. Urs Jenal, my supervisor, for giving me the opportunity to work on this exciting research project and for very fruitful scientific discussions.

I would also like to give thanks to my collaborator to Prof. Patrick Viollier for his great work.

To wonderful friends and Colleagues Jutta, Annina, Svetlana, Sören and the rest of the Jenal Lab

To my family

5.3 Curriculum Vitae

Curriculum Vitae



▶ Personal Information

Surname/Given name	Cohen Yaniv
Address	Bruderholzallee 126, 4059 Basel
Telephone	061 361 00 21
Email	yaniv.cohen@unibas.ch
Marital status	Married, two children
Date of birth	23 June 1975
Nationality	CH, IL

▶ Education and work experience

Since 2008	<p>PhD Molecular Microbiology, Growth and Development Department of Microbiology, Biozentrum, University of Basel Supervisor Prof. Urs Jenal</p> <p>Second messenger-mediated flagellum assembly during the <i>Caulobacter crescentus</i> cell cycle</p>
Winter 2011	<p>Venture challenge Commission for Technology and Innovation, University of Basel</p> <p>Strategic principles of success for young entrepreneurs</p>
2007 – 2008	<p>Master Molecular Microbiology, Infection Biology Department of Microbiology, Biozentrum, University of Basel Supervisor Prof. Guy R. Cornelis</p> <p>The Type III secretion system - The LcrV secretion signal</p>
Summer 2006	<p>Internship Roche, Basel</p> <p>Development of Avastin production process Data analysis, QA and Validation standards</p>
2002 – 2006	<p>Bachelor Molecular Biology, University of Basel</p>